CYANOBACTERIAL CYCLIC ELECTRON FLOW DRIVES PROTON PUMPING THROUGH NDH-1 COMPLEXES

By

NEIL MILLER

Bachelor of Science in Biology
John Brown University
Siloam Springs, AR
2013

Submitted to the Faculty of the
Graduate College of the
Oklahoma State University
in partial fulfillment of
the requirements for
the Degree of
DOCTOR OF PHILOSOPHY
December, 2020

CYANOBACTERIAL CYCLIC ELECTRON FLOW

DRIVES PROTON PUMPING THROUGH NDH-1

COMPLEXES

Dissertation Approved:

Robert L Burnap

Dissertation Adviser

Rolf A. Prade

Wouter D. Hoff

Erika I. Lutter

William J. Henley

ACKNOWLEDGEMENTS

Firstly, I want to thank my advisor and mentor Robert Burnap who has provided untold support, advice, and scientific development throughout the course of my time at Oklahoma State. I also appreciate the devotion of the time and efforts of my committee members for developing my scientific mind.

I am eternally grateful to the other members of the Burnap lab present and current who have helped develop my lab skills and provided camaraderie in pursuit of our own academic goals. I'm thankful to Steven Holland, Juliana Artier, and Han Bao for teaching me skills I would use in development of my physiological assays, and I'm thankful to Anton Avramov for being a companion and friend as we pursued our different projects, and providing an invaluable sounding boards for each other's experimental development. I'm thankful to Ross Walker and Clark Jett for their interest in the continuation of our project, and I'm so excited to see the directions they take it in.

I'm thankful to my professors in my undergraduate education for preparing me for my PhD and for instilling in me the fire needed to drive me into academic research. I thank Brian Greuel for teaching and guiding me through my understanding of molecular biology and genetics, and for making me believe in my scientific abilities. I thank Joel Funk for teaching me the basics of molecular biology research and for introducing me to the world of microbiology. I thank Tim Wakefield for deepening my interest in the animal world, research in general, and for pushing me toward opportunities that would ultimately change the course of my life and education.

I'm thankful for my dear friends who are like the brothers and sisters I never had. I thank Alex and Danielle Evers for their constant friendship and being very forgiving of living with a scatter-brained scientist. I thank Ryan and Shelbye Spencer for their optimism and love for playing games, which have always provided needed escapes from the lab. I'm thankful for Heather Sudduth and Chuck McClary for their friendship and support from far away, and their deep thinking on difficult topics. I'm thankful for my friendship with Thomas Kiser, who has been a sounding board, home brewing partner, and inspiration to me for many years.

Finally, I'm thankful for all of the love and support that my family has given me. I thank Steven and Debra Miller, my parents, for instilling in me a joy in reading and the pursuit of knowledge and for supporting me throughout my endeavors. I thank my grandparents Tom and Jean Miller and Marie and Fred Martin for their unwavering support and beliefs that I'm "a smart cookie." I thank my aunts, uncles, and cousins, too numerous to list here, for helping to inspire me that this was something I could do and do well.

This dissertation was made possible due to financial support from the U.S. Department of Energy (DOE), Office of Science, Basic Energy Sciences, grant no. DE-FG02-08ER15968.

Name: NEIL MILLER

Date of Degree: DECEMBER, 2020

Title of Study: CYANOBACTERIAL CYCLIC ELECTRON FLOW DRIVES PROTON PUMPING THROUGH NDH-1 COMPLEXES

Major Field: MICROBIOLOGY AND MOLECULAR GENETICS

Abstract: In cyanobacteria and other photosynthetic organisms, cyclic electron flow (CEF) around Photosystem I (PSI) is a crucial mechanism for balancing the photosynthetically produced energy carriers NADPH and ATP that are utilized to accumulate biomass. This is accomplished via the oxidation of NADPH by membrane oxidoreductases which pass the electrons into the membrane-soluble PQ pool and back to PSI where ferredoxin (Fd) and $NADP^+$ are reduced, completing the cycle. This cyclic flow drives the pumping of protons across the thylakoid membrane, driving the operation of ATP-synthase and thereby increasing the ATP/NADPH ratio with no net consumption of NADPH. A major participant in CEF are the NDH-1 complexes, homologs to respiratory complex I. Cyanobacteria possess four versions of this complex that participate in CEF as well as CO_2 uptake. While the activity of these complexes in pumping protons is known in other organisms, and the closely related chloroplast NDH-1 had recently been shown to do so, information on these complexes in cyanobacteria is lacking regarding proton pumping activity. As well, in cyanobacteria, these complexes were demonstrated to utilize Fd as a reductant source instead of NAD(P)H as is typical for its homologs. Cyanobacteria also possess a system to regulate the redox state of the Fd/NADPH pools by exchanging electrons between them, termed the Fd:NADP-oxidoreductase (FNR). Some cyanobacteria, like *Synechocystis* sp. PCC6803, possess two isoforms of FNR, FNR_S and FNR_L, that share a gene and are differentially expressed by different translation initiations, and are thought to primarily operate in NADPH oxidation and $NADP^+$ reduction respectively, though there are still large gaps in understanding their physiological functions. In this work, it is hypothesized that CEF is a major driver of proton pumping and that NDH-1 complexes are the driving force of that proton pumping. It is also hypothesized that the activity of FNR_S feeds NDH-1 with reduced Fd, allowing enhancement of proton pumping during acclimation to fluctuating light conditions, a major stressor of photosynthetic organisms.

TABLE OF CONTENTS

Chapter Page

LIST OF TABLES

Table Page

LIST OF FIGURES

Figure Page

CHAPTER I

INTRODUCTION

The atmosphere of early Earth was anaerobic, and the first organisms were almost certainly anaerobes (reviewed in (Zubay 1996, Fischer *et al.* 2016, Martin *et al.* 2017)). This era came to a close when the ancestors of the phylum Cyanobacteria acquired the ability to perform oxygenic photosynthesis, a process which produces O_2 and H^+ from light and H_2O, causing a rise in atmospheric O_2 (reviewed in (Lyons *et al.* 2014, Sanchez-Baracaldo *et al.* 2020)). The oxidation of water by oxygenic photosynthesis drives electron flow toward metabolic reductant in the form of NADPH and ferredoxin (Fd), which is consumed to power carbon fixation for the accumulation of sugars, or used to drive the formation of the Proton Motive Force (PMF) to power ATP synthesis (Alberts *et al.* 2017). A critical aspect of the photosynthetic mechanism is its adaptation to fluctuations in the environment that influence the pools of metabolic reductant and ATP (reviewed in (Shikanai *et al.* 2017)). Plants, algae, and cyanobacteria have evolved several mechanisms to dissipate excess reductant to adjust to the environmental and subsequent metabolic demand changes, but one shared by all of the oxygenic photosynthesizers is the NAD(P)H Dehydrogenase 1 (NDH-1) complex

Cyanobacterial NDH-1 complexes are versatile and important complexes for maintaining healthy growth. These complexes have high sequence and structural homology to respiratory

Complex I (NADH Dehydrogenase) of most respiring organisms, and they have been shown to function in electron transport in a similar way, in that they accept electrons from a reducing agent (ferredoxin in cyanobacteria and NADH in heterotrophs) and then use that energy to pump protons across a membrane to help establish the proton motive force (PMF) for ATP synthesis. While NDH-1 complexes are homologous to Complex I, the nomenclature between the organisms that possess them can be varied. In plants, algae, and cyanobacteria, the complexes also participate in cyclic electron flow (CEF) around Photosystem I (PSI) as a means of returning electrons into the plastoquinone pool that ultimately supplies PSI with electrons to reduce NADPH or ferredoxin (Fd). In this process, protons are thought to be pumped across the thylakoid membrane for ATP synthesis, and this is hypothesized to be used to increase the [ATP] with no net change in [$NADP^+$/NADPH], thereby balancing the NADPH/ATP ratio within the cell as needed. While this activity has been confirmed in the closely related chloroplast NDH-1 (Strand *et al.* 2017), such activity had not been confirmed in cyanobacteria until this work (Chapter IV).

Unlike in other organisms, cyanobacteria have four versions of the NDH-1 complex, differing by the presence of variable subunits connected with a common core sub-complex as discussed in section 1.3. Two of the variant forms (NDH-$1_{1/2}$) function similarly to the traditionally studied NDH-1 complexes in that they participate in electron transport and presumably proton pumping. The other two complexes (NDH-$1_{3/4}$) possess an extra protein subunit with carbonic anhydrase (CA) activity that hydrates CO_2 to HCO_3^- while also participating in electron transport. These two complexes experience different patterns of regulation, with one being constitutively expressed with low affinity and high flux (NDH-1_4) and the other being inducible by low external inorganic carbon concentrations with high affinity and low flux (NDH-1_3). These complexes accomplish this with the unique CupB or CupA proteins, respectively, attached to the variable parts of the NDH-1 complex. Since these proteins possess

carbonic anhydrase activity, and the removal of a H^+ from the active site of CAs is rate limiting, it is hypothesized that the removal of that proton is energized by proton pumping action of NDH-$1_{3/4}$ complexes. The work of Strand et al has shown that chloroplast NDH-1 complexes were able to couple proton pumping to electron flow in similar ratios to that seen for the well-studied homolog complex I (Strand *et al.* 2017, Strand *et al.* 2017), however, the extent of this activity and the roles of the various forms of the cyanobacteria NDH-1 complex remain poorly understood in this regard. It is a hypothesis of this work that the cyanobacterial NDH-1 complexes couple electron transfer to the PQ pool to proton pumping, that this activity varies among the complexes, and that CEF is able to drive PMF formation through these complexes to a considerable degree.

Abbreviations: PSII, photosystem II; PSI, photosystem I; cyt. b_6f, cytochrome b_6f; COX, cytochrome oxidase; NDH-1, NADPH Dehydrogenase 1; FNR, ferredoxin:NADP-oxidoreductase; PQ, plastoquinone; LEF, linear electron flow; CEF, cyclic electron flow; Fd, ferredoxin; PMF, proton motive force AO, acridine orange; CBB, Calvin Benson Basham; CEF, cyclic electron flow; CCCP, Carbonyl cyanide *m*-chlorophenyl hydrazone; DCMU, 3-(3,4-dichlorophenyl)-1,1-dimethylurea; DCCD, *N*,*N*′-Dicyclohexylcarbodiimide; Val, valinomycin; PAM, pulse-amplitude modulated fluorometry;

CHAPTER II

REVIEW OF LITERATURE

2.1 *Synechocystis* sp. PCC 6803: a model organism for studying photosynthesis and CO_2 uptake

The unicellular cyanobacterium *Synechocystis* sp. PCC 6803 (hereafter *Synechocystis*) is able to grow photoautotrophically and heterotrophically given the appropriate carbon and light sources (Stanier *et al.* 1977). Cyanobacteria in general make for fantastic model organisms with which to study CO_2 uptake and photosynthesis because they contribute greatly to the production of O_2 by their presence in lakes and oceans (Luz *et al.* 2011) and because they share many qualities with eukaryotic plants and algae (Martin *et al.* 2002). A variety of properties have made *Synechocystis* an experimental model for the study of photosynthetic processes. *Synechocystis* possesses the full suite of proteins required for photosynthetic electron transport and carbon fixation, with structural, functional, and sequence similarity to higher plants and algae. It possesses two photosystems and antennae apparatuses, synthesizes chlorophyll and carotenoids for energy absorption, and splits water as an electron source, much like higher plants and algae. This cyanobacterium was also the first photosynthetic organism whose genome was completely sequenced (Kaneko *et al.* 1996). This yields the advantage of rich literature on the species, and it has been used extensively as a model organism for photosynthesis. In addition to these factors, *Synechocystis* possesses the machinery for natural competence, allowing DNA to be taken up

with a simple incubation in the light at a high concentration of cells (Nakasugi *et al.* 2006, Eaton-Rye 2011). This results in transformation by homologous recombination without single-crossover events, provided the exogenous DNA contains homologous sequences within it (Williams 1988, Yoshihara *et al.* 2001, Eaton-Rye 2011). *Synechocystis*' competence, relationship to higher plants, and rich background literature allow it to be used effectively to explore the functions of photosynthetically related genes by the relatively simple creation of deletion mutants, complementations, and point mutations.

2.2 Cyanobacterial photosynthetic electron transport chain

Photosynthetic electron transport (PSET) is the primary means of establishing Proton Motive Force (PMF) in the light in cyanobacteria and other photosynthetic organisms (Mullineaux 2014, Shikanai *et al.* 2017). Cyanobacteria, being physiologically similar to chloroplasts in many ways, are useful in the study of this mechanism as they are genetically tractable and able to be measured as whole cells quite easily. There are two ways that PSET is accomplished, termed Linear Electron Flow (LEF) and Cyclic Electron Flow (CEF). The movement of electrons in LEF utilizes light energy to oxidize water and move electrons through PSII, the Plastoquinone (PQ) pool, cytochrome b_6f, and uses light energy again at PSI to produce Fd_{red} and NADPH (Mullineaux 2014). In CEF, PSI is the only photosystem active, and NADPH/Fd_{red} and carbon skeletons are consumed by thylakoid oxido-reductases and subsequently replenished by PSI driven reduction in order to produce PMF for ATP synthesis with no net NADPH/Fd_{red} production (Mullineaux 2014). The cell may switch which form of electron flow is dominant by moving the light-harvesting phycobilisomes to the relevant complexes depending on factors both external and internal that affect the oxidation state of the PQ pool (Mullineaux 2014). The light harvesting phycobilisomes dissociate from PSII when the PQ pool becomes over-reduced, allowing for their relocation to PSI to prevent too much further reduction of PQ by limiting LEF, with excess energy being devoted to either the formation of

PMF or the dissipation of the energy as heat and other mechanisms via interactions of the phycobilisome with Flv and OCP proteins (Mullineaux 2014). (Bhatti *et al.* 2020)The movement of the phycobilisomes between photosystems is termed a "state transition." When the phycobilisomes largely associate with PSII, the cells are in "state 1," which is regulated by oxidation of the PQ pool in an unknown manner. Transition to "state 2" requires reduction of the PQ pool, which triggers the dissociation of phycobilisomes from PSII and their movement to PSI, focusing the light energy there (Mullineaux *et al.* 1990, Ranjbar Choubeh *et al.* 2018, Bhatti *et al.* 2020). On a longer timescale, the movement of the membrane-integral NDH-1 complexes into proximity with PSI, allowing for the formation of a supercomplex that appears to function in rapidly dissipating excess reductant produced by PSI activity back into the PQ pool (Gao *et al.* 2016). The slowest adaptation to higher CEF is the production of more PSI and CEF components, which can take several hours (Fujita *et al.* 1988). The cell exerts strict controls over the PSET chain, as the energetics conducted within it are vital to the cells' photosynthetic activity. The energetics of both LEF and CEF will be discussed, with a more in-depth discussion of CEF as it more heavily involves the NDH-1 complexes.

2.2.1 Linear electron flow

Linear electron flow begins when a photon is absorbed by a special pair of chlorophyll at the reaction center (RC) of PSII which initiates photochemistry as a charge separation, forming the $P680^{+}Q_{A}^{-}$ state, where Q_{A}^{-} passes electrons to Q_B which, when fully reduced and protonated, diffuses into the thylakoid membrane and into the PQ pool (Barber *et al.* 2001). An important note to make is that charge separation is a vectorial process in that the positive charge is located on the lumenal side (P-side) and the negative charge is on the cytoplasmic (N-side) of the membrane, contributing to PMF generation. The positive charge at $P680^{+}$ is utilized for the oxidation of water and after four successive charge separations at PSII, two molecules of H_2O are oxidized and one molecule of O_2 is produced along with the deposition four protons into the

luminal space of the thylakoid membrane and contributing to the thylakoid ΔpH. Alongside the water oxidation, charge separation and electron transport drives the movement of electrons in to the PQ pool via Q_B reduction to quinol. The quinol diffuses through the thylakoid membrane to the cyt. b_6f complex, where it undergoes oxidation via the so-called Q cycle and deposits $2H^+$ per electron ($4H^+$ per PQH_2 oxidized) to the thylakoid lumen while transferring electrons to plastocyanin. This then transports the electrons to PSI, where another light-driven excitation event occurs upon photoexcitation of the PSI reaction center Chls, designated P700, which undergo and vectorial charge separation and electron transfer to Fd_{ox}, producing Fd_{red}, which may then transfer electrons to NADPH via Fd:NADP oxidoreductase (FNR) (Jensen *et al.* 2007). LEF carries forward at a H^+/e^- ratio of 3, with one proton coming from water splitting, and the other two coming from activity of the cyt. b_6f complex (Sacksteder *et al.* 2000). This produces the bulk of protons needed for ATP synthesis (Kramer *et al.* 2011), and LEF is shown in this work to be the heaviest contributor to proton pumping upon the dark to light transition (Chapter IV), likely due to the high abundance of PSII compared to CEF components such as NDH-1 along with the faster reaction rate of PSII (Zhang *et al.* 2004). Based on understandings of the structure of cyanobacterial ATP synthase (Pogoryelov *et al.* 2007), 3 ATP are made per 14 protons translocated, which does not satisfy the ratio of 1.5 required by the CO_2 fixing Calvin-Benson-Bassham-cycle (CBB-cycle) (Allen 2002). The PMF lacking to produce ATP therefore must be supplied by other means, such as cyclic electron flow around PSI, as discussed below.

2.2.2 Cyclic electron flow

It has been known for over 60 years that ATP can be photosynthetically produced in the absence of CO_2 fixation, with this activity being attributed to PSI alone (Arnon *et al.* 1954). Cyclic electron flow, which is observed in plants, algae, and cyanobacteria, begins when electrons produced from the linear electron transport chain are returned to the PQ pool via the electron transport chain. A model of this focusing on the subunits covered by this work is shown

in **Fig. 1**. This recycling of electrons contributes the proton gradient, and therefore ATP synthesis, with no net accumulation of Fd, NADPH, nor the reduction of CBB intermediates. Thus, the primary function of this action is hypothesized to be the cyclic oxidation and re-reduction of Fd or NADPH, while driving the accumulation of ATP with no net change in the redox state of the NADPH pool (Battchikova *et al.* 2011, Bernat *et al.* 2011). In cyanobacteria, the two major contributors to the consumption of reductant are Succinate Dehydrogenase (SDH) (Mi *et al.* 1992, Cooley *et al.* 2001, Bernat *et al.* 2011) the four forms of the cyanobacterial NDH-1 complexes (discussed below). The NDH-1 complexes most closely related to those in chloroplasts, NDH-$1_{1,2}$ complexes, appear to be the major contributors to CEF among the NDH-1 complexes in cyanobacteria (Bernat *et al.* 2011). The differences between the four NDH-1 complexes will be further discussed below, but briefly: the NDH-$1_{1/2}$ complexes are heavily active in CEF and respiration, and the NDH-$1_{3/4}$ complexes are involved in smaller fluxes of CEF, but also capture CO_2 as HCO_3^- in a manner necessary for growth in air levels of CO_2. The NDH-1 complexes also act as a protective mechanism for PSI, forming a supercomplex under conditions such as high light or salt stress and thereby providing the spatially close consumption of photosynthetically produced electrons, preventing ROS generation (Zhang *et al.* 2020). It was shown that the NDH-1-PSI supercomplex stabilizes PSI (Zhao *et al.* 2017), with the function of the supercomplex likely being to consume electrons for CEF as quickly as possible, limiting the space needed for Fd_{red} to diffuse (Gao *et al.* 2016). This accelerated consumption of electrons is thought to act as an antioxidant mechanism in this way, especially when stresses such as high light leads to increased Fd reduction. Recently, it was shown that exposure to high light caused heavy accumulation of the NDH-$1_{3/4}$ complexes, indicating their CO_2 uptake activity in addition to their CEF activity may play a role in the NDH-1 antioxidant mechanism (Zhang *et al.* 2020). The tightly regulated response of cyanobacteria to these stresses highlights the importance of this mechanism for the protection and acceleration of PSI-CEF when needed, thereby providing electron transport pathways necessary to prevent overreduction and ROS generation. Another

component of the cyanobacterial energy budget for safely dissipating excess reductant involves the activity of flavodiiron proteins, which act in a manner to reduce O_2 to H_2O in a so-called "water-water cycle" as a means of protection for the photosystems, reducing the opportunity for ROS to appear (Shikanai *et al.* 2017). The activities of both LEF and CEF occur in the light, but their activities share not only a membrane but electron carriers with respiration, which also functions to couple electron transport to the production of ATP.

2.2.3 Respiratory electron flow

Cyanobacteria are energetically unique among photosynthetic organisms in that they possess cytochrome oxidase (COX) in the same compartment as PSII, which consume and generate oxygen respectively in order to drive PMF production (Mullineaux 2014). In the dark, cyanobacteria consume the glycogen and monosaccharides they produced in the light, utilizing catabolic pathways typical to respiring organisms (Mullineaux 2014). The catabolically produced electrons are transferred, generally via the redox carriers NADPH and Fd, into the PQ pool through NDH-1 and SDH and through the cyt. B_6/f complex and, eventually to O_2 via COX. The electron flow through NDH-1, cyt. B_6/f, and COX couples to proton deposition in the thylakoid lumen and results in the generation of PMF and ATP in the dark, allowing maintenance metabolism to proceed in the absence of photosynthesis (Falkner *et al.* 1976, Peschek *et al.* 1985, Belkin *et al.* 1987). The balance between respiratory and photosynthetic metabolisms must be tightly regulated to prevent bottlenecks in the electron transport chain, especially during the diurnal illumination cycle or conditions of fluctuating illumination. As noted, respiration occurs in the dark, when light energy is not being utilized and accumulated sugars are being catabolized (Mullineaux 2014). Once illuminated, the cells switch toward a photosynthetic metabolism and shut down COX, allowing for them to accumulate carbon in the light. While the photosystems are not involved in respiration, many of the other electron transport components are shared, such as the PQ pool, cyt b_6f, and the NDH-1 complexes. Because of this shared activity, the dark ΔpH

produced by respiration and its effect on the oxidation state of the PQ pool must be considered as a technical point in observing proton pumping in the dark to light transition, since the light induced increases in PMF may build upon the existing PMF formed by respiration in the dark.. This becomes especially important in measurements of the proton pumping activity of the various NDH-1 complexes, as discussed in Chapter 3. Electron flow through photosynthetic NDH-1 complexes is well studied by following the redox state of the PQ pool using Chl fluorescence yield measurements or spectroscopically using the redox state of PSI during the course of the photosynthetic reactions of cyanobacterial cells (Battchikova *et al.* 2011, Bernat *et al.* 2011, Gao *et al.* 2016, Zhang *et al.* 2020). The other hypothesized action of cyanobacterial NDH-1 complexes, proton pumping, remains especially understudied. An important focus of this work is to elucidate CEF/PMF formation coupling and to explore specifically the contributions of the NDH-1 complexes as they are abundant and important members of the photosynthetic electron transport chain.

2.2.4 Electron carriers and redox balance

In cyanobacteria, electrons produced from either photosynthesis or catabolism are stored in the form of NADPH and Fd_{red} and are subsequently consumed by the various membrane complexes which dump those electrons into the PQ pool and plastocyanin, which then pass the electrons either back to PSI to participate in CEF, or passed through COX for respiration. The same carriers are utilized in the same membrane for all forms of electron flow in cyanobacteria, so the redox state of these pools must be tightly regulated. One of the balancing acts that must occur is in the redox state of the NADP(H)/$Fd_{ox/red}$ pools. This is broadly accomplished by the actions of Ferredoxin:NADP oxidoreductases (FNR), which possess the ability to either reduce $NADP^+$ by Fd_{red} oxidation or reduce Fd_{ox} by NADPH oxidation (van Thor *et al.* 1999, van Thor *et al.* 2000, Thomas *et al.* 2006, Korn *et al.* 2009, Korn 2010). Cyanobacteria that are capable of heterotrophy, such as *Synechocystis*, possess two isoforms of FNR that differ in the the presence

(FNR_L) or absence (FNR_S) of a phycobilisome linker-like domain (Thomas *et al.* 2006). The FNR_L isoform appears to be more heavily expressed under growth conditions, and generally associates with phycobilisomes. The FNR_S isoform is expressed to a lesser degree under growth conditions and is thought to locate to the cytoplasm as a soluble protein (Korn 2010). The current thinking is that FNR_L largely participates in the reduction of $NADP^+$, while FNR_S oxidizes NADPH to feed heterotrophic growth as it is required for chemoheterotrophic growth (Korn 2010), potentially by providing Fd_{red} for NDH-1 driven proton pumping and PQ reduction. The expression of each isoform is determined at the transcript level, with the FNR_S isoform being more heavily expressed in stressful conditions like nitrogen limitation or high light (Thomas *et al.* 2006). The two isoforms are produced by alternative transcription start sites in the same gene, allowing for this differential expression (Thomas *et al.* 2006). Two mutants were constructed by Dr. Ghada Aijlani's group which express only FNR_a (mutant termed FS1) or FNR_L (mutant termed MI6), and have been utilized to begin understanding the roles that each of these isoforms play in cyanobacterial photosynthesis. One of the major findings was that the FS1 mutant, expressing only FNR_S, had increased NDH-1 CEF, evidenced by an increased post-illumination chlorophyll fluorescence rise, associated with NDH-1 CEF activity (Korn 2010). What has remained unclear is the differences between these two isoforms with regard to their ability to participate in CEF by contributing to reductant pools, as well as how the presence or absence of each isoform effects proton pumping. The relationship these isoforms have to CEF and proton pumping by NDH-1 will be explored by this dissertation.

2.3 Cyanobacterial NDH-1 complexes: electron transport, CO_2 uptake, and proton pumping

The four NDH-1 complexes in cyanobacteria have unique functions within the cell. The NDH-1 complexes are comprised of two large parts: a core redox module (NDH-1M) that is common to all four variants of the complex and one of four distal modules that vary to make the different complexes that each participate in electron flow, and are hypothesized to couple the

redox activity in the core module to the distal subunits for proton pumping. (**Fig. 2**). Both the core redox module and the distal modules are multi-polypeptide protein complexes consisting of 15and 2-5 polypeptides, respectively (Laughlin *et al.* 2019, Schuller *et al.* 2019, Schuller *et al.* 2020, Zhang *et al.* 2020). This core redox module contains the proteins necessary for accepting electrons from Fd, the proteins that hold Fe-S clusters for e^- transport to PQ, and one of the three putative proton pumping subunits (Zhang *et al.* 2004, Laughlin *et al.* 2019, Schuller *et al.* 2019, Schuller *et al.* 2020). This core module attaches to the specialized distal subunits (NdhD1/2/3/4 and NdhF1/3/4) to allow for the complexes to be active (Herranen *et al.* 2004, Zhang *et al.* 2004, Folea *et al.* 2008) (**Fig. 2**). The NDH-1 complexes are named here based on the NdhD protein that associates with them, as each complex possesses an unique NdhD subunit. The subunits NdhD1 or D2 pair with NdhF1 and NDH-1M to produce the NDH-1_1 and NDH-1_2 complexes respectively (Zhang *et al.* 2004, Folea *et al.* 2008, Laughlin *et al.* 2019, Schuller *et al.* 2019). The other two complexes are associated with CO_2 hydration activity and are comprised of NdhD3, NdhF3, CupA, and CupS pairing with NDH-1M to make the NDH-1_3 complex, and NdhD4, NdhF4, and CupB pairing with NDH-1M to make the NDH-1_4 complex (Folea *et al.* 2008). The NDH-$1_{3/4}$ complexes possess the CupA and CupB carbonic anhydrase-like proteins which have no homologs among any other known carbonic anhydrase (CA) (Shibata *et al.* 2001). While these subunits are unique to cyanobacteria, the complexes as a whole have shown sequence homology to the Complex I seen in other organisms such as *E. coli*, *Thermus thermophilus* (hereafter *T. thermophilus*), and even subunits in Eukaryote complex I in organisms like *Yarrowia lipolytica* and *Bos taurus*. The structure of these complexes had been solved earlier in these organisms than cyanobacteria, allowing for in depth study of the mechanisms involved (Kaneko *et al.* 1996, Galkin *et al.* 1999, Shibata *et al.* 2001, Galkin *et al.* 2006, Battchikova *et al.* 2011). The structures for the cyanobacterial NDH-1 complexes have only recently been published, so hypotheses about their mechanisms are still forming, though they are generally expected to behave like the more well studied complex Is due to their homology (Laughlin *et al.* 2019,

Schuller *et al.* 2019, Schuller *et al.* 2020, Zhang *et al.* 2020). All four complexes are powered by reductant in the form of Fd, and putatively pump protons while simultaneously transferring electrons into the plastoquinone (PQ) pool (Battchikova *et al.* 2011, Battchikova *et al.* 2011, He *et al.* 2015, Laughlin *et al.* 2019, Schuller *et al.* 2019). This function allows for CEF around PSI, which is thought to cause the production of ATP while keeping the [NADPH] relatively constant by cycling the electrons from NADPH/Fd to the PQ pool and then back to NADPH via cyt. b_6f and PSI (**Fig. 1**) (Battchikova *et al.* 2011, Bernat *et al.* 2011). Given the homology of the cyanobacterial complexes to those with established and well-studied structures, one can infer that the cyanobacterial complexes function similarly in their mechanisms. The complexes have similar subunit composition, with residues seen to be vital to proton pumping in other organisms conserved in the cyanobacterial complexes. The modular NdhD and F proteins are homologous to the two proton pumping subunits most distal to the base module (Efremov *et al.* 2011, Efremov *et al.* 2012, Sato *et al.* 2014, Sazanov 2015). The proton pumping subunit homologs to NdhD and F are composed of several transmembrane helices that contain half-channels on either side of the membrane to allow proton pumping. In addition to this, the NdhF protein and its homologs have a long C-terminal helix that spans the length of the membrane arm. The current thinking is that the helix functions in anchoring the membrane arm to the hydrophilic arm via interactions along the membrane subcomplex (Wirth *et al.* 2016). The coupling of electron transport and proton pumping is thought to be carried out via conformational changes that occur upon reduction of quinone (Q) and are carried along the complex through the membrane via a series of conserved charged amino acids along the membrane axis, gating the transport of protons across the membrane (Wirth *et al.* 2016). The H^+/e^- stoichiometry of Complex I is under some debate, however a consensus of $2H^+/e^-$ is generally accepted (Galkin *et al.* 1999, Galkin *et al.* 2006). The complex has even been seen to be reversible in mitochondria, and potentially chloroplasts, indicating a possible role as a "pressure relief valve" that is utilized to dissipate the ΔpH when the difference across the membrane becomes too great, or to spend ATP to generate $NADPH/Fd_{red}$

(Kotlyar *et al.* 1990, Vinogradov 1998, Strand *et al.* 2017). This reverse action in mitochondria is only seen in specially prepared submitochondrial particles under specific conditions, however this activity has been seen *in vivo* in organisms with unique energy budgets such as *Nitrospira* or *Thaumarchaea* (Aleem 1966, Lucker *et al.* 2010, Simon *et al.* 2013, Konneke *et al.* 2014, Chadwick *et al.* 2018) The energetics and mechanisms known about homologous complexes allow the following questions to be asked about cyanobacterial NDH-1 complexes: Do the NDH-1 complexes pump protons? Are electron transport, proton pumping, and CO_2 hydration coupled? Which pathways of electron flow and sources of reductant are utilize *in vivo*, and how might these pathways vary when challenged with the stress of fluctuating redox conditions?

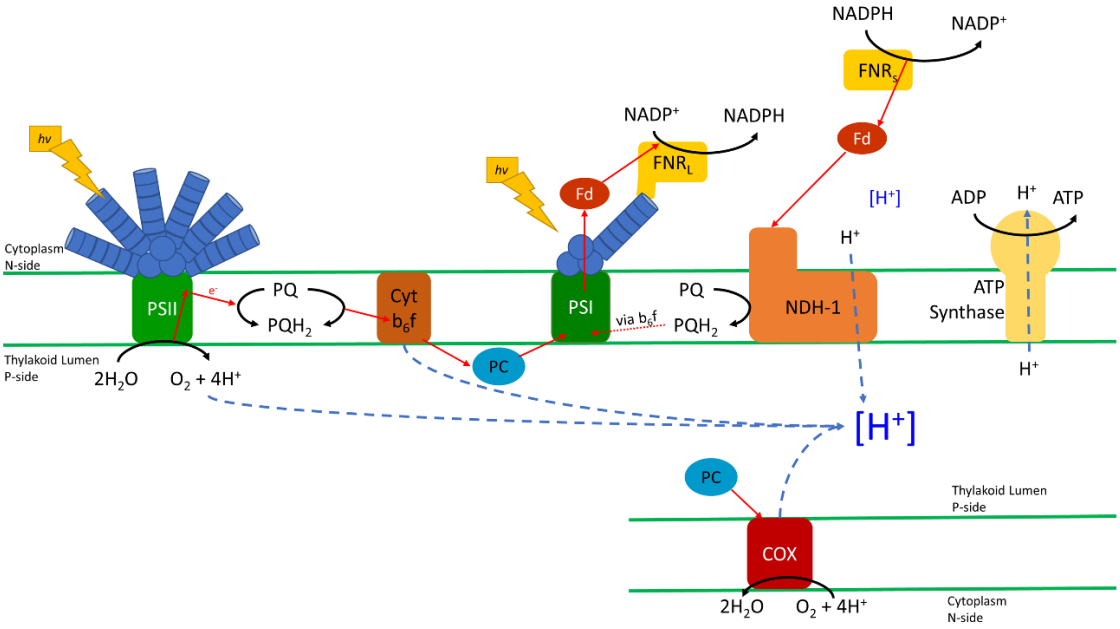

Figure 1. Model of electron transport and proton pumping in the thylakoid membrane of cyanobacteria. Electron transport routes are highlighted in red, sources of protons for PMF are shown with blue arrows, and the general reactions shown with a black arrow.

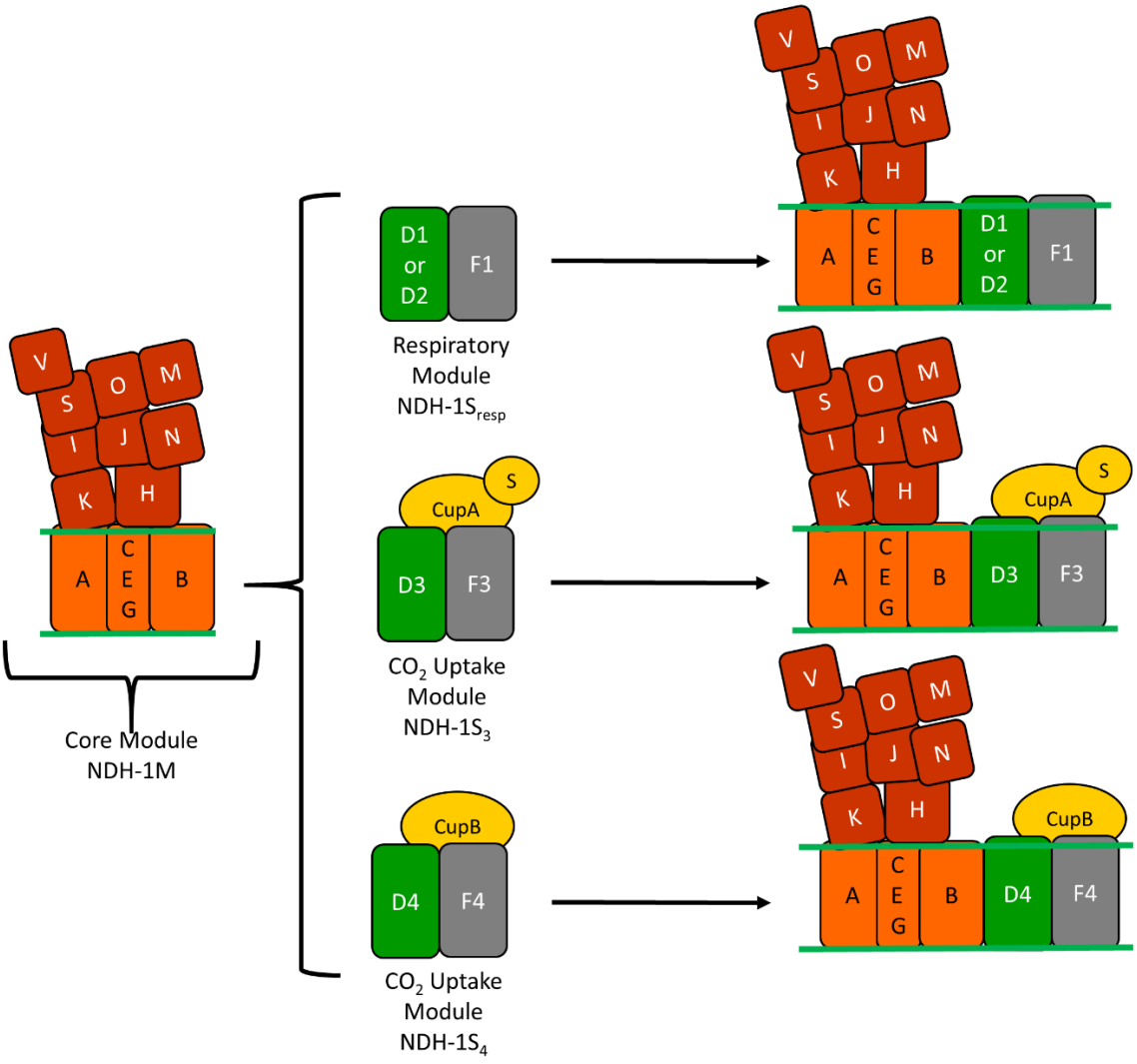

Figure 2. The modularity of NDH-1 complexes in cyanobacteria. All four NDH-1 complexes in cyanobacteria share a common core sub-complex that is paired with distal subunits to produce functional complexes. The variable modules provide functions largely split between NDH-$1_{1/2}$ complexes and NDH-$1_{3/4}$ complex which are primarily involved in CEF/respiration or CO_2 uptake respectively. The Fd oxidation subunits are colored red, the quinone binding and membrane subunits of the core module are highlighted in orange, the NdhD and NdhF proteins in green and black respectively, and the CO_2 uptake associated CupA/B/S highlighted in yellow.

Table 1. Subunits of NDH-1, notes on their function, and homologs in other organisms.

Associated module of NDH-1	Subunit in cyanobacteria	*E. coli*	*T. thermophilus*	*B. taurus*	*Y. lipolitica*	Subunit notes
PQ reductase in core module	NdhA	NuoH	Nqo8	ND1	NU1M	PQ-binding, half antiporter-like fold
	NdhB	NuoN	Nqo14	ND2	NU2M	Antiporter like, proton pumping
	NdhC	NuoA	Nqo7	ND3	NU3M	PQ-binding site
	NdhE	NuoK	Nqo11	ND4L	NULM	
	NdhG	NuoJ	Nqo10	ND6	NU6M	
	NdhH	NuoD	Nqo4	49 kDa	NUCM	Fd-binding
	NdhI	NuoI	Nqo9	TYKY	NUIM	Fd-binding, FeS clusters
	NdhJ	NuoC	Nqo5	30kDa	NUGM	
	NdhK	NuoB	Nqo6	PSST	NUKM	Terminal FeS cluster, PQ binding
NAD(P)H oxidase in core module		NuoF	Nqo1	51kDa	NUBM	NAD(P)H dehydrogenase domain
		NuoE	Nqo2	24kDa	NUHM	NAD(P)H dehydrogenase domain
		NuoG	Nqo3	75kDa	NUAM	NAD(P)H dehydrogenase domain
Fd oxidase in core module	NdhL					
	NdhM					
	NdhN					
	NdhO					Fd-binding, negative regulator of activity
	NdhP					Single transmembrane helix
	NdhQ					Single transmembrane helix
	NdhS					SH3-like Fd binding domain
	NdhV					Fd-binding, positive regulator of activity

Distal membrane subunits	NdhD1	NuoM	Nqo13	ND4	NU4M	Antiporter-like
	NdhD2	NuoM	Nqo13	ND4	NU4M	Antiporter-like
	NdhD3	NuoM	Nqo13	ND4	NU4M	Antiporter like, high affinity CO_2 uptake
	NdhD4	NuoM	Nqo13	ND4	NU4M	Antiporter like, low affinity CO_2 uptake
	NdhF1	NuoL	Nqo12	ND5	NU5M	Antiporter-like
	NdhF3	NuoL	Nqo12	ND5	NU5M	Antiporter like, high affinity CO_2 uptake
	NdhF4	NuoL	Nqo12	ND5	NU5M	Antiporter like, low affinity CO_2 uptake
Carbonic Anhydrase-like subunits	CupA/ChpY					Carbonic anhydrase-like, Zn binding, high affinity CO_2 uptake
	CupB/ChpX					Carbonic anhydrase-like, likely Zn binding, low affinity CO_2 uptake
	CupS					

2.3.1 Strucutre, function, and mechanism of homologous complexes

Until recently, hypotheses about the mechanism of cyanobacterial NDH-1 complexes could only be inferred from the mechanism of complex I of heterotrophs that had already been crystalized and studied. Thanks to recent works, the structure of the *Thermosynechococcus elongatus* (hereafter *T. elongatus*) cyanobacterial NDH-1 was solved, confirming the close relation to the more well studied complexes, allowing the mechanism hypotheses to now be more closely analyzed (Laughlin *et al.* 2019, Schuller *et al.* 2019). Since the mechanism has been well studied in organisms like *E. coli* and *T. thermophilus*, the conclusions reached by them will inform some of the tests presented in this work.

In general, these complexes perform two functions: proton pumping and electron transport. Since the proton pumping occurs against a pH gradient, it must be energetically coupled. It is hypothesized that electron transfer from NADH to Quinone (Q) via FeS clusters causes electronically based conformational changes among charged residues in the membrane axis that allows for the deposition of protons against the pH gradient.

Complex I proton pumping

The membrane domain of complex I from *E. coli* had its structure determined via X-ray diffraction by Efremov and Sazanov in 2011 (Efremov *et al.* 2011). Since before this point the structure had not been determined to a degree precise enough to assign sequences to the trans-membrane helices, this work allows for the sequence/structure/function comparison of this complex to homologous complexes in other organisms, including cyanobacteria. In this work, they attain a resolution of 3.0Å, allowing for the group to observe the placement of residues within the helices. The two subunits NuoM and NuoL are located distally within the membrane to the hydrophilic subunits and are homologous to the NdhD and NdhF proteins of cyanobacteria respectively, and **Table 1** shows the nomenclature differences between the species, along with their known and hypothesized functions. An important not here is that while the different versions of the NdhD/F proteins are homologous to NuoM/L and Nqo13/12, the Nuo and Nqo proteins lack specialized abilities like CO_2 uptake. After determining the structure, they mapped out the locations of various residues and utilized previous works to determine their effects on proton pumping and the putative functions they may have in translocating protons across the membrane. They saw that none of the channels seen are solvent accessible from both sides of the membrane, indicating there is some sort of gate between the channels. In the structure, they saw that each of the proton pumping subunits is comprised of 14 transmembrane (TM) helices, with NdhF having additional 15^{th} and 16^{th} helices that traverse the entire membrane domain, parallel to the plane of the membrane of the complex, and anchor it to the subunits near the hydrophilic domain. The common helices are grouped into a highly conserved core (TMs 4-13) and then the less conserved

TMs 1-3 and 14. In the conserved core, TMs 4-8 and 9-13 can be superimposed upon one another by a rotation of ~180^{o} along the axis lying in the membrane. The structures of the helices are conserved throughout both mitochondria and bacteria (Efremov *et al.* 2011, Baradaran *et al.* 2013, Wirth *et al.* 2016). TMs 7 and 12 are symmetrically related, and both contain helices that are interrupted by a 5-7 residue loop in the middle of the membrane. These loops contain a conserved proline and are important for proton/ion transport because they introduce flexibility and charge into the center of the membrane (Screpanti *et al.* 2007). Partial charges are introduced into the middle of the membrane through positive and negative dipole ends at the N and C termini of the helices respectively. Unlike typical α-helices, the internal hydrogen bonds of the backbone of the extended peptide in the discontinuous helices are not fully saturated, thereby helping to increase polarity at the center of the membrane and creating a space for ion binding. Other polar residues can also be used to help stabilize ion binding (Screpanti *et al.* 2007). TM8 lies at the interface between the proton tunnels created by TMs 7 and 12, and it contains a proline-less kink that disrupts local secondary structure via a π-bulge. These are seen in some protein active sites, and is hypothesized to connect the two half-channels in the NuoL and NuoM proteins by utilizing the charged residues and the flexibility inherent in a π-bulge (Cooley *et al.* 2010, Efremov *et al.* 2011, Sharma *et al.* 2015, Di Luca *et al.* 2017). They saw that the channel formed by TM7 is accessible to the cytoplasm and that the channel formed by TM12 is accessible to the periplasm (this would be the thylakoid lumen in cyanobacteria since the complexes localize to the thylakoid membrane). In their analysis, they concluded that conformational changes in the Q-reduction subunits that are proximal to the hydrophilic subcomplex upon reduction by NADH can be transmitted to the membrane subunits of the core complex, and then transmitted further by the long helix of NuoL (NdhF) to TM7 of NuoN (NdhB), NuoM (NdhD), and NuoL itself (Efremov *et al.* 2011, Sharma *et al.* 2015, Di Luca *et al.* 2017, Fedor *et al.* 2017). This notion seems to have been abandoned for an explanation involving conformational changes starting at the Q-binding site and propagating down the membrane arm via an axis of charged residues in the center of the

membrane (discussed below). Protonation of LysTM7 occurs in the oxidized state by connection to the cytoplasm, and upon reduction, LysTM7 and GluTM5 move away from each other, forcing the donation of a proton to the link between the half channels, and then to Glu/LysTM12 which remains protonated, potentially from a combination of local conformation changes and/or interaction from the neighboring subunits' TM5. When the conformation returns to the oxidized state, the proton is ejected from Lys/GluTM12 and LysTM7 is protonated to reload the pump (Sazanov 2015, Haapanen *et al.* 2018). These Glu and Lys residues are highly conserved in the cyanobacterial homologs to these proteins.

Coupling electron transport to proton pumping

Many efforts have been made by various groups to determine the mechanism by which NDH-1 complexes couple proton pumping to electron transport, however the specifics remain somewhat difficult to determine. Based on the structural information gained thus far, explanations have been provided for the mechanism of complex I (Baradaran *et al.* 2013, Sazanov 2015, Sharma *et al.* 2015, Di Luca *et al.* 2017, Fedor *et al.* 2017). One of the most challenging aspects of developing an explanation for the mechanism of complex I is answering the question: how is a redox reaction coupled to proton pumping that occurs up to 200Å away? The predominant explanation in the literature states that initially in complex I, NADH donates an electron to FMN, then through FeS clusters down to quinone. Since only one e^- can be transferred by each FeS cluster, and most of the FeS clusters are reduced in physiological steady state, it is thought that the rate limiting step is the binding and release of quinone (Fedor *et al.* 2017). The terminal FeS cluster is coordinated by 4 Cys residues. One pair is uniquely consecutive in the sequence, since in most FeS coordinations the Cys residues are separated spatially (Berrisford *et al.* 2009, Sazanov 2015). This results in interesting geometry, where one of the consecutive residues will disconnect from the cluster upon reduction of the FeS cluster. The midpoint potential of this cluster is pH dependent, therefore its reduction is thought to be related to proton binding (Ohnishi 1998). The disconnected Cys upon reduction is thought to result in a significant conformational

change in nearby helices. This may also be driven by the binding and protonation of the quinone, releasing it only when the conformational changes and proton pumping have been completed. Under the current hypothesis, reduction of quinone triggers a conformational change of charged residues to occur near the quinone binding pocket. A heavily conserved part of this pocket, NuoH, not only helps bind quinone, but also composes a part of one of the four proton pathways through complex I (Sazanov 2015). This proximity allows for the hypothesis that reduction/protonation of the quinone triggers the proton pumping action of complex I, since NuoH is both a part of the charged membrane axis and the quinone binding site. The charged axis is located in the middle of the membrane and the residues are located in the proton channels or areas that connect them, and at/near their discontinuous helices (Sazanov 2015). The conformational changes occurring at NuoH are hypothesized to initiate the cascade of conformational changes that allow proton pumping.

In general, proton translocating channels have some common traits. They have chemical groups that have a tunable pKa, and a switch that allows the channel to be opened and closed for proton translocation (Wang *et al.* 2009, Sazanov 2015, Wickstrand *et al.* 2019). In NDH-1 complexes, it is thought that an axis of 5 Lys residues and one Glu residue lie within the membrane and are present in the center of each half channel in the proton pumping subunits, and they have their pKa, and therefore their protonation state, regulated by Glu in TM5. TM5 is thought to be able to move via conformational changes such that the Glu residue is able to affect the pKas of the cytoplasmic side pathway within the same subunit (TM7 channel), or the periplasmic side pathway of the neighboring subunit (TM12 channel). The origin of this conformational change is thought to reside in the quinone binding subunits, which start the chain of charged residues to the highly conserved residues of the membrane subcomplex. The charged residues are arranged along an axis that runs parallel to and in the middle of the membrane subcomplex, allowing the complex interaction of charged residues from neighboring subunits to

accomplish proton pumping. Included in these subunits are 3 proteins that are related to the Mrp Na^+/H^+ antiporters, and likely each pump one proton per $2e^-$ donated. The fourth proton is likely transported by a similarly constructed channel that is comprised of four protein subunits, some of which also function in quinone binding. The subunits may even be able to re-distribute protons that have been accumulated via routes that connect the subunits, potentially overcoming the relatively high $[H^+]$ of the cytoplasm compared to the periplasm. The periplasmic side of each antiporter-like subunit, on the other hand, only has one putative proton extrusion route, TM12, which seems to control the extrusion of protons on that side of the membrane. It was hypothesized that electron transfer to the quinone from the terminal FeS cluster initiates a cascade of conformational changes in a charged tunnel that culminates in a Glu-Asp quartet, which can then interact with the nearest Mrp-like antiporter subunit, which in turn can interact with the further away antiporter-like subunits via ProTM12-GluTM5 interactions between neighboring subunits. To summarize the hypothesized mechanism: upon reduction of quinone, conformational changes occur along the charged axis. The LysTM7 residues open to the cytoplasm are thought to be protonated in the oxidized state of the enzyme. The conformational changes induced by quinone reduction closes the cytoplasmic side of the channels and moves GluTM5, thereby moving TMs 7 and 8 close enough to allow proton transfer, and then to Lys/GluTM12 in the periplasmic/lumen side channel. The proton is ejected upon a return to the oxidized state and the pump is primed with protons again. This accounts for the transport of three protons, the fourth likely goes through a similar process, however its path passes near the Q-binding domain. Observing the conserved residues in sequence and structural homology models can allow the determination of which residues may be important in modulating the pKa of the charged residues within the proton pump channel, and how these channels are gated.

The quinone binding site is located proximally to the hydrophilic subcomplex and is composed of several subunits. Currently, it is thought that the hydrophilic arm accepts electrons

from NADH (or in the case of cyanobacteria, Fd (He *et al.* 2015, Laughlin *et al.* 2019, Schuller *et al.* 2019, Zhang *et al.* 2020)) and then passes them down the FeS clusters to the Q-reduction site, deep within the Q-binding subunits, and on to quinone for quinol formation (Wirth *et al.* 2016). According to previous data, it takes about 100μs for electrons to travel to the terminal cluster near the Q-reduction site, while the enzyme turnover rate is on the millisecond scale (Verkhovskaya *et al.* 2008). EPR data has shown that the redox chemistry of reducing quinone is a stepwise process with energetic barriers between each step to stabilize the radical intermediates formed during the reduction. To explain this, the two-state stabilization change mechanism has been proposed (Brandt 2011). This mechanism states that quinone reduction and proton pumping are strictly separate events, and that energy released during the stabilization of the quinone radicals drives conformational changes near the Q-reduction site that are passed on via charged residues to the rest of the complex, thereby allowing proton pumping. It also suggests that the FeS clusters serve as a reservoir for electrons to be passed along to the next step as they are needed, keeping the redox poise of the system at ~-250mV or less. This cycling between an electron transporting state (E-state) and proton translocating state (P-state) is thought to be the main mechanism behind the coupling of electron transport to proton pumping. Because not only the proton pumping subunits, but the electron transport subunits are well conserved in cyanobacteria (Laughlin *et al.* 2019, Schuller *et al.* 2019, Schuller *et al.* 2020), similar constraints can be applied to observe how these complexes might behave.

Stoichiometry of complex I electron transport coupled to proton pumping

The stoichiometry of the NDH-1 complex's redox coupled proton pumping is currently under debate, with the complex either pumping 4 protons per NADH or 3, depending on the experimental conditions utilized (Wikstrom *et al.* 2015). In 1999, the Galkin *et al* group (Galkin *et al.* 1999) prepared submitochondrial particles and utilized pH dependent dyes to measure the absorbance change in the solution and inside the particles, allowing determination of the rates of acidification and alkalization of the prepared particles. Then, utilizing a series of inhibitors,

teased apart the signal obtained to determine the $H^+/2e^-$ ratio in bovine heart mitochondria. Utilizing this method, they obtained a ratio of $4H^+/2e^-$, or $4H^+$/NADH. The Galkin *et al* group (Galkin *et al.* 2006) additionally isolated complex I from the fungus *Yarrowia lipolytica* mitochondria, then produced proteoliposomes containing the complex. They first measured the stoichiometry in intact mitochondria using methods in the 1999 paper, confirming a ratio of $4H^+/2e^-$. Then, utilizing a dye called oxonol VI, they measured the red shift in the spectrum, which indicates an accumulation of protons inside the proteoliposomes by accumulating to the lipid phase when the inside of the proteoliposome is positively charged. The amplitude of the oxonol response is indicative of the electric potential across the membrane, was seen to be responsive to additions of NADH to the medium, and was essentially proportional to the concentration of NADH added. Utilizing the rate of the decay of the pH gradient after NADH addition, indicating protons re-entering the external media from the Q pool, it is possible to obtain the stoichiometry ratio by dividing by the concentration of NADH added. When this was done with the proteoliposomes, they found that the ratio varied depending on the amount of NADH added. In values below the k_m, the rate was seen to be closer to $2H^+/2e^-$, while in concentrations near/above the k_m, the rate was seen to be about $4H^+/2e^-$. This works with the structural data, since the model proposed by Efremov and Sazanov (Efremov *et al.* 2011) includes four antiporter-like channels in the membrane domain, with one comprised of two proteins residing proximally to the hydrophilic domain. Works by Wikstrom *et al* (Wikstrom *et al.* 2012) have predicted a ratio closer to $3H^+/2e^-$ based on known energetics of the redox span of NADH usage and the energy stored in the proton gradient in rat mitochondria (Wikstrom *et al.* 2012). In order to achieve a ratio of $4H^+/2e^-$ the redox span of NADH must be larger if the proton gradient energy is accepted, or the proton gradient energy must be considerably lower if the redox span of NADH is accepted. They also argue that since the measurements done previously have issues in performing their experiments in non-physiologically relevant conditions, the proton gradient energy may fluctuate, allowing the ratio to reach $4H^+/2e^-$. This author also points out studies

where ATP synthesis is considered in the energetics equation, determining the proton pumping ratio in complex I of both sub-mitochondrial particles and in whole *E. coli* cells. The group utilized an equation relating the known energetics of ATP synthesis (8 protons per 3 ATP, or 2.67 H^+/ATP), the ATP/$2e^-$ ratio determined from rat mitochondria, and the $H^+/2e^-$ ratio. They determined that with these constraints, a ratio of $3H^+/2e^-$ provides 97% coupling efficiency, while a ratio of $4H^+/2e^-$ provides only 73%. This group hypothesizes that the presence of the putative pump proximally to the hydrophilic arm of complex I acts as a proton pump channel only under conditions in which the proton motive force is low. By understanding the stoichiometry and rates of H^+/e^- transport in the cyanobacterial complexes, their contributions to photosynthesis and their mechanisms, especially that of CO_2 hydration, may be studied in the future.

2.3.2 Functions of cyanobacterial NDH-1 complexes

The cyanobacterial NDH-1 complexes participate in some very important energetic processes in the cell. They participate in CEF around PSI, consuming reductant from the NADPH/Fd pool and putatively pumping protons to help balance the NADPH/ATP ratio, keeping the pools from getting over-reduced. This action is thought to be coupled to the known reduction of the PQ pool by the consumption of that reductant. In addition to this, two of the four complexes possess unique subunits (CupA/CupB) that perform CO_2 hydration, an action not yet seen in any other phylum's NDH-1 complexes. The mechanism behind this action is unknown, and the Cup proteins have no homology to known carbonic anhydrases which perform the same reaction, making them somewhat difficult to study, though recently structures have been proposed for these complexes that will ease mechanistic studies. Because these proteins are associated with the variable membrane pieces of the NDH-1 complexes, it may be possible to use the more well studied *E. coli* and *T. thermophilus* complexes to design point mutations in the membrane subunits to address questions about the relationship between CO_2 hydration and the putative proton pumping subunits.

Cyclic electron flow and respiration

In respiratory heterotrophs, complex I is a member of the respiratory electric transport chain. In photosynthetic organisms, NDH-1 complexes not only do this, but also possesses a unique function within the thylakoid membrane, that of CEF around PSI. To study some of the roles these complexes have in CEF, Bernat *et al* (Bernat *et al.* 2011) performed a series of experiments to answer the following questions: Are NDH-$1_{3/4}$ complexes involved in CEF around PSI? Which is the major respiratory pathway to PQ? How do the pathways interact? To answer these, they analyzed $P700^+$ oxidation and reduction kinetics to observe respiratory and cyclic electron transport rates in various mutants. To separate the components of electron transport, they utilized far red light to select for activity of PSI over PSII. Both the maximum oxidation during the light pulse and the subsequent dark reduction give information on electron transport through the PQ pool and cytochrome b_6f. To isolate cyclic, PQ reducing, and PQ oxidizing respiratory routes, they utilized a suite of inhibitors that specifically block the electron pathways at key locations. They posit that the rate of $P700^+$ rereduction, k_1, should reflect the difference between electron transport rates into and out of the PQ pool, represented by the equation: $k_1 = k_A + k_B - k_C$. where k_A represents NDH-1 dependent PSI mediated electron transport, k_B represents electrons transport from metabolic sources to PQ via NDH-1/SDH, and k_C represents electron flow from PQ to O_2 mediated by terminal oxidases. In the presence of KCN, k_C is blocked, therefore the $P700^+$ kinetics, k_2, reflects $k_A + k_B = k_2$, and the difference between k_1 and k_2 reflects the electron transport rate through k_C. Electron donation from PSI to the PQ pool was inhibited by utilizing the PSI electron acceptor methyl viologen. Pairing this with KCN allows probing of only the k_B route, with a rate constant equal to k_3. Subtracting this from k_2 gives the rate constant through k_A. These rate constants were then utilized to calculate the electron transfer rates of the separate pathways. When they measured the oxidation of $P700^+$ upon far red illumination, they saw that electron transport rates were similar to the wild type in mutants Δ*ndhF*$_{3/4}$ or Δ*ndhF*$_{1/3/4}$, but faster

in the mutant only lacking *ndhF₁*, indicating highly efficient $P700^+$ oxidation in the last mutant. In contrast, the reduction kinetics were similar in the wild type and Δ*ndhF₁*, but faster in the Δ*ndhF₃/₄* mutant, and very slow in the Δ*ndhF₁/₃/₄* mutant. The reduction kinetics measured for these mutants show inhibition of respiratory electron flow to PQ in all cases of NDH-1 inactivation. Addition of KCN lowered $P700^+$ oxidation levels and produced a slower rise and faster decay than without the inhibitor in the wild type, Δ*ndhF₃/₄*, and Δ*ndhF₁* mutants, indicating a more reduced PQ pool in the presence of KCN, showing a significant transport of electrons to O_2 via terminal oxidases in these strains. In contrast, the Δ*ndhF₁/₃/₄* mutant was unaffected by KCN, showing a low rate of respiratory electron transport. When methyl viologen was added to the KCN treated cells, $P700^+$ oxidation was relatively unaffected in the wild type, Δ*ndhF₃/₄* and Δ*ndhF₁/₃/₄* resulting in nearly identical k_2 and k_3 values for these strains. These high k_3 values for the wild type an Δ*ndhF₃/₄* indicate a high capacity for electron donation from metabolites to PQ. Contrastingly, the rate of oxidation of $P700^+$ in the Δ*ndhF₁* was increased, and the rate of reduction in the dark was decreased, indicating a strong suppression of electron flow from respiratory routes and very active cyclic transport through the NDH-$1_{3/4}$ complexes. Since cyclic routes are minor contributors to $P700^+$ reduction in the wild type and Δ*ndhF₃/₄* mutant, the contribution of the PQ reducing pathways appears flexible and potentially dependent upon other pathways. The authors suggest that electron flow in different routes may suppress one another or become activated when a pathway is closed. Earlier work in probing the cyanobacterial NDH-1 complexes and their participation in CEF by observing $P700^+$ kinetics has been performed with mutants lacking the gene for the vital core subunit *ndhB* (therefore lacking all NDH-1 complexes), and in conditions of high and low C_i (Mi *et al.* 1992, Deng *et al.* 2003). The Mi *et al* (Mi *et al.* 1992) group observed that the NDH-1 complexes are the major electron donors to PSI in CEF dependent on metabolically generated reductant, providing a base for further exploration of the contributions of these complexes. The Deng *et al* (Deng *et al.* 2003) group observed that the abundance and activity of NDH-1 complexes increases in low CO_2 conditions. The Ohkawa *et*

al (Ohkawa *et al.* 2000) group showed that the deletion of the NdhB subunit in the core redox module abolished CO_2 uptake and the ability to grow at air levels of CO_2, requiring supplementation. This provides some evidence that the CO_2 hydrating NDH-1 complexes contribute to CEF.

The NDH-1 complexes not only participate in CEF, but also in the respiratory electron flow (REF). Cyanobacteria have an interesting energetics problem in the thylakoid membrane: both photosynthesis and respiration utilize the PQ pool, and occur in the same membrane/lumen system! If both were active at the same time, the PQ pool could become over-oxidized. To get around this, cyanobacteria appear to regulate their respiratory machinery by light intensity (Mullineaux 2014), with respiration increasing in lower light intensities and darkness. There are several components to REF, including the NDH-1 complexes, SDH, cyt b_6f, and COX.

The NDH-$1_{1/2}$ complexes are the primary participants in REF among NDH-1 complexes, but actually make up a smaller proportion of the total REF compared to Succinate Dehydrogenase (SDH) (Cooley *et al.* 2001). which catalyzes the conversion of succinate to fumarate in the TCA cycle. In cyanobacteria, the same PQ pool is used for both PSET and respiration and are utilized by the "light" and "dark" reactions respectively (Nagarajan *et al.* 2016). Cooley and Vermaas in 2001 (Cooley *et al.* 2001) utilized chlorophyll fluorescence, oxygen consumption assays, determination of the concentrations of TCA cycle intermediates, and reduction states of the PQ and NAD(P)H pools to observe the contributions of SDH, NDH-1, and NDH-2 to respiratory electron flow. In their work, they saw that the NDH-1 complexes contribute to about 5-10% of respiratory electron flow. The majority of respiratory electron flow is contributed by SDH, and in fact a lack of carbon skeletons appears to be the reason the PQ pool is hyper oxidized in NDH-1 deletion mutants since the oxidation is rescued by the addition of succinate (Cooley *et al.* 2001). Their work implies at least two things about the NDH-1 complexes: 1) NDH-1 complexes are not the major contributors to respiratory electron flow; 2) The availability of carbon skeletons is

partially dependent upon the activity of NDH-1 complexes. This is likely due to the CO_2 hydration activity of the NDH-$1_{3/4}$ complexes, as their deletion causes mutants to be perpetually carbon starved (Artier *et al.* 2018). While their contribution to the reduction of PQ may be minimal compared to SDH in terms of respiration, it is clearly important for helping to manage the PQ pool and Fd/NADP(H) pool reduction states. While the SDH complex does not directly contribute to the formation of ΔpH, it does contribute to the reduction of the PQ pool, which can be utilized by the cyt. b_6f complex in a Q-cycle to deposit protons on the P-side of the membrane.

The cyt. b_6f complex is a major enzymatic junction between PSET/CEF and respiration. It performs the action of removing electrons from the PQ pool and passing them along to either PSI or a terminal oxidase such as Cytochrome *c* oxidase (COX) utilizing electron carriers (Nagarajan *et al.* 2016). Because it is at this intersection and both processes utilize many of the same components, there must have tightly controlled electron flow toward either PSET or respiration. According to Nagarajan and Pakrasi in 2016 (Nagarajan *et al.* 2016), the electron transport capacities of the various components were compiled, and it was seen that PSI has the highest capacity of electron transfer (μmol electrons h^{-1} (mg Chl)$^{-1}$), while PSII and cyt. b_6f have ~1/3 the capacity of PSI, but 5x the capacity of SDH and COX, and 50x the capacity of NDH-1 complexes. Because of the inherent flux capacities, when light intensity is high there is more flow through PSII/PSI, while when light is limiting the respiratory pathway can utilize the available electrons faster than the PSET pathway. This allows for the expression of both systems simultaneously and gives the cell adaptability to best utilize its electrons depending upon the conditions it's faced with. Another part of the regulation may be pH sensitivity of the cyt. b_6f complex, which, in plants, is seen to become inhibited at lower pH observed at high light intensities (Kramer *et al.* 1999).

The heavy contribution of the NDH-$1_{1/2}$ complexes to CEF makes these complexes a prime target for mutation and analysis of their proton pumping efficacy. If CEF drives proton

pumping, and the removal of NDH-$1_{1/2}$ complexes results in reduced CEF, then CEF-driven proton pumping should similarly be reduced by the deletion of these complexes. In fact, this was observed, as discussed further in Chapter IV. While this addresses some of the activity of the NDH-$1_{1/2}$ complexes, it does not say much about the activity of their cousins: the CO_2 hydrating NDH-$1_{3/4}$ complexes.

Cyanobacterial NDH-1 complexes and the CO_2 concentrating mechanism

The unique copies of the NdhD and F ($NdhD_{3/4}$/$NdhF_{3/4}$) proteins along with their counterparts CupA and CupB allow for cyanobacterial NDH-1 complexes to have a function unique to the phylum: CO_2 hydration (Shibata *et al.* 2001, Maeda 2002). There are two CO_2 hydration sub-complexes that perform this action, and they are distinguished by 2 general factors: their affinity/v_{max}, and their regulation. The constitutive complex, NDH-1_4, has low affinity and high v_{max}, while the low C_i inducible NDH-1_3 complex has high affinity and low v_{max} (Shibata *et al.* 2001, Maeda 2002, Artier *et al.* 2018). The components of each complex colocalize in to the thylakoid (Zhang *et al.* 2004), and the genetic components of the NDH-1_3 complex, *ndhF3/ndhD3/cupA/S*, are found in an operon and are transcriptionally repressed by the LysR-type regulator NdhR in C_i replete conditions (Wang *et al.* 2004). The components of the NDH-1_4 complex, however, are somewhat more dispersed in the genome. The genes *ndhF4* and *ndhD4* are located together and are expressed as an operon, but *cupB* is located elsewhere. In both complexes, all the components are required for their CO_2 hydration action (Ohkawa *et al.* 2000, Shibata *et al.* 2001), implying a functional relationship in their association.

Not only have these complexes shown that they perform CO_2 hydration, but they also participate in CEF, returning electrons to the PQ pool, though at a much slower rate than occurs in the NDH-$1_{1/2}$ complexes (Bernat *et al.* 2011). This electron transport activity is hypothesized to be coupled to proton pumping not only in the respiratory-like complexes, but the CO_2 hydration complexes as well since there is such high homology between the membrane subunits of the

complexes. Since CO_2 hydration is a carbonic anhydrase like activity, it was investigated whether the Cup proteins were related to known carbonic anhydrases (Shibata *et al.* 2001). Alas, it was shown that they do not share an evolutionary history with known carbonic anhydrases, making the hypothesis of the mechanism more difficult. Recently, the CupA/S proteins' structures were solved with Cryo-EM along with the rest of the NDH-$1_{3/4}$ complex, and the active site of CA activity was seen to be quite different from the traditionally studied CAs, possessing an Arg residue near the Zn^{+2} binding site. While the mechanism of the Cup proteins remains a mystery for now, this structure will help develop point mutation targets for the exploration of this unique activity. The Cup proteins share sensitivity to the same inhibitors as CAs, and they also catalyze the same reaction. Because of these shared traits, the general reaction model of known carbonic anhydrases can be used to hypothesize the mechanism of Cup, and when doing that the rate limiting removal of a proton to regenerate the enzyme reaction becomes interesting to the idea of CO_2 hydration coupled to electron coupled proton pumping The hydration of CO_2 is thought to occur as a nucleophilic attack of the Zn-OH^- on CO_2, occurring in a two-step ping-pong mechanism (Baird *et al.* 1997). The binding of CO_2 in the hydrophobic region near the Zn promotes nucleophilic attack by Zn-OH^- forming HCO_3^-, which is later displaced by the random diffusion of water to the active site. The transfer of a proton from the bound water at the Zn to an acceptor in the bulk solvent is the rate limiting step, and is required to regenerate the hydroxide needed for attack of the next CO_2 molecule (Baird *et al.* 1997, Boone *et al.* 2014). Since this step is rate limiting and vital to the priming of CA after the catalyzed reaction, it is important that there is a proton acceptor outside the CA to help drive the reaction toward CO_2 hydration. The removal of the proton from the bound water occurs on the order of 10^6 s^{-1} (Boone *et al.* 2014). Because the removal of the proton from the bound water is so important to the cycle of the enzyme, and CupA/B require $NdhD_{3/4}/F_{3/4}$ to function, it is reasonable to hypothesize that the NDH-$1_{3/4}$ complexes utilize their proton pumping activity to pull the CA reaction of the Cup proteins toward CO_2 hydration by removing the Zn-bound water's proton, allowing formation of

$Zn\text{-}OH^-$. While the mechanism will not be explored here, it will be demonstrated by this work that the NDH-$1_{3/4}$ complexes are involved in proton pumping to at least some degree.

2.4 Questions and goals

The cyanobacterial NDH-1 complexes are vital for the maintenance of the cell's energetics, and function not only to balance the ATP/NADPH ratio, but to help ensure a high concentration of C_i within the cell for carbon fixation. While it has been assumed because of their homology to the proton pumping Complex I, the connection between their known electron transport activity to proton pumping has been little explored. The variety of NDH-1 complexes in cyanobacteria allow for several questions to be asked about their activities: Does CEF power proton pumping through NDH-1? Do each of them contribute to PMF formation? Is the contribution of the respiratory-like complexes to PMF greater than the CO_2 hydration complexes? How is Fd_{red} produced to power NDH-1 proton pumping?

The hypotheses here are that CEF drives proton pumping; respiratory NDH-$1_{1/2}$ complexes are the primary drivers of CEF proton pumping; that CEF is unable to fully compensate for the loss of LEF; that NDH-1 complexes, powered by Fd_{red} produced by FNR_S, is an important part of acclimation to fluctuating light conditions; that FNR_L is able to power this, but requires longer illumination periods to do so. The aims of this study were:

- Develop an Acridine Orange based fluorescence assay to measure the establishment and dissipation of PMF generated by photosynthetic activity.
- Utilizing mutants defective in NDH-1 complex activity along with inhibitors to observe the contributions of the NDH-1 complexes to PMF.
- Utilize mutants defective in FNR_S or FNR_L to observe the impacts the different isoforms have on the PQ and NADPH pools while also observing their impacts on proton pumping during fluctuating light conditions.

CHAPTER III

METHODOLOGY

In general, results reported were obtained with three biological replicates, with technical replicates noted. Standard Deviation (SD) was calculated for the necessary measurements, and is reported with the tables. Graphs plotted and best fit lines calculated using Kaleidagraph software (Synergy).

3.1 Culture and growth conditions

For general culture maintenance, cells were struck on to standard BG-11 medium (Allen 1968), pH8 supplemented with 20mM HEPES-NaOH and 1.5% agar. The Wild Type (WT) was maintained without antibiotics at air-level CO_2, 30ºC, with ~50 µM photons/m^2/s provided by Cool White Fluorescent lamps. The deletion mutants were maintained with appropriate antibiotics. Antibiotics were utilized at the following concentrations: Spectinomycin (Sp) 25 µg/mL; Kanamycin (Km) 25 µg/mL; Gentamycin (Gm) 7 µg/mL (agar plates) or 1 µg/mL (liquid cultures). Deletion mutants were grown under the same external conditions as the WT except for the M55 mutant, which required growth in a chamber supplemented with 5% CO_2. For growth in shaking flasks, cells were grown in BG-11 pH8 supplemented with 20mM HEPES-NaOH at 30ºC with ~50 µM photons/m^2/s provided by Cool White Fluorescent lamps. For mutants, appropriate antibiotics were provided, and M55 was bubbled with 5% CO_2 by passing

water bubbled 5% CO_2 through a sterile 0.2 µm filter (Whatman polydisc TF filter, GE Healthcare) and through a sterile tube to bubble the culture as it was shaken. Liquid cultures were grown to OD_{750} ~0.7-1.0 for physiological measurements. For plates, a clear plastic box with a sealing door and shelving was used, and the CO_2 gassing system hooked up to a port on the side of the box. Similar light intensities were achieved in the CO_2 box.

Absorbance spectra and optical densities were performed with a UV-Vis Scanning Spectrophotometer (UV-2101PC, Shimadzu, Japan).

3.2 Strains and molecular constructs

Details for the construction of strains for each study are detailed in their chapter's methods section. In general, PCR reactions were performed with the Q5 High Fidelity 2x master mix (NEB) following manufacturer instructions. The Gibson Assembly technique (Gibson *et al.* 2009) utilizing a commercially available kit (NEB). *Escherichia coli* (*E. coli*) DH5α (NEB) cells were used for general plasmid maintenance and for receiving constructed plasmids. Plasmids were isolated from *E. coli* with the E.Z.N.A. ® Plasmid Mini/Midi kits (Omega, Bio-tec). Restriction enzymes employed were used according to their manufacturer specifications (NEB). Molecular constructions were confirmed by PCR.

The cyanobacterium *Synechocystis* sp. PCC 6803 (here *Synechocystis*, Genbank GCA_000009725.1) was used as the wild-type (WT) organism in the physiological experiments as well as the background strain for mutant construction. To transform *Synechocystis*, the basic protocol from Eaton-Rye 2011 (Eaton-Rye 2011) was used, with some slight modifications. WT or mutant cells were grown from colonies in 100mL cultures in 250mL flasks with their appropriate antibiotics and gassing to an OD_{750} of greater than 0.2 but less than 0.5. The cells were then pelleted at 4000xg for 10 minutes and resuspended in 1-2mL of sterile BG-11 media. The OD_{750} of the resuspension was measured, and the proper dilution calculated to make transformation reactions of 0.5mL with an OD_{750} of 2.5. The cells were then added to appropriate

aliquots of BG-11, along with 2-10µg of plasmid DNA in 2-10µL and incubated at 30ºC in ~50 µmol m^{-2} s^{-1} light for 3 hours, shaken gently, and incubated for 3 more hours. At the end of this period, the 0.2 µm Whatman filters were placed onto BG-11 containing either no antibiotic (in the case of the WT), and appropriate antibiotic (for mutants), and 200µL of cells plated on each plate. The plates were then incubated overnight in ~50 µmol m^{-2} s^{-1} of light with CO_2 gassing in the case of mutants that need it. After ~18h, the filters were transferred to "low antibiotic" plates (5µg/mL Km and Sp) and incubated in the light with CO_2 gassing until colonies arose after ~10 days. Colonies were then picked and struck out onto "moderate antibiotic" plates (12µg/mL Km and Sp) and grown for ~7 days. Colonies were then picked again and struck out on full antibiotic plates (values listed above) for two more weeks. Colony PCR was then performed to check whether deletion or integration had occurred completely, or if the strain was not yet segregated. Segregation was confirmed by extracting the genomic DNA using the Quick-DNA™ Fungal/Bacterial Kit (Zymo Research) from 100mL of shaking culture and utilizing PCR to check the deletion of the gene. DNA was quantified using both a NanoDrop 1000 (Thermo) and comparing band intensity to the 1Kb Plus DNA Ladder (Invitrogen) on a 1% agarose gel.

3.3 Cell sample preparation

100mL cultures between OD_{750} ~0.7-1.0 were collected by centrifugation at 6000xg for 10min at RT for use in both acridine orange and chlorophyll fluorescence assays. Cells were then washed in 50 mM tricine with either 25 mM NaCl or 25 mM KCl (TCN and TCK buffer respectively) depending on the experiment. Cells were centrifuged again and resuspended in TCN/TCK buffer and their chlorophyll (Chl) concentration checked by spectrophotometry utilizing the extinction coefficient 12.95 (Ritchie 2006). Cells were diluted to 5.9 µg Chl/mL in 20-25 mL in a small Erlenmeyer flask. For samples preparing for Acridine Orange (AO) fluorescence measurement, 5µM AO was added to the sample and it was allowed to incubate gently shaking in the dark for 20min to allow uptake of the dye (Teuber *et al.* 2001). For samples

preparing for chlorophyll fluorescence measurement, they were simply allowed to shake in the dark gently for 5min before measurement.

3.4 Chl and NADPH fluorescence

Changes in PSII activity and the redox state of the PQ pool were assessed by variations in Chl fluorescence upon illumination. Assays were performed as previously described (Holland *et al.* 2016) with the variation that assays were carried out with cells suspended in TCN or TCK buffer. Cells were diluted to 5µg Chl/mL in the measuring cuvette by the addition of extra TCN or TCK buffer. The DualPAM-100 (Walz, Germany) was used to measure the fluorescence of Chl a and NADPH over time courses. The pulse amplitude modulated (PAM) fluorometer included an attached emitter-detection-cuvette assembly (ED-101US/MS) with a DUAL-DR mode. The fluorometer contains a single red (620nm) LED measuring light as well as an LED array (COB, 24 reds, 635nm) for actinic light (AL) as well as saturating pulses (SP) and multiple turnover flashes (MT), though only MTs were used in these experiments. The 9-AA/NADPH module was attached to the fluorometer, allowing for the detection of NADPH fluorescence as well as the fluorescence of some pH sensitive dyes such as 9-aminoacridine or acridine orange. The DUAL-ENADPH (emitter) with a 365nm measuring light (ML) was set up at a 90^{o} angle from the DUAL-DNADPH (detector) with a blue-sensitive photomultiplier (420-550nm) and an ML intensity of 20. The Chl fluorescence emitter had its ML set to an intensity of 15, and it was located at a 90^{o} angle from its detector. For all measurements, cells were added in the dark. Any inhibitors were added in the dark and, regardless of inhibitor addition, the sample stirred by small stir bar for 4min with a 1min rest after. Dark adapted cells were then measured, with either a 60sec or 10sec dark period for either the 5min illumination traces or the 15sec illumination traces, followed by illumination with AL for the specified time, and another dark period for 200 or 40 seconds respectively. MT flashes (20,000 µmol m^{-2} s^{-1}) were utilized on the 5min traces before, during, and after illumination with AL (at 15, 300, and 540 sec), and utilized toward the end of

AL illumination for the 15sec traces (at 22sec) for measuring the proportion of available PSII (q_p) as determined by the equation: $q_p = (F'_m - F_s)/(F'_m - F_0)$ outlined in (Campbell *et al.* 1998). The precise programs for each measurement were designed in the DualPAM-100 software on trigger mode. Points were collected at a rate of one per millisecond, and the trace smoothed with a running average of 100 points. 200µM KCN was added where indicated.

3.5 Acridine orange fluorescence in the DUAL PAM-100

The DualPAM-100 unit as described above was utilized to measure AO fluorescence in the dark and over long illuminations. The parameters above applied to these measurements, with the exception that a 534/20nm bandpass filter (Edmund Optics) was included before the DUAL-DNADPH module's photomultiplier, allowing for the finer detection of the wavelengths associated with AO fluorescence. The DUAL-ENADPH module is able to excite AO fluorescence, but to a minimal degree (Schreiber *et al.* 2009). AO fluorescence was measured stirring in the dark using the same ML intensities described above for NADPH fluorescence detection to observe the effect of inhibitor addition on dark AO fluorescence. Following the dark measurement, a new measurement was started with the 5min illumination parameters outlined above.

3.6 Acridine orange fluorescence in the JTS-100

The JTS-100 pump-probe spectrometer (Biologic) was utilized to measure quick changes in AO fluorescence upon illumination with actinic light. A 534/20nm bandpass filter (Edmund Optics) was placed between the sample and detector, and the BG39 filter (Biologic) was utilized in the JTS-100 the measuring beam and the reference detector. A 450nm lamp was utilized for the excitation of AO, allowing greater excitation of the dye than in the DualPAM-100. The user interface was utilized to write a program that would measure one point per second in the dark, and one per 100ms in the light for either 15 or 120 seconds utilizing the following programs (D, detection pulse; G, actinic light on; H actinic light off):

20(D1s)TG[600uE]150(98msH20usD10usG[600uE])H60(D1s)

20(D1s)TG[600uE]1200(98msH20usD10usG[600uE)H120(D1s)

The light intensity was changed as needed for light intensity dependence experiments, but 600 µmol m^{-2} s^{-1} was generally used as the AL light intensity for rate determination.

Cells prepared in TCN or TCK buffer were diluted to 5 µg Chl/mL with either 1 M KCl to 150 mM (TCN buffer) or with excess TCK buffer. Inhibitors were added in the cuvette in the dark and were incubated without measuring for 5min. Following this, the sample was illuminated for 15 sec with 630 nm actinic light intensities that varied from 50 to 600 µmol m^{-2} s^{-1} depending on the particular experiment noted. In Chapter IV, utilizing TCN buffer, samples incubated with the background inhibitors were measured three times with a 5min dark incubation between each measurement as minimal drift was seen on repeated measurements. This measurement was performed at differing light intensities for the light intensity dependence measurements and was performed at 600 µmol m^{-2} s^{-1} for other measurements. DCMU was added to the samples after the measurements with the background inhibitors, incubated for 5min, and measured again. A fresh sample with DCMU and CCCP was prepared for the final measurements. For the data collected for Chapter V, cells were prepared in TCK buffer to avoid contributions of Na^+/HCO_3^- and Na^+/H^+ pumps. Dark adapted samples were refreshed after each measurement to avoid light-induced drift upon repetition of measurement under these conditions with the mutants utilized. Each sample was given the inhibitors upon refreshing and given 5min in the dark before measurement, and three technical replicates collected for each condition in this manner. To light adapt samples, dark-adapted cells treated with inhibitors were illuminated with 600 µmol m^{-2} s^{-1} actinic light for 2 minutes, followed by darkness for 5 minutes. Samples were then illuminated for 15sec with 600 µmol m^{-2} s^{-1} actinic light. This was repeated on the same sample three times for each condition. Averages of AO data collected by the JTS-100 were plotted in Kaleidagraph, and

the rates of quenching of each biological replicate were calculated by plotting a fit line through the linear portion of data collected after 4 seconds of illumination to avoid fast changes that occur immediately after illumination and to observe proton pumping. The rates provided by the biological or technical replicates were utilized for statistical analysis.

CHAPTER IV

ELECTRON FLOW THROUGH NDH-1 COMPLEXES IS THE MAJOR DRIVER OF CYCLIC ELECTRON FLOW-DEPENDENT PROTON PUMPING IN CYANOBACTERIA

4.1.1 Abstract

Cyclic electron flow (CEF) around Photosystem I is vital to balancing the photosynthetic energy budget of cyanobacteria and other photosynthetic organisms. The coupling of CEF to proton pumping has long been hypothesized to occur, providing proton motive force (PMF) for the synthesis of ATP with no net cost to [NADPH]. This is thought to occur largely through the activity of NDH-1 complexes, of which cyanobacteria have four with different activities. While a much work has been done to understand the steady-state PMF in both the light and dark, and fluorescent probes have been developed to observe these fluxes *in vivo*, little has been done to understand the kinetics of these fluxes, particularly with regard to NDH-1 complexes. To monitor the kinetics of proton pumping in *Synechocystis* sp. PCC 6803, the pH sensitive dye Acridine Orange was used alongside a suite of inhibitors in order to observe light-dependent proton pumping. The assay was demonstrated to measure photosynthetically driven proton pumping and used to measure the rates of proton pumping unimpeded by dark ΔpH. Here, the cyanobacterial NDH-1 complexes are shown to pump a sizable portion of proton flux when CEF-driven and LEF-driven proton pumping rates are observed and compared in mutants lacking some or all NDH-1 complexes. It is also demonstrated that PSII and LEF are responsible for the bulk of light-induced proton pumping, though CEF and NDH-1 are capable of generating ~40% of the

proton pumping rate when LEF is inhibited

4.1.2 Introduction

NADH dehydrogenase complex I, or complex I, is a widely distributed bioenergetic complex, with homologs seen in archaea, bacteria, and eukaryotes (Chadwick *et al.* 2018). The core structure of these complexes and their subunit composition have been largely conserved throughout these phyletic kingdoms, with the bacterial complexes possessing the fewest subunits, and eukaryotes possessing accessory subunits, but retaining a core that is conserved across the domains of life (Sazanov 2007, Sazanov 2015, Laughlin *et al.* 2019, Schuller *et al.* 2019, Schuller *et al.* 2020, Zhang *et al.* 2020). These complexes are vital parts of a diverse variety of electron transport chains and have been shown to couple proton pumping to electron transport from ferredoxin (Fd) or NAD(P)H to a quinone to increase the proton motive force (PMF) for ATP production in heterotrophic bacteria as well as mitochondria and chloroplasts (Matsushita *et al.* 1987, Galkin *et al.* 1999, Galkin *et al.* 2006, Sazanov 2007, Strand *et al.* 2016, Jones *et al.* 2017, Strand *et al.* 2017). These complexes have also been shown to act in reverse to dissipate PMF while producing low potential reductant (e.g. NAD(P)H), though this has only been observed under special inhibitor conditions with the addition of succinate in mitochondria and submitochondrial particles (Kotlyar *et al.* 1990) or in chemoautotrophic bacteria and archaea with unique energy budgets such as *Nitrospira* or *Thaumarchaea* respectively (Aleem 1966, Lucker *et al.* 2010, Simon *et al.* 2013, Konneke *et al.* 2014, Chadwick *et al.* 2018).

Cyanobacteria also possess complex I, however they are unique in possessing four functional versions of complex I, and they are termed NDH-1 for NADPH Dehydrogenase 1 complex, though they have recently been shown to utilize Fd for their reductant over NADPH (He *et al.* 2015, Zhang *et al.* 2020). Recently, the structure of two cyanobacterial NDH-1 complexes have been solved (Laughlin *et al.* 2019, Schuller *et al.* 2019, Schuller *et al.* 2020, Zhang *et al.* 2020), covering representatives of the major functions of these complexes: Cyclic

electron flow (CEF), respiratory electron flow, and CO_2 uptake. A summary of the components of photosynthetic electron flow, their actions on proton pumping, and inhibitors utilized here are shown in **Fig. 3A**. These NDH-1 complexes share a common "core" subcomplex, NDH-1M, with modular attachments that confer a specific function, such as CO_2 uptake (Zhang *et al.* 2004, Laughlin *et al.* 2019, Schuller *et al.* 2019, Schuller *et al.* 2020) (**Fig. 3B**). The core subcomplex contains the redox active subunits that participate in electron transfer from Fd_{red} to the plastoquinone (PQ) pool, and it pairs with specific NdhD and NdhF proteins in the membrane arm to assemble the functional complexes (Laughlin *et al.* 2019, Schuller *et al.* 2019, Schuller *et al.* 2020) (**Fig. 3B**). These assembled complexes participate in CEF around Photosystem I (PSI) by accepting electrons from Fd_{red} produced through photosynthetic electron flow and passing them into the PQ pool (Battchikova *et al.* 2011, Bernat *et al.* 2011) while presumably pumping protons to contribute to PMF, though proton pumping by the cyanobacterial NDH-1 complexes had not been experimentally demonstrated until this work. The NDH-1 complexes contribute majorly to CEF in cyanobacteria, but it has also been shown that another major route is through succinate dehydrogenase (SDH) (Cooley *et al.* 2001), though its CEF activity is able to be limited based on the illumination, inhibitor additions, and mutations in the strains measured (Ryu *et al.* 2003). The PQ pool electrons are then passed through the photosynthetic electron transport chain, including cytochrome b_6f Q-cycles, to pass them back to PSI and inevitably to $Fd_{ox}/NADP^+$, thereby keeping the redox state of [Fd_{red}/NADPH] relatively constant while, it is hypothesized, contributing to PMF to drive [ATP] synthesis. Quantitative information on the thylakoid PMF in cyanobacteria has been obtained using electron spin resonance probes (Belkin *et al.* 1987) and by measuring the distribution of radioactive pH-sensitive probes (Falkner *et al.* 1976, Peschek *et al.* 1985). These have provided a relatively consistent picture with the cyanobacterial cytoplasm at approximately pH 7.0 and a lumen pH of about 5.0-5.5 in the dark, supported by respiration. Photosynthetic electron transport was observed to increase the pH in the cytoplasm and decrease the pH in the lumen by approximately 0.5 pH units each, thereby increasing the ΔpH by about

one unit (Belkin *et al.* 1987). This would produce a lower lumen pH than the more moderate values estimated for chloroplast thylakoids (Kramer *et al.* 1999), nevertheless is in line with responses seen in plants and algae. Importantly, the electrical and proton concentration components of the PMF, $\Delta\psi$ and ΔpH respectively, were shown to be interconvertible using classical techniques employing ionophores and protonophores (Peschek *et al.* 1985). The steady-state pH of the lumen in the light appears to be regulated by various mechanisms allowing for photosynthetic electron transport while preventing over-acidification and allowing for photosynthesis to continue with minimal ROS production (reviewed in (Tikhonov 2013, Morales *et al.* 2018)).

The four cyanobacterial NDH-1 complexes are termed here based on the identity of the NdhD protein they possess, as each complex has an unique NdhD protein associated with it. Of the four complexes in cyanobacteria, two of them, the NDH-1_1 and NDH-1_2 complexes, are primarily active in CEF and respiratory electron flow (Cooley *et al.* 2001, Bernat *et al.* 2011). While the NDH-$1_{1/2}$ complexes share a common NdhF protein termed NdhF1, the physiological differences between the NDH-$1_{1/2}$ complexes are largely unknown. It has been shown to that the deletion of *ndhF1* severely inhibits CEF, and that NDH-$1_{1/2}$ complexes are responsible for the bulk of NDH-1 driven electron flow (Bernat *et al.* 2011). These complexes have also been shown to form super complexes with PSI in cyanobacteria as a means of protecting against stresses such as high light or salt or in the absence of PSII activity after treatment with DCMU, a PSII inhibitor (Gao *et al.* 2016, Zhao *et al.* 2017). It was shown that the NDH-1-PSI supercomplex stabilizes PSI (Zhao *et al.* 2017), with the function of the supercomplex likely being to consume electrons for CEF as quickly as possible, limiting the space needed for Fd_{red} to diffuse (Gao *et al.* 2016). This accelerated consumption of electrons is thought to act as an antioxidant mechanism in this way, especially when stresses such as high light leads to increased Fd reduction. Recently, it was shown that exposure to high light caused heavy accumulation of the NDH-$1_{3/4}$ complexes,

indicating their CO_2 uptake activity in addition to their CEF activity may play a role in the NDH-1 antioxidant mechanism (Zhang *et al.* 2020). The deletion of the NDH-$1_{1/2}$ complexes causes a hyper-oxidation of the PQ pool, locking the photosynthetic machinery in State 1 where the bulk of light harvesting is focused around PSII (Ogawa *et al.* 2013, Ogawa *et al.* 2015). Reduction of the PQ pool can trigger a "state transition" to State 2, where the bulk of light harvesting is focused around PSI. These state transitions are dependent upon the redox state of the PQ pool, and, when the photosynthetic electron transport chain is intact, there is normally a state transition upon the dark-light shift from State 2 to State 1 (Papageorgiou *et al.* 2007, Papageorgiou *et al.* 2011, Kana *et al.* 2012). This suggests that the NDH-$1_{1/2}$ complexes are important for mediating the reduction of the PQ pool both in the dark during respiration and in the light during photosynthesis. The tightly regulated response of cyanobacteria to these stresses highlights the importance of this mechanism for the protection and acceleration of PSI-CEF when needed, thereby providing electron transport pathways necessary for photosynthetic metabolism.

The other two complexes, NDH-1_3 and NDH-1_4, possess unique subunits that have carbonic anhydrase activity, termed $\underline{C}O_2$ $\underline{U}$ptake or "Cup" proteins, and they participate in the $\underline{C}O_2$ $\underline{C}$oncentrating $\underline{M}$echanism (CCM), which functions to increase the internal concentration of inorganic carbon (C_i) to 1000-fold the external concentration, hydrating CO_2 to HCO_3^-, thereby trapping it in the cytoplasm (Shibata *et al.* 2001, Price *et al.* 2002). These two complexes differ in their gene expression, affinity for CO_2, and flux of CO_2 hydration, with the NDH-1_3 complex being essential for growth in air (Artier *et al.* 2018). They contribute relatively little to CEF compared to their NDH-$1_{1/2}$ cousins, but do still participate (Bernat *et al.* 2011). These complexes require all of their unique components in order for CO_2 uptake to occur, and lacking them or a component of the core subcomplex, NdhB, results in an inability to grow in limiting concentrations of CO_2 (Zhang *et al.* 2004, Artier *et al.* 2018).

Evidence of proton pumping in cyanobacterial NDH-1 complexes and their physiological contributions to that activity will provide relevant data in terms of accounting for photosynthetic electron flow driven proton pumping, as well as provide insight into the mechanism of the unique cyanobacterial CO_2 trapping system of the NDH-$1_{3/4}$ complexes. While the e^- transport activity of NDH-1 complexes in general has been well probed (Mi *et al.* 1992, Mi *et al.* 2000, Cooley *et al.* 2001, Ryu *et al.* 2003, Battchikova *et al.* 2011, Bernat *et al.* 2011), many questions remain in understanding the coupling of this electron transport to their potential proton pumping activity. Do NDH-1 complexes pump protons? Is that activity light dependent? Given the multiplicity of forms of cyanobacterial NDH-1 complexes, which are responsible for the bulk of proton pumping activity? Does CEF couple to proton pumping? Here, a pH sensitive fluorescent dye called Acridine Orange (AO) that locates to both the cytoplasm and thylakoid lumen (Teuber *et al.* 2001) was utilized to observe the formation of ΔpH across the thylakoid membrane in strains deficient in NDH-1 activity. This was done alongside chlorophyll (Chl) fluorescence measurements for the comparison of proton pumping activity with photosynthetic electron transport activities. In this work, it is hypothesized that CEF drives proton pumping, respiratory-like NDH-$1_{1/2}$ complexes are responsible for the bulk of CEF driven proton pumping, and that CEF is incapable of reaching the rate of proton pumping reached by LEF.

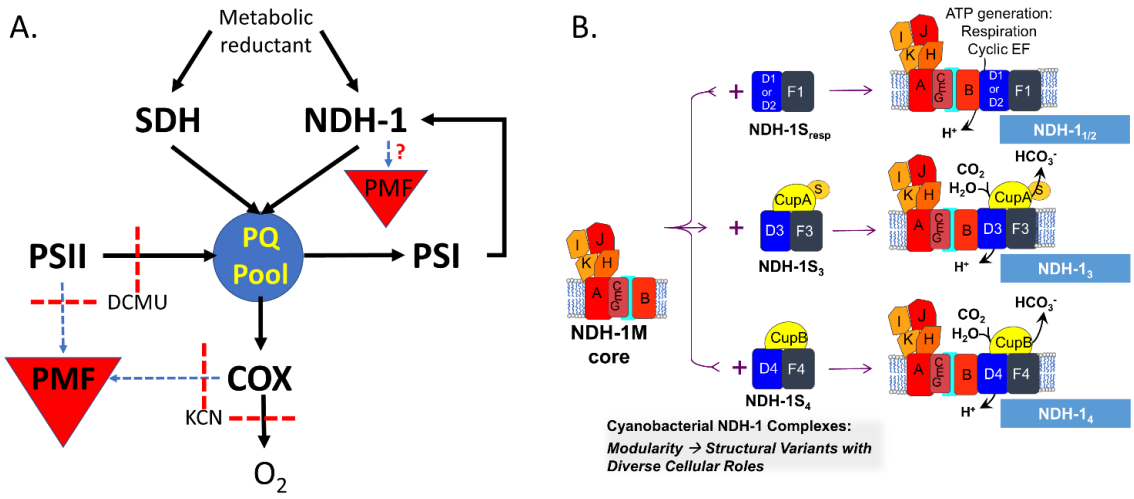

Figure 3. Photosynthetic electron flow and proton pumping in cyanobacteria. Panel A. The enzymatic components are shown, connected by arrows representing electron transfer. Blue dashed arrows indicate contribution to PMF, and red dashed lines represent a blocking of electron flow or proton pumping upon addition of an inhibitor. **Panel B**. The modularity of the cyanobacterial NDH-1 complexes. They share a common core (NDH-1M) containing NdhA,B,C,E,G,H,I,J,K, but differ in their distal membrane subunits, and are named based on the proteins they possess. The variable modules provide two major functions that are largely split between the NDH-$1_{1/2}$ and NDH-$1_{3/4}$ complexes, which are primarily involved in CEF/respiration and CO_2 uptake, respectively. The CEF/respiration complexes (NDH-S_{resp}) modules contain the NdhD1 (or NdhD2), NdhF1 proteins plus smaller polypeptides, whereas the CO_2 uptake modules contain either NdhD3/NdhF3/CupA/CupS for high affinity CO_2 uptake or NdhD4/NdhF4/CupB/ for low affinity CO_2 uptake.

4.2 Methods

4.2.1 Strains and molecular constructs

Strains of *Synechocystis* sp. PCC 6803 (hereafter, *Synechocystis*) were maintained on pH 8 BG-11 (Allen 1968) with 1.5% agar supplemented with 18 mM sodium thiosulfate and containing the appropriate antibiotics for each mutant (7 µg/mL Gentamycin (Gm) for Δ*ndhF1*, 50 µg/mL Kanamycin (Km) for M55), with WT maintained under ~70 µmol m^{-2} sec^{-1} light,

Δ*ndhF1* 70 µmol m^{-2} sec^{-1} light, and M55 50 µmol m^{-2} sec^{-1} light. Experimental material was obtained from 100 mL cultures grown in 250 mL Erlenmeyer flasks with rotary shaking (200 rpm) under ~100 µmol m^{-2} sec^{-1} Cool White fluorescent lighting (GE). Cultures were harvested upon reaching an OD_{750} 0.7-1.0. The M55 strain was grown under 5% CO_2 with an autoclaved gassing apparatus consisting of a 0.2 µm filter attached to tubing put through a foam cap, sterilized, used to replace the foam cap of the regular shaking BG-11 cultures, with a long enough tube to gently bubble the media with CO_2 while shaking.

The plasmid used to construct Δ*ndhF1*, pUCF1-Gm, was produced using Gibson assembly (Gibson *et al.* 2009) by amplifying ~500 bp upstream and downstream regions of the *ndhF1* gene from wild-type chromosomal DNA utilizing the primers shown in **Table S1**. The Gm antibiotic resistance cassette was amplified from *Synechocystis* HT-3 genomic DNA (Debus *et al.* 2001) with the primers also shown in **Table S1**. The primers above were designed with overlaps for Gibson Assembly according to manufacturer's specifications (NEB). The three PCR generated fragments were assembled in the presence of pUC18 digested with NdeI and PstI (NEB) by Gibson Assembly according to the manufacturer specifications to create pUCΔF1. M55 was provided to our group by professor Teruo Ogawa from Nagoya University in Nagoya, Japan.

4.2.2 Chlorophyll fluorescence

Cells were harvested by centrifugation, washed with 50mM Tricine pH 8 + 25 mM NaCl (TCN) and resuspended to 5.9 µg/mL Chl, measured by in a UV-Vis spectrophotometer (Shimadzu) (Ritchie 2006). Following this, each sample was diluted to 5 µg/mL Chl in the cuvette with the Tricine buffer. Measurements of Chl fluorescence yield were measured using the Dual PAM-100 (Walz) with the 9-AA/NADPH module. For 5-minute illumination period measurements, a nominal light intensity of 53 µmol m^{-2} sec^{-1} was utilized except in experiments measuring LEF saturation as a function of light intensity, or experiments observing fluorescence

in saturating light. Values for q_p were produced using the equation outlined in (Campbell *et al.* 1998) utilizing multiple turnover flashes (300 milliseconds, nominally 20,000 µmol m^{-2} sec^{-1}).

4.2.3 Acridine orange fluorescence quenching

Acridine orange (AO) has been used as a fluorescent dye for measuring proton pumping across a membrane in both whole cyanobacterial cells and membrane vesicles (Palmgren 1991, Teuber *et al.* 2001, Nakamaru-Ogiso *et al.* 2010, Checchetto *et al.* 2012). Cells were grown and washed with TCN buffer as above for Chl fluorescence. Samples were diluted to 5.9 µg/mL Chl had acridine orange added to 5 µM, and were incubated shaking gently in the dark for 20 minutes to allow acridine orange penetration into the cell (Teuber *et al.* 2001). Samples of the cells were then added to a cuvette, and 1 M KCl added to 150 mM to dilute the cells to 5 µg/mL and provide K^+ to exchange across the thylakoid when Valinomycin (Val) was added to 10 µM to dissipate $\Delta\psi$. DCCD was added to 500 µM to inhibit ATP synthase and prevent proton leakage. KCN was added to 200 µM to inhibit cytochrome oxidase (COX) and respiratory proton pumping as well as to maintain the photosynthetic electron transport chain in a State 2 like poise (Ogawa *et al.* 2013). Samples were then stirred for 5 minutes in the dark, and the fluorescence measured with the JTS-100 (Biologic) or Dual-PAM 100 (Walz). A 534/20 nm bandpass filter (Edmund Optics) was placed between the sample and the detector in both instruments. The 9-AA/NADPH attachment (Walz) was used on the Dual-PAM 100 to excite AO, however, the wavelength used does not allow for maximal excitation (Schreiber *et al.* 2009), unlike with the JTS-100.

The Dual-PAM 100 proved useful for measuring dark fluorescence and some larger scale changes in AO fluorescence, while the JTS-100 was primarily used to observe rates of proton pumping in response to illumination. Dual-PAM 100 data was generated by exporting the data averaging 100 points, resulting in one point per 100ms, with inhibitors (Val, DCCD, KCN) added in the dark. Upon reaching a steady-state, a new measurement was performed on the same sample with a 5 minute actinic illumination with multiple turnover flashes (parameters above) before,

during, and after illumination. The multiple turnover flashes were included for measurement of Chl fluorescence parameters at the same time (**Fig. S1**) and were not greatly taken into account for the AO measurements.

For the AO fluorescence data recorded on the JTS-100, points were collected once per second in the dark and once per 100ms in the light, with light intensity varying by experiment. Each sample was recorded after a 5 minute dark incubation after the addition of inhibitors with 5 minutes of additional stirring in the dark between each technical replicate. The rates and depths of quenching were relatively unaffected by repeated measurements or a slight drift in these conditions (discussed below). The inhibitors Val (10 μM), KCN (200 μM), and DCCD (500 μM) were added to samples measured in the JTS-100 to ensure the measurement of maximal rates, as discussed below. Accordingly, these formed the standard set of inhibitors for most experiments used to observe proton pumping here. Utilizing the same conditions in the instrument, DCMU was added in some case to the sample to 10μM and measurements recorded after a 5 minute incubation period in the dark with stirring, and measurements recorded as described above. A fresh sample was then prepared with the standard inhibitors along with the addition of 10 μM DCMU and 250 μM CCCP, incubated for 5 minutes with stirring, and measurements recorded as described above. To obtain sufficient signal/noise ratios, 3 to 6 technical replicates were recorded per condition for each of 3 biological replicates. AO data collected on the JTS-100 was provided by averaging the data of all 3 biological replicates for each condition with a line plotted through the data after about 4 seconds of illumination and extending for 4-10 seconds, depending on the shape of the trace and the ability to plot a line through the linear portion of quenching. The traces were arbitrarily zeroed to the beginning of the linear portion of quenching. Rates were determined by plotting the line through each biological replicate and using those to determine the average rate and standard deviation. Significance in text calculated with a two-tailed t-test assuming unequal variance.

4.3 Results

4.3.1 Proton pumping activity in whole *Synechocystis* sp. PCC 6803 cells

In cyanobacteria, the pH sensitive dye AO has been shown to report the changes in pH across the thylakoid membrane by fluorescence changes (Teuber *et al.* 2001, Checchetto *et al.* 2012). The cyanobacterial thylakoid membrane presents a unique challenge because both photosynthesis and respiration occur in the same membrane and utilize the common electron carriers (Vermaas 2001, Mullineaux 2014). Therefore, a suite of inhibitors was used to isolate the contributions of specific complexes, including NDH-1 complexes, to ΔpH. Firstly, a significant fraction of PMF is stored as a K^+ ion gradient, contributing to the electrical component, ΔΨ, of PMF (Peschek *et al.* 1985, Belkin *et al.* 1987, Checchetto *et al.* 2012), and there is a considerable efflux of K^+ ions from the thylakoid lumen upon illumination to create a cation deficit in the thylakoid lumen to drive the accumulation of H^+ (Checchetto *et al.* 2013). The ΔΨ component can cause variations in proton pumping measurements using AO (Checchetto *et al.* 2012), therefore, Val was used to dissipate the K^+ gradients across the membranes with the addition of 150 mM KCl to remove the ΔΨ component of PMF from measurements. ATP synthase was inhibited with 500 µM DCCD to prevent the flow of protons through the membrane from affecting the measurements. Finally, in some cases, 200 µM KCN was added to block COX, thereby pushing dark-adapted cells into a State 2-like poise, where more light harvesting occurs at PSI than in State 1, since the NDH-1 mutants used have the potential to be locked in State 1 (Ogawa *et al.* 2013). The addition of KCN also allows for the isolation of the photosynthetic components of ΔpH formation as there is a considerable the ΔpH in the dark when COX is active (Peschek *et al.* 1985) (**Fig. 4A-C**).

The presence of the dark ΔpH provides PMF which must be overcome in order for photosynthetically driven proton pumping to occur. The electrochemical back-pressure of positive charges within the thylakoid lumen ultimately has an effect on the ability of light induced

proton pumping (Checchetto *et al.* 2012), so dissipating these pressures can allow observation of photosynthetically driven proton pumping unimpeded by the effects of that back-pressure. The contribution of respiratory activity in dark-adapted cells to their trans-thylakoid PMF can be observed as an increase in AO fluorescence (loss of quenching), as the dark ΔpH dissipates upon the addition of KCN as detected using a PAM fluorometer due to the loss of COX activity (**Fig. 4A**). This dissipation was enhanced when Val and DCCD are included with KCN. The addition of any of these alone did not result in as strong a dissipation as when all three are included (not shown), indicating the combination of these additions was necessary for the disruption of dark ΔpHf. These results are indicative of the dissipation of dark PMF associated with respiration. This was further shown in **Fig. 4B**, where AO fluorescence arbitrarily zeroed to the fluorescence before illumination was seen in the absence and presence of KCN in addition to the background inhibitors. In the presence of KCN, quenching occurs to ~1.5x the value seen in its absence and was considerably faster (**Fig. 4C**). This suggests that respiration in the dark indeed exerts some amount of electrochemical back-pressure that impedes the rate ΔpH formation upon illumination. Slower kinetic processes are also apparently occurring simultaneously. Superimposed upon the rapid light-induced AO quenching, we observe a more gradual increase in AO fluorescence (**Fig. 4B**). This can be attributed to the previously observed alkalinization of the cytoplasm occurring in the minutes time frame, potentially due to CBB-cycle activity (Falkner *et al.* 1976, Peschek *et al.* 1985, Belkin *et al.* 1987, Wang *et al.* 2002).

Comparison of Chl fluorescence induction kinetics with and without KCN revealed a reduction of the PQ pool in the dark, and some alterations in the rates of secondary transitions, likely involving S-state transitions and the activation of the CBB cycle, but otherwise photosynthetic electron transport was unaffected, save for the dramatic rise in both F_0 and post-illumination fluorescence upon addition of KCN, likely due to the lack of COX as an electron

sink exacerbating the actinic effect of the PAM measuring light and thwarting the consumption of photosynthetically-produced reductant during the light-to-dark transition (**Fig. S1**).

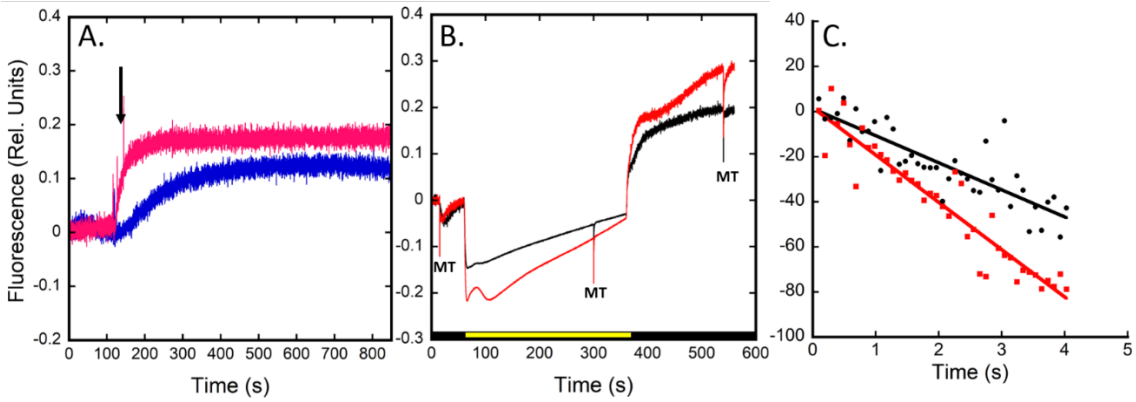

Figure 4. Respiratory electron flow contributes to ΔpH in the dark. Panel A: Acridine fluorescence in the Walz DUAL PAM-100 instrument. Cells were dark adapted with acridine orange (5 µM) in TCN buffer with KCl (150 mM). Either only KCN (200 µM) (blue trace) or KCN plus Val (10 µM) and DCCD (500 µM) (pink trace) were added (arrow). **Panel B:** Acridine fluorescence in the DUAL PAM-100. Cells were incubated in the dark for 5 min. with background inhibitors in the absence (black) or presence (red) of KCN and AO fluorescence was collected over the course of a 5 min. illumination period, including multiple turnover flashes before, during, and after illumination. The MT flashes were employed for evaluating characteristics of the simultaneously measured Chl fluorescence (e.g. Fig. S1). Data was acquired using same instrument settings and scale, and the traces zeroed to F_0 to account for small drifts in baseline and sample differences. **Panel C:** Acridine fluorescence in the BioLogic JTS-100 instrument. Cells were dark adapted with acridine orange (5µM) for 20 min, then a sample prepared with KCl (150 mM) and either Val (10 µM) and DCCD (500 µM) (black circles), or with the inclusion of KCN (200 µM) (red squares) and the sample stirred in the dark for 5 min. Traces are typical of three replicates.

4.3.2 Proton pumping activity dominated by photosynthetic linear electron flow

To evaluate the activity of different photosynthetic membrane complexes with respect to proton pumping, initial rates of light-induced AO fluorescence quenching in the presence of the three background inhibitors (KCN, Val, DCCD), were tested in a shorter experiment. Steady state AO fluorescence in the dark, F_0, was recorded for 20 sec, followed by quenching due to the application of 600 μmol m^{-2} sec^{-1} actinic illumination for 15 seconds, followed by darkness to observe the recovery phase (**Fig. 5**). The quenching of fluorescence upon illumination indicates the acidification of the thylakoid lumen due to the activity of photosynthetic electron flow upon a dark-to-light transition. The rate of this quenching during the linear phase after illumination (~4-8 or 4-14 sec depending on the strain and additional inhibitors added) was termed j_{H^+}. The quenching occurred from F_0 to an extent, termed $F_{\Delta pH}$ (**Fig. 5**). Cessation of illumination led to an increase in AO fluorescence indicating a collapse of ΔpH across the thylakoid (Teuber *et al.* 2001). This rise appears to be biphasic, occurring first rapidly and then slowly. There was additionally some upward drift in fluorescence seen after the cessation of illumination. As this was not seen in dark adapted cells (**Fig. 4A**), it is hypothesized that this may be due to the processing of reducing equivalents produced during illumination. A considerable gradient was still formed upon the addition of DCMU and inhibition of PSII, albeit to smaller extent in the time measured (**Fig. 5**). The inclusion of the uncoupler CCCP with DCMU causes a cessation of light-induced proton pumping, giving a baseline against which to compare the other data. DCMU was always added with CCCP, because unless PSII was inhibited the solution slowly acidifies due to water oxidation activity (not shown). These data indicate that LEF, including the strong contribution of protons released from water oxidation, is the major contributor to the proton gradient formation during the dark-to-light transition, although the contribution of CEF is very substantial.

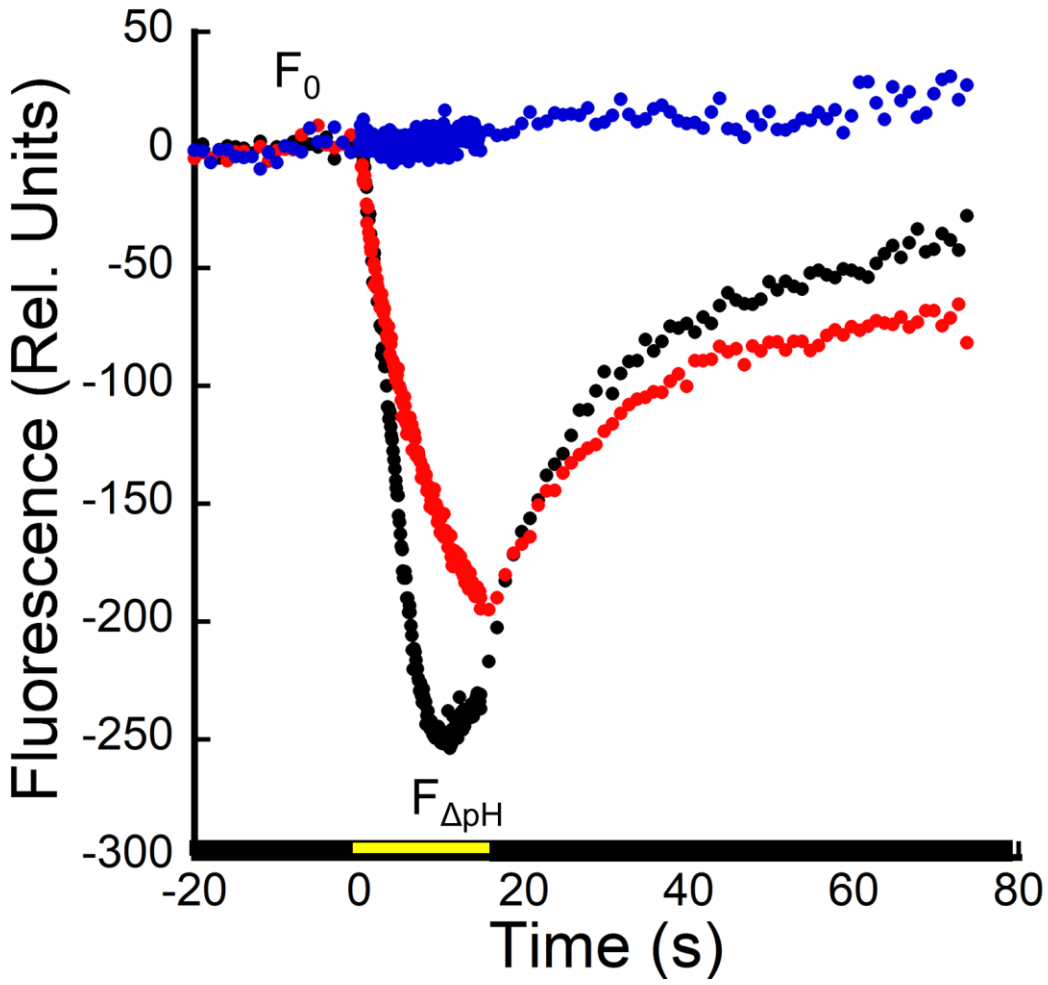

Figure 5. Light-induced acidification of the thylakoid lumen. Acridine orange fluorescence of dark-adapted WT cells in the JTS-100 representing the formation and dissipation of ΔpH across the thylakoid lumen upon the activation and cessation of actinic illumination. Cells were dark adapted with acridine orange (5 µM) for 20 min, then a sample prepared with KCl (150 mM) plus Val (10 µM), DCCD (500 µM), and KCN (200 µM) and stirred in the dark for 5 min. Actinic illumination (630 nm, 600 µE) was applied for 15 seconds. Black symbols, standard additions; red symbols, standard additions plus DCMU, blue symbols, standard additions plus DCMU and the uncoupler CCCP. The plots are typical of three biological replicates, each with three technical replicates. Steady state fluorescence in the dark is labeled F_0. Steady-state fluorescence in the light is termed $F_{\Delta pH}$. The linear portion of the section of fluorescence quenching between F_0 and

$F_{\Delta pH}$ was used to calculate the rate of quenching (j_{H^+}). The rise in fluorescence associated with ΔpH collapse is termed F_R.

4.3.3 Proton pumping rate is dependent upon light intensity

To examine the components of proton pumping activity in the dark-to-light transition, the WT was measured in j_{H^+} as a function of light intensity to observe the dependence of proton pumping on photosynthetic performance. As can be seen in in **Fig. 6A, C**, increasing light intensity caused an increase in the depth of AO quenching reached within the time measured. The depth of quenching only increased to a point, and intensities greater than 300 μmol m^{-2} sec^{-1} did not appreciably increase the depth of quenching. Upon addition of DCMU to the cells (**Fig. 6 B, D**), blocking PSII water oxidation, there was no appreciable difference observed between the different light intensities in the depth of quenching. Because the quenching is light dependent, it is indicative of photosynthetic activity, however quenching due to photosynthetic activity is apparently at its maximum even at lower light intensities. When plotting the rates of the linear portions of AO quenching, the clear dependence of the rate of proton pumping on light intensity can be observed (**Fig. 7A**). As reflected in the depth of quenching without DCMU, the rate of quenching does not appreciably increase at intensities greater than 300 μE (p=0.324), indicating saturation of the rate of light-induced proton pumping. This was reflected by the proportion of open PSIIs, q_p, which shows that PSIIs are largely occupied when ≥300 μE light was applied (**Fig. 7B, Fig. S2**). When DCMU was added and the rates plotted (**Fig. 7A**, red squares), little difference was seen between the rates regardless of light intensity. At even 70 μmol m^{-2} sec^{-1}, CEF dependent proton pumping is at approximately maximal value, with minimal variation seen as light intensities climb, and none significantly different from one another (p ≥0.188). This indicates that CEF driven proton pumping, while dependent upon light to operate, is incapable of compensating for the lack of PSII. To determine whether this inability to compensate was due to stoichiometric limitations of CEF machinery or a lack of substrates to participate in electron

transport, glucose was added to DCMU treated cells. Previous work has shown that addition of glucose to cells significantly increases the amount of reductant available for P700 re-reduction (Holland *et al.* 2016). Interestingly, the addition of glucose had very little effect on DCMU treated cells, in fact slightly slowing the proton pumping rate (**Fig. S4**). This indicates that even without glucose, CEF-driven proton pumping is saturated at low light intensities, and that the difference in predicted versus observed proton pumping activity of CEF to LEF is due to the available complexes and their catalytic parameters, not a lack of reductant. While these results indicate that CEF indeed drives proton pumping, lending further credence to a long-standing hypothesis, further experiments are needed to determine which complexes contribute to CEF-driven ΔpH formation in the dark-to-light transition, as well as their relative contributions.

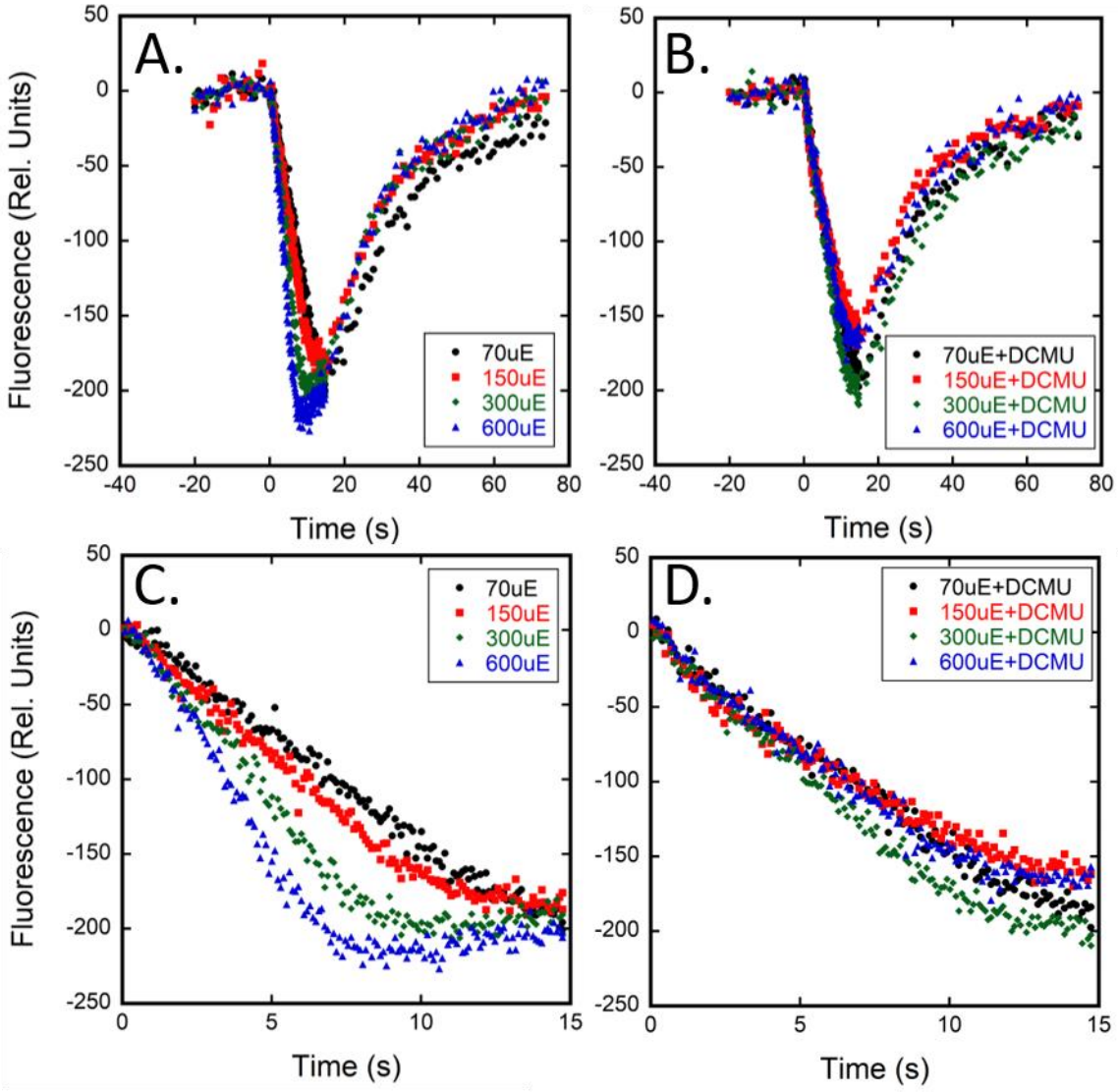

Figure 6. Light dependent proton pumping in the absence (A,C) or presence (B,D) of DCMU at varying light intensities. Acridine orange fluorescence of dark adapted WT cells in the JTS-100 in response to increasing light intensities, representing the formation and dissipation of ΔpH across the thylakoid membrane in response to the dark-to-light and light-to-dark transitions respectively. Cells were dark adapted with acridine orange (5µM) for 20 min, then a sample prepared with KCl (150mM) plus Val (10µM), DCCD (500µM), and KCN (200µM) and stirred in the dark for 5 min. For panels C and D, 10µM DCMU was used. Actinic illumination (630 nm, 600 µE) was applied for 15 seconds. These plots are typical of 3 technical replicates.

Panel A: The formation and dissipation of light dependent ΔpH formation when LEF and CEF are both active. **Panel B**: The formation and dissipation of light dependent ΔpH formation when only CEF is active. **Panel C**: A closer look at the light dependent formation of ΔpH when LEF and CEF are active. **Panel D**: A closer look at the light dependent formation of ΔpH when only CEF is active.

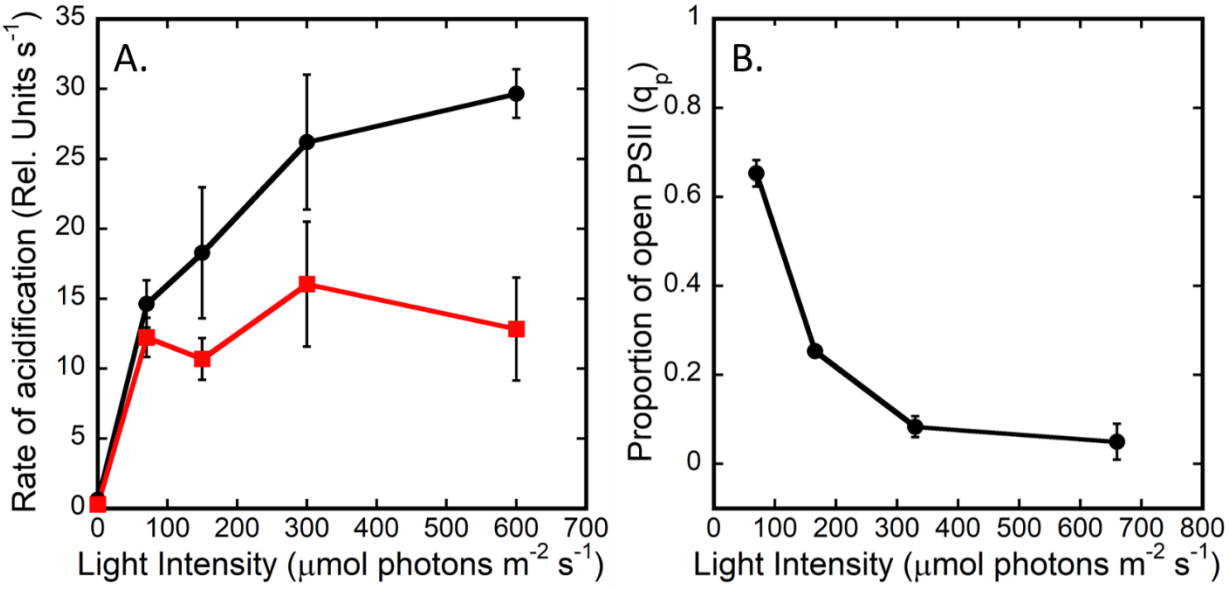

Figure 7. Proton pumping rates and photochemical quenching (q_p) as a function of light intensity. Panel A: Rates of proton pumping as a function of light intensity determined from JTS-100 data in the WT without (black circles) or with 10µM DCMU (red squares). WT cells were dark adapted in TCN buffer with AO (5µM), KCl (150mM), Val (10µM), DCCD (500µM), and KCN (200µM). Actinic illumination (630 nm, 600 µE) was applied for 15 seconds. Each point is representative of the rate estimates of 3 biological replicates with 3 technical replicates. **Panel B:** The proportion of open PSII reaction centers as a function of light intensity as estimated as photochemical quenching (q_p), in cells suspended to 5µg/mL Chl in TCN buffer + 150mM KCl. Photochemical quenching ($q_p=(F_m-F_s)/F_m-F_0)$) was obtained from Chl fluorescence yields using a PAM fluorometer (Campbell *et al.* 1998).

4.3.4 NDH-$1_{1/2}$ complexes are largely responsible for NDH-1 driven proton pumping

To determine which NDH-1 complexes are responsible for CEF-driven proton pumping, mutants in the cyanobacterial NDH-1 complexes were utilized in proton pumping experiments. The mutants Δ*ndhF1* and M55, lacking functional NDH-$1_{1/2}$ and all NDH-1 complexes respectively, were utilized to observe whether these complexes pump protons, and what contribution they have to proton pumping in the dark-to-light transition. As can be seen in **Table 2** and **Fig. 8**, there was little difference between the strains when PSII is active, further highlighting its importance in the establishment of ΔpH upon illumination, however, there was a steady decline in the rates as NDH-1 complexes are removed, with M55 having the slowest rate. The rates of proton pumping in WT and M55 with the background inhibitors are significantly different (p=0.03), indicating the NDH-1 complexes may be important for proton pumping in the dark-light transition, even when PSII is active. Upon inhibition of PSII, WT shows a slowing of j_H^+ to about 40%, however the formation of ΔpH in the Δ*ndhF1* and M55 strains was dramatically slowed or eliminated, respectively (**Table 2, Fig. 8**). While Δ*ndhF1* was still able to form a gradient at ~5% the rate of its no DCMU control and was significantly different than the traces with DCMU+CCCP (p=0.038), the M55 strain remains approximately in line with conditions measured with the protonophore CCCP near baseline (p=0.5) (**Fig. 8B,C**, red and blue symbols respectively). When Chl fluorescence of the WT and Δ*ndhF1* was measured, it was seen that, in accordance with previous work (Ogawa *et al.* 2013), chlorophyll fluorescence in the dark increases in the presence of KCN, indicating a more reduced PQ pool (**Fig. S5**). M55, on the other hand, was relatively unaffected by the addition of KCN. As well, the characteristic post-illumination fluorescence rise associated with NDH-1 activity (Battchikova *et al.* 2011, Holland *et al.* 2015, Artier *et al.* 2018, Zhang *et al.* 2020) was observed in both the WT and Δ*ndhF1*, with its magnitude being enhanced by the addition of KCN, though to a much greater degree in the WT both with and without KCN. M55 had no rise in either condition. Together these results indicate that in the dark-to-light transition, the NDH-$1_{1/2}$ complexes are major contributors to

CEF-driven proton pumping in addition to their established role in electron flow, and they may indicate that the NDH-$1_{3/4}$ complexes are also involved, but to a lesser extent.

Table 2. Relative rates of acidification. The rate of acidification, j_{H^+}, upon illumination in WT, Δ*ndhF1*, and M55 in the presence of the background inhibitors with either no additional inhibitors, with DCMU, or DCMU and CCCP added. Values are averages of three biological replicates with 3 averaged technical replicates each. Data is presented with the standard deviation. Data normalized to [Chl]/OD_{750} of the WT to account for differences in the Chl content per cell in the different strains.

Inhibitors added	Wild-type	ΔndhF1	M55
Val+DCCD+KCN	33.77 ± 8.09 s^{-1}	23.24 ± 6.99 s^{-1}	20.25 ± 4.45 s^{-1}
Val+DCCD+KCN+DCMU	14.07 ± 2.33 s^{-1}	0.72 ± 0.59 s^{-1}	-0.70 ± 0.47 s^{-1}
Val+DCCD+KCN+DCMU+CCCP	0.46 ± 0.22 s^{-1}	-0.99 ± 0.07 s^{-1}	-1.46 ± 1.16 s^{-1}

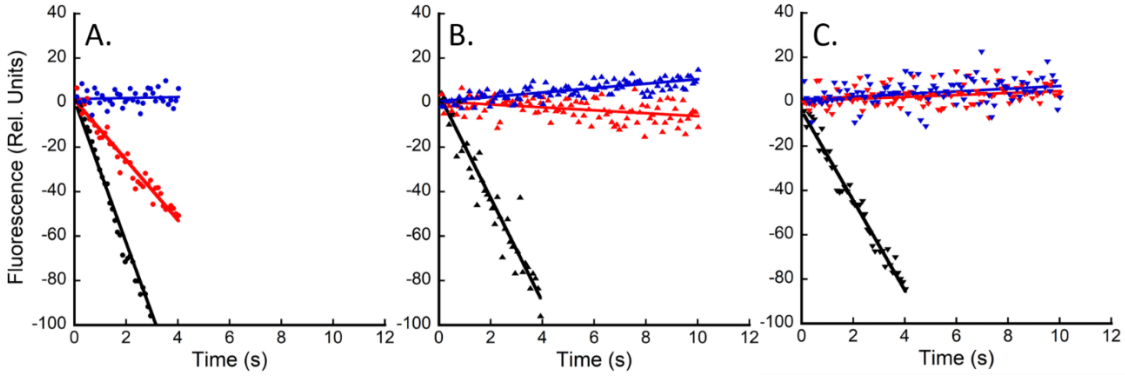

Figure 8. Rates of acidification, j_{H^+}, upon illumination in the WT and mutants deficient in NDH-1 complexes. Acridine orange fluorescence in the JTS-100. Cells were dark adapted in TCN buffer with acridine orange (5µM) for 20 min, then a sample prepared with KCl (150mM) plus Val (10µM), DCCD (500µM), and KCN (200µM) and stirred in the dark for 5 min. Actinic illumination (630 nm, 600 µE) was applied for 15 seconds. These plots are typical of 3 technical replicates. WT (**A**), Δ*ndhF1* (**B**), and M55 (**C**) after the addition of background inhibitors (black

symbols), with the addition of 10µM DCMU (red symbols), and with the addition of DCMU and 250µM CCCP (blue symbols). Data is representative of the averages of 3 biological replicates with at least 3 technical replicates each. Data was normalized to [Chl]/OD_{750} of the WT to account for differences in [Chl] per cell.

4.4 Discussion

Since the discovery that PMF and ion gradients are central to virtually all bioenergetic processes (Mitchell 1961), there has been considerable work done to understand certain characteristics of the cyanobacterial PMF both in the thylakoid and the cytoplasm (Falkner *et al.* 1976, Peschek *et al.* 1985, Belkin *et al.* 1987). Despite this work, the kinetics of proton pumping in cyanobacteria have been little explored with regards to the contributing protein complexes and the impacts of those components on rates of gradient formation. Here, the analysis of proton pumping by *Synechocystis* has revealed components that contribute to the formation of ΔpH upon the illumination of the cells by actinic light. An interesting advantage that whole cell cyanobacteria have over heterotrophic species in this sort of measurement is that the photosynthetic electron transport chain is light inducible, allowing for the control of redox components by controlling the actinic illumination. This allows for the relatively easy assaying of photosynthetic ΔpH formation in whole cell cyanobacteria, which provides opportunities to observe the effects of cellular metabolism on the proton gradient.

To best observe the contribution of the photosynthetic complexes to light-dependent proton pumping in whole cells, various parameters needed to be considered to compare rates of photosynthetically driven proton pumping, particularly in regard to the NDH-1 complexes. It has been shown that the amount of K^+ available in the thylakoid affects the ability of the cells to pump protons, providing an electrochemical back-pressure against which protons must be pumped as they both have a positive charge (Checchetto *et al.* 2012). Val was added to the samples to alleviate this constraint. The inhibitor DCCD was also included to prevent the forward

or reverse action of ATP-synthase from deducting from or contributing to the formation of the gradient. Because respiration occurs in the dark, it is reasonable to suppose that the dark ΔpH will also affect the observed rate and amplitude of light-induced AO quenching since it will have start from a 'pre-energized' membrane exerting an electrochemical backpressure as photosynthetic electron flow initiates. The existence of the dark ΔpH was demonstrated when cells were treated with KCN, causing the dark ΔpH to collapse, an effect enhanced by the addition of Val and DCCD alongside KCN (**Fig. 4A**). Indeed, by eliminating the dark ΔpH the rate and depth of light-induced AO quenching increased (**Fig. 4B,C**), indicating that in the absence of a a 'pre-energized' membrane, proton pumping is faster and that it is light-dependent proton pumping. This supports the conclusion that light-induced proton pumping can be limited, under in vivo conditions, to some degree by the electrochemical back-pressure due the dark ΔpH. Although AO fluorescence technique is not amenable to pH calibration, previous estimates of the dark ΔpH in cyanobacteria in the presence of Val is approximately 1.5 pH units and that value further increased to ~2.5 pH units under illumination (Falkner *et al.* 1976, Peschek *et al.* 1985, Belkin *et al.* 1987). The observation that actinic illumination of dark-adapted samples in the presence of KCN produced a larger and more rapid quenching of AO fluorescence than in its absence (**Fig. 4B**) is consistent with these estimates. Overall, removing the dark ΔpH and ΔΨ allows for the determination of rates of light-dependent proton pumping that are closer to maximal within live cells.

While observing the major components of photosynthetically driven PMF formation, PSII was seen to be the major contributor to ΔpH formation in all strains measured. This is an expected result, as the water oxidation reaction produces $4H^+/O_2$, and PSII is both abundant in the cell and has a fast reaction rate compared to NDH-1 of other organisms (Fato *et al.* 1996, Zhang *et al.* 2004, Dismukes *et al.* 2009, Hirst 2013, Strand *et al.* 2017). This is demonstrated here by the sharp reduction in the rates of ΔpH formation upon the addition of DCMU in all strains tested

(**Fig. 5**, **Fig. 6, Fig. 7A, Fig. 8, Table 2**), with that reduction most pronounced in strains lacking NDH-1 complexes. While the rates of proton pumping when PSII is active are similar in all the strains, there is a small reduction in the rates as NDH-1 complexes are removed. Nevertheless, the rates remain fast in all the strains, indicating that the NDH-1 complexes are important for proton pumping even when LEF is active, though their contributions are partially masked by LEF and PSII activity, as discussed below. The removal of PSII activity by the treatment of the WT with DCMU still allows for a substantial gradient to be formed upon illumination, indicating that CEF drives the formation of ΔpH in the absence of PSII activity, though ~60% less effectively (**Table 2, Fig. 5, Fig. 7A, Fig. 8A**). While the rate is decreased, it quenches to approximately 80% the $F_{\Delta pH}$ without DCMU, potentially indicating that the reduced rate is incapable of completely overcoming the dissipation mechanisms that allow $F_{\Delta pH}$ to be established (**Fig. S3**). AO quenching in DCMU treated cells is light dependent (**Fig. 5, Fig. 6**, **Fig.7A**), indicating that it is due to CEF activity. The light intensity dependence of CEF-driven proton pumping saturates at lower intensities than when LEF is active, possibly indicating the upper limits of the proton pumping capability of CEF, as at lower light intensities it is able to match the proton gradient formation rates seen when PSII is active (**Fig. 7A**). When accounting for known and assumed H^+/e^- ratios for photosynthetic electron flow, some interesting parameters can be seen. One turnover of LEF results in $3H^+/e^-$ (Sacksteder *et al.* 2000), 1 H^+ from PSII, and 2 from the Q-cycle in Cyt.-b_6f. In addition to this, a turnover of CEF through the NDH-1 complexes adds $2H^+/e^-$, assuming a stoichiometry similar to that observed in their relatives (Strand *et al.* 2017) and no additional turnover of b_6f, for a total of $5H^+/2e^-$ from a single turnover of both LEF and CEF. With LEF inactivated by the addition of DCMU, $4H^+/e^-$ are accounted for, with 2 from NDH-1, and 2 from cyt.-b_6f, resulting in 80% of the protons per turnover, with more protons moved per electron. Why is the rate of proton pumping when treated with DCMU only 40% of the no addition control (**Table 2**)? This may be explained by the slower rate of complex I in other organisms: ~200 e^-/s (Fato *et al.* 1996, Hirst 2013) compared to 1-400 PSII turnovers/s

(Dismukes *et al.* 2009), along with the relative abundance of PSII compared to NDH-1 in cyanobacterial thylakoid membranes (Zhang *et al.* 2004). Alternatively, there may be sufficient CEF components, but limiting reductant. To test this, glucose was added to WT cells treated with DCMU, as glucose is known to increase available reductant (Holland *et al.* 2016), and AO quenching observed (**Fig. S4**). The addition of glucose did not increase the rate and in fact decreased it some, indicating that the limitation of CEF-driven proton pumping is not due to the lack of reductant, and is more likely due to the numbers of complexes and their respective turnover rates.

To analyze the contribution of NDH-1 complexes to proton pumping, the mutants Δ*ndhF1* and M55, lacking only NDH-$1_{1/2}$ complexes or all NDH-1 complexes respectively, were utilized in AO assays. Interestingly, NDH-1 complexes are contributing to proton pumping even during conditions dominated by LEF since initial rates slowed to nearly 60% upon upon complete elimination of all NDH-1 complexes (in M55) and almost as much in the Δ*ndhF1* strain, though only M55 is significantly different from the WT (**Table 2**). Thus, during the dark-to-light transition, NDH-1 complexes make a strong contribution to proton pumping. In the Δ*ndhF1* strain, the remainder of the cellular complement of NDH-1 complexes is comprised of only the forms involved in CO_2-uptake, NDH-$1_{3/4}$. Therefore, these complexes must contribute only a minor amount to the total CEF, at least under these growth conditions. Recent data on the presence of the Flv1/3 system consuming electrons in their Mehler-like reaction (resulting in no additional proton pumping and acting as an electron sink to compensate for the loss of the NDH-$1_{1/2}$ systems (Nikkanen *et al.* 2020)) alongside the data presented here implies that the NDH-$1_{3/4}$ complexes are incapable not only of dealing with the excess reductant but also of compensating for the loss of the NDH-$1_{1/2}$ complexes in terms of either electron transport or proton pumping in these conditions. The proton pumping results are consistent with studies of Bernat and colleagues, showing that the respiratory forms of the NDH-1 complexes (NDH-$1_{1/2}$) dominate the

corresponding cyclic electron fluxes and that the CO_2-uptake forms (NDH-$1_{3/4}$) contribute less strongly (Bernat *et al.* 2011). The dominance and essentiality of NDH-$1_{1/2}$ in CEF proton pumping can also be seen in **Fig. 8** and **Table 2**, where both Δ*ndhF1* and M55 are severely impaired compared to the WT when treated with DCMU. The NDH-1 null mutant, M55, was unable to form significant ΔpH in the dark-to-light transition in the time measured when treated with DCMU (**Fig. 8C**), highlighting the importance of the function of NDH-1 complexes in proton pumping under these conditions. The importance of the NDH-$1_{1/2}$ complexes is especially highlighted by the Δ*ndhF1* mutant, which is still able to form a gradient when treated with DCMU, however at ~5% the rate of the WT when treated with DCMU (**Fig. 8A**, **B**). That said, the Δ*ndhF1* strain when treated with DCMU still performs light-dependent proton pumping, indicating that deletion of only the NDH-$1_{1/2}$ complexes is not sufficient to completely eliminate CEF-driven proton pumping, while the removal of all four NDH-1 complexes is sufficient, as seen by the absence of quenching in M55 cells treated with DCMU (**Fig. 8C**). These data indicate that the NDH-$1_{1/2}$ complexes are the primary drivers of proton pumping in these conditions, but also imply the NDH-$1_{3/4}$ complexes are participants as well, though to a much lesser degree than their cousins. Whether this is due to a difference in the number of NDH-1 complexes of each sort available, or some activity intrinsic to NDH-$1_{3/4}$ complexes remains to be understood. The heavy activity of the NDH-$1_{1/2}$ complexes in proton pumping is consistent with their activity in e^- transport (Bernat *et al.* 2011, Ogawa *et al.* 2013). Because it is known the NDH-1 complexes participate in CEF based on measurements such as post-illumination fluorescence rise (PIFR), which is eliminated by the deletion of NDH-1 complexes (Ryu *et al.* 2003, Ma *et al.* 2005, Strand *et al.* 2017). It is shown here that deletion of NDH-1 complexes similarly disrupts CEF-driven H^+ pumping (**Fig. 5B, C**), indicating that the two activities are coupled by these enzyme complexes, and that NDH-1 complexes are responsible for the bulk of CEF-driven proton pumping in the dark-to-light transition. This has implications for the partitioning of electrons flowing through PSI, and cells may favor the NDH-1 complexes in times when more proton

pumping, and therefore ATP production, is needed, while SDH is activated when less proton pumping is needed, but reductant must still be consumed. Given the recent structural data on the cyanobacterial NDH-1 complexes, the development of this assay system enables measurement of the impact of point mutations on proton pumping, allowing for deep understandings of the mechanisms underlying their Complex I-like activities, as well as the unique CO_2 hydration activities of the NDH-$1_{3/4}$ complexes.

4.5 Conclusions

While it has been observed that Complex I/NDH-1 pumps protons to generate PMF in heterotrophic bacteria and archaea, mitochondria, and chloroplasts, we are the first to demonstrate activity among the unique NDH-1 medley present in cyanobacteria. Among the processes that generate PMF, PSII and LEF are responsible for the bulk of this activity in the dark-to-light transition. The NDH-1 complexes, however, contribute to this action to a great degree, with the ability to compensate for ~40% of the rate of proton pumping when LEF is inactivated. This is particularly important regarding the findings that changes in light intensity is one of the many stresses that photosynthetic organisms face in their natural environments.

CHAPTER V

CYCLIC ELECTRON FLOW COUPLED TO PROTON PUMPING IN *SYNECHOCYSTIS* SP. PCC 6803 IS DEPENDENT UPON NADPH OXIDATION BY THE SOLUBLE ISOFORM OF FERREDOXIN NADP-OXIDOREDUCTASE

5.1.1 Abstract

Ferredoxin:NADP-oxidoreductase (FNR) catalyzes the reversible exchange of electrons between the one electron carrier ferredoxin (Fd) and the two-electron carrier $NADP^+$. Reduction of $NADP^+$ by Fd via FNR is essential in the terminal steps of the photosynthetic electron transfer chain as light activated electron flow produces NADPH for CO_2 assimilation. However, FNR also catalyzes the reverse reaction in photosynthetic organisms, transferring electrons from NADPH to Fd, which is important for example, for the reduction of inorganic nutrients in plant root plastids and in cyanobacterial metabolism for respiration and cyclic electron flow (CEF). The cyanobacterium *Synechocystis* sp. PCC 6803 possesses two isoforms of FNR, a long form attached to the phycobilisome (FNR_L) and a short form that is soluble (FNR_S). While both isoforms are capable of NADPH oxidation or $NADP^+$ reduction, FNR_L is most abundant during optimal growth conditions, whereas FNR_S accumulates under conditions of stress, especially those that require enhanced CEF. Because CEF-driven proton pumping in the light-dark transition is due to NDH-1 complex activity and that NDH-1 complexes are powered by reduced Fd, CEF driven proton pumping and the redox state of the PQ and NADP(H) pools were investigated in mutants possessing either FNR_L or FNR_S. The FNR_S isoform is shown to facilitate proton

pumping in the dark-light transition, contributing more to CEF than FNR_L. FNR_L was shown to provide reducing power for CEF-driven proton pumping, but only after an adaptation period to illumination.

5.1.2 Introduction

Cyclic electron flow (CEF) is an important mechanism in photosynthetic organisms as a means of recycling excess reductant while simultaneously driving the synthesis of ATP by the generation of proton motive force (PMF) (Battchikova *et al.* 2011, Bernat *et al.* 2011). In plants, algae, and cyanobacteria the reducing power produced by the photosynthetic light reactions is stored in the form of NADPH and Fd_{red}, which is then consumed by anabolic processes, mainly CO_2 fixation via the Calvin-Benson-Bassham (CBB) cycle. This process is driven by linear electron flow (LEF) since electrons derived from the oxidation of water by photosystem II (PSII) follow a linear sequence of transfers through the photosynthetic electron transport chain, on through photosystem I (PSI), and ultimately terminating in the reduction of inorganic substrates for biomass production. During CEF, however, accumulated NADPH and Fd_{red} follow an alternative path that returns the energized electrons back to the membrane where they are oxidized by protein redox complexes in the electron transport chain, where the may, depending on the pathway, drive the formation of PMF and thereby contribute to ATP production without net production of NADPH and Fd_{red}. The fraction of electrons recycled through CEF relative to LEF provides a mechanism for cells to adjust the ouptput ratio of NADPH and ATP to accommodate different metabolic demands and fluctuating environmental conditions. Recently, cellular ATP concentrations were shown to modify the rate of CEF through a competitive inhibition of Fd oxidation by the NDH and FQR/PGR5 pathways in plant chloroplasts providing a relatively simple feedback mechanism for adjusting this output ratio of phosphorylating and reducing power(Fisher *et al.* 2019). Although different cyclic paths involving different membrane complexes have been discovered, in all cases electrons are transferred to the plastoquinone (PQ)

pool, thereby re-entering the electron transport chain to be further utilized to produce NADPH and Fd_{red} via PSI. This process is not a simple one, with many potential electron sources and contributing components. The electron flow can be direct from the acceptor side of PSI via Fd, or indirectly from the oxidation of photosynthetically produced NADPH, or carbohydrates (Mi *et al.* 1992, Mi *et al.* 1995, Holland *et al.* 2015, Zhang *et al.* 2020). One of the mechanisms by which the redox state of the NADPH/Fd pool is maintained in these organisms is by the presence of Ferredoxin:NADP-oxidoreductase (FNR). In many cyanobacteria, only one form of FNR is present (FNR_L), and it attaches to the phycobilisome (PBS), posising it to function in photosynthetic $NADP^+$ reduction from the acceptor side of PSI (Schluchter *et al.* 1992, Thomas *et al.* 2006, Korn *et al.* 2009, Korn 2010, Liu *et al.* 2019). FNR_L localization in proximity the photosynthetic membrane via attachment to the PBS is likely thought to facilitate fast rates of LEF. Specifically, it would minimize macromolecular diffusion constraints during the interaction of PSI, Fd, and FNR for the rapid production of more quickly diffusing NADPH, which is in high demand and undergoes fast recycling between the oxidized and reduced forms as it communicates reductant from photosynthetic electron transport to the CBB cycle and anabolic metabolism in the cytoplasm (Moal *et al.* 2012). Some cyanobacteria, such as the glucose tolerant *Synechocystis* sp. PCC6803, possess two isoforms of FNR. The second isoform is smaller, and therefore referred to as FNR_S. It was discovered to be produced by the same gene (Thomas *et al.* 2006) and is produced by an alternative initiation of translation, potentially via sRNAs or secondary structures. The isoform primarily observed in cyanobacteria is FNR_L, which may have arisen due to a gene recombination event of FNR_S with a PBS-linker domain, eventually resulting in the genetic conversion FNR_S to FNR_L in most of these bacteria (Thomas *et al.* 2006). This is consistent with the observation that *Gloeobacter violaceus,* a primitive cyanobacterium, possesses the FNR_S form (Thomas *et al.* 2006). Cyanobacteria capable of heterotrophy, on the other hand, have retained the ability to recapitulate the FNR_S isoform through regulated alternative translational initiation codon utilization, and it is expressed under conditions of heterotrophy, or stress conditions like

high light intensity and nutrient limitation (Thomas *et al.* 2006), conditions which necessitate CEF activity (Battchikova *et al.* 2011). The fact that these organisms have kept the ability to express the FNR_S isoform suggests that it is an important part of their photosynthetic mechanism. Data on the kinetics of these isoforms has led to the hypothesis that FNR_S operates as a soluble NADPH oxidase, while FNR_L acts more as an $NADP^+$ reductase associated with the PBS, though both isoforms are capable of performing either reaction (Korn *et al.* 2009). Because cyanobacterial NDH-1 complexes utilize Fd as their source of reductant (Schuller *et al.* 2019, Zhang *et al.* 2020) and their contribution to proton pumping can be observed by AO fluorescence (Chapter IV), the coupling of electron transport and proton pumping data can be used to explore the dynamics of the relationship between these two isoforms, CEF, and proton pumping. Here, this relationship is explored by utilizing these techniques and strains lacking either FNR_S or FNR_L.

5.2 Methods

5.2.1 Strains and molecular constructs

Strains of the glucose tolerant *Synechocystis* sp. PCC 6803 (hereafter, *Synechocystis*) were maintained on pH 8 BG-11 (Allen 1968) with 1.5% agar supplemented with 18mM sodium thiosulfate and containing the appropriate antibiotics for each mutant (25µg/mL spectinomycin for FS1 and MI6) with and maintained under ~70 µmol m^{-2} sec^{-1} light and air levels of CO_2. Experimental material was obtained from 100mL cultures grown in 250mL Erlenmeyer flasks with rotary shaking (200 rpm) under ~100 µmol m^{-2} sec^{-1} Cool White fluorescent lighting (GE). Cultures were harvested upon reaching an OD_{750} 0.7-1.0.

The strains MI6 and FS1 were generated and provided by the lab of Ghada Ajlani from the Centre National de la Recherche Scientifique in Paris, France (Thomas *et al.* 2006).

5.2.2 Chlorophyll and NADPH fluorescence

Cells were harvested by centrifugation, washed with 50mM Tricine pH 8 + 25mM KCl (TCK) and resuspended to 5.9µg/mL Chl, measured by in a UV-Vis spectrophotometer (Shimadzu). Following this, each sample was diluted to 5µg/mL Chl in the cuvette with the Tricine buffer. Measurements of Chl and NADPH fluorescence yield were measured using the Dual PAM-100 (Walz) with the 9-AA/NADPH module. For 5-minute illumination period measurements, a nominal actinic light intensity of 53 µmol m^{-2} sec^{-1} was utilized with multiple turnover (MT, nominally 20,000 µmol m^{-2} sec^{-1}) flashes occurring before, during, and after illumination to visualize the approximate proportion of open PSII. The application of an MT in NADPH fluorescence measurements produces an artifactual feature that was not included in its entirety in the graphical representations of the data.

5.2.3 Acridine orange fluorescence quenching

Acridine orange (AO) has been used as a fluorescent dye for measuring proton pumping across a membrane in both whole cyanobacterial cells and membrane vesicles (Palmgren 1991, Teuber *et al.* 2001, Nakamaru-Ogiso *et al.* 2010, Checchetto *et al.* 2012) and the assay protocol outlined in Chapter IV was utilized with minor modifications. Cells were grown as described above and washed with TCK buffer as above for Chl fluorescence. Samples were diluted to 5.9µg/mL Chl had acridine orange added to 5µM, and were incubated shaking gently in the dark for 20 minutes to allow acridine orange penetration into the cell (Teuber *et al.* 2001). Samples of the cells were then added to a cuvette and diluted the cells to 5µg/mL in TCK buffer and the inhibitors applied as described in Chapter IV. Samples were then stirred for 5 minutes in the dark, and the fluorescence measured with the JTS-100 (Biologic), describe in greater detail below. A 534/20nm bandpass filter (Edmund Optics) was placed between the sample and the detector.

Data points in the JTS-100 were collected once per second in the dark and once per 100ms in the light, with 600 µmol m^{-2} s^{-1} actinic light applied. For dark-adapted samples, cells

incubating in the dark were provided with an additional 5 min dark incubation with stirring after the addition of inhibitors. Samples were then illuminated with actinic light for 15 sec, and then actinic illumination was ceased. Samples were refreshed after each measurement to avoid drift associated with repeated illumination. For light-adapted samples, cells were pre-illuminated with 600 µmol m^{-2} s^{-1} actinic light for 2 min, followed by a 4 min dark incubation with stirring. The cells were then illuminated with actinic light for 15 sec as stated above. Samples were measured repeatedly as there was minimal drift seen with repeated illuminations. The raw data and rates were treated essentially as described in Chapter IV.

5.3 Results

5.3.1 FNR_S has a large contribution to NDH-1 cyclic electron flow

Chlorophyll fluorescence kinetics have long been used to observe electron flow through the PQ pool in cyanobacteria (Renger *et al.* 1986, Schreiber *et al.* 1995), and the post-illumination kinetics are especially indicative of NDH-1 driven CEF (Battchikova *et al.* 2011, Holland *et al.* 2015, Artier *et al.* 2018, Zhang *et al.* 2020). Chlorophyll fluorescence traces for WT, MI6, and FS1 are shown in **Fig. 9**. During a 5 minute illumination in the TCK assay buffer, WT has typical initial kinetics following the initiation of illumination characterized by a gradual approach to an intermediate level of PQ reduction state toward the end of the five minute continuous illumination period (~growth light intensity) indicative of a balance of linear electron flow and the consumption of electrons for CO_2 fixation. The MI6 mutant exhibits several strikingly different Chl fluorescence features. Firstly, the maximal levels of fluorescence yield are considerably higher than either FS1 or the WT, perhaps indicating high levels of PSII (**Fig. 9C**) seen both with the levels upon brief high intensity MT flashes as well as in response to the initiation of continuous actinic illumination. Secondly, the first MT flash was higher yield than the subsequent MT flashes suggesting that the cells are already in State-1 in the dark. Thirdly, following the initiation of five minute continuous illumination period, the initially high level of fluorescence yield progressively decreases toward levels values nearer the WT than FS1 (**Fig.**

9A,C,E). It appears that the MI6 mutant has a stronger tendency to induce non-photochemical excitation energy quenching compared to the wild type and starting the illumination period with a relatively unquenched configuration and/or having aberrant State transition characteristics. In contrast to MI6, the level of reduction of the PQ pool increases during the actinic illumination period in FS1, potentially obscuring the small peak at ~20-30 sec of illumination corresponding to activation of the CBB cycle in the light (**Fig. 9A,E**) (Holland *et al.* 2015). Instead of maintaining a steady state after the CBB cycle activation as with the WT, the increasingly reduced PQ pool in FS1 indicates that either utilization of the photosynthetically generated reductant was impaired and/or an enhanced rate of CEF was concurrently re-reducing the PQ pool. Post-illumination in these conditions, the WT and MI6 have very minimal fluorescence rises while FS1 has a large rise that seems to include both the fast and slow components, associated with CEF involving oxidation of Fd and consumption of photosynthetically produced reductant, respectively (**Fig. 9A,C,E**) (Holland *et al.* 2015). This indicates that in the WT and MI6 under these conditions, electrons are not flooding back into the PQ pool via complexes like NDH-1 after illumination, or if they are, they are being removed from the PQ pool at a similar rate to that which they are entering. This was not the case in FS1, where electrons flood the PQ pool after illumination, and there was little consumption of those electrons after illumination (**Fig. 9E**). When KCN was added to the samples, preventing cytochrome oxidase (COX) activity oxidizing the PQ pool, some stark changes are seen to fluorescence yield. Over the course of the 5min illumination, WT starts out with a very reduced PQ pool, which becomes even more reduced over the illumination to near Fm levels (**Fig. 9B**). The initially reduced state of the PQ pool can be ascribed to the continued donation of electrons to the NDH-1 and perhaps other complexes, leading to accumultation of reductant in the PQ pool due to blockage of COX. MI6 exhibits a large initial reduction of PQ upon illumination, followed by the typical quenching associated with CBB cycle activation (**Fig. 9D**), which was followed by a slight increase of fluorescence over the course of illumination indicating slight reduction of the PQ pool. These

results suggest that MI6 has a relatively oxidized PQ pool in the dark despite the inactivation of COX with KCN. As shown in **Fig. 9F**, FS1 also appears to have a more oxidized PQ pool in the dark, albeit not as oxidized MI6, as evidenced by relatively low level of F_0 compared to the maximal fluorescence yield levels. Following the intiation of continuous actinic illumination, there is a typical initial reduction followed by a brief oxidation and then a sustained steady reduction of the PQ pool over the course of illumination. The post illumination rise was similar in the WT and MI6 in terms of magnitude, but the reduction state of MI6 remains high by comparison as measurement continues. This rise was further investigated in **Fig. 10**, compiling and highlighting the post-illumination period of the measurements in **Fig. 9B,D,F**. As can be seen, FS1 has the sharpest initial rise after illumination and reaches the highest fluorescence yield. This initial rise was also seen in MI6 and the WT, but not to the magnitude seen in FS1. After this initial rise, a second rise occurs over the course of ~12-30 seconds after the cessation of illumination. This slower rise occurs at similar rates for all of the strains in these conditions, but the peak of fluorescence yield and its dissipation was shifted in the mutants, most severely so in FS1 (**Fig. 9B,D,F, 10**). To further investigate the post-illumination rise in the absence of inhibitors, 15sec illuminations were performed with a MT flash at 13sec of illumination. Illuminations of this length were observed to produce strong post-illumination rises without inhibitors and were utilized to observe the differences between dark-adapted strains. The FS1 and WT had similar initial slopes of the post-illumination rise, however the FS1 had a greater magnitude, associated with greater CEF activity, especially via NDH-1 (**Fig. 11**). The MI6 mutant, on the other hand, had a small rise, with dissipation of the post-illumination fluorescence occurring well before either FS1 or the WT had reached their peak and begun their own dissipations (**Fig. 11**).

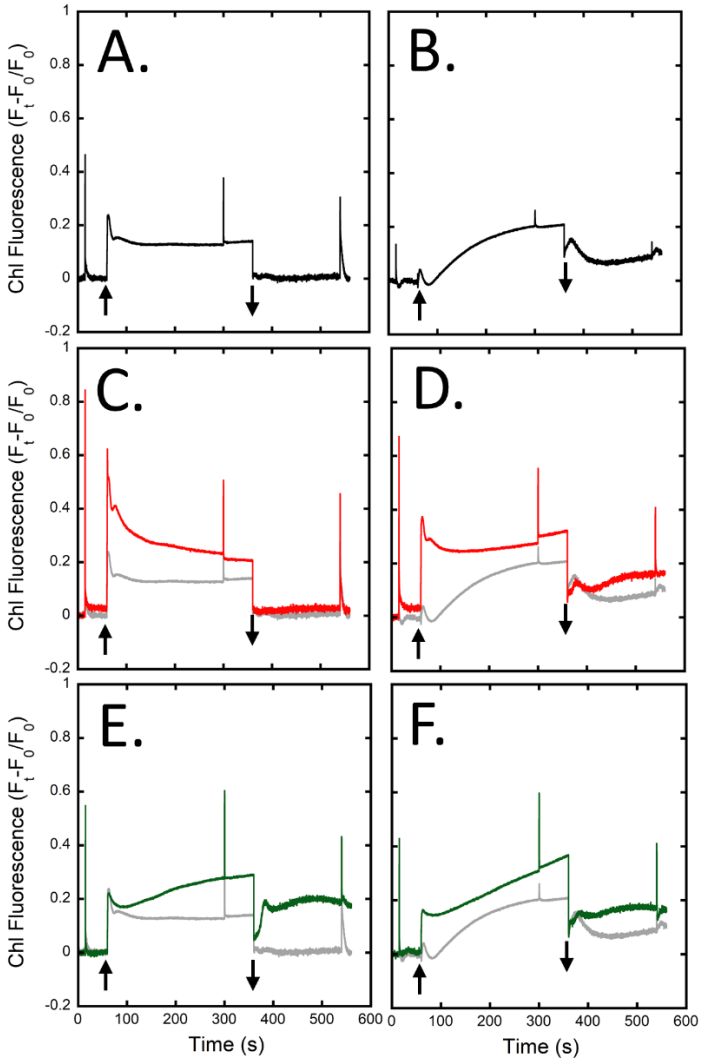

Figure 9. Chlorophyll fluorescence kinetics distinct in strains lacking an FNR isoform. Panel A: Chlorophyll fluorescence in the DUAL PAM-100 of dark-adapted WT cells in TCK buffer upon illumination for 5 min with 53 µmol m^{-2} s^{-1} with multiple turnover flashes before, during, and after illumination. Arrows indicate actinic light on (up) or off (down). **Panel B:** Chlorophyll fluorescence of the WT after treatment with KCN. The trace of the WT with and without KCN is repeated in panels C-F in grey for illustrative purposes. **Panel C**: Chlorophyll fluorescence of the MI6 strain. **Panel D:** Chlorophyll fluorescence of MI6 after treatment with KCN. **Panel E:** Chlorophyll fluorescence of the FS1 strain. **Panel F:** Chlorophyll fluorescence of FS1 after treatment with KCN.

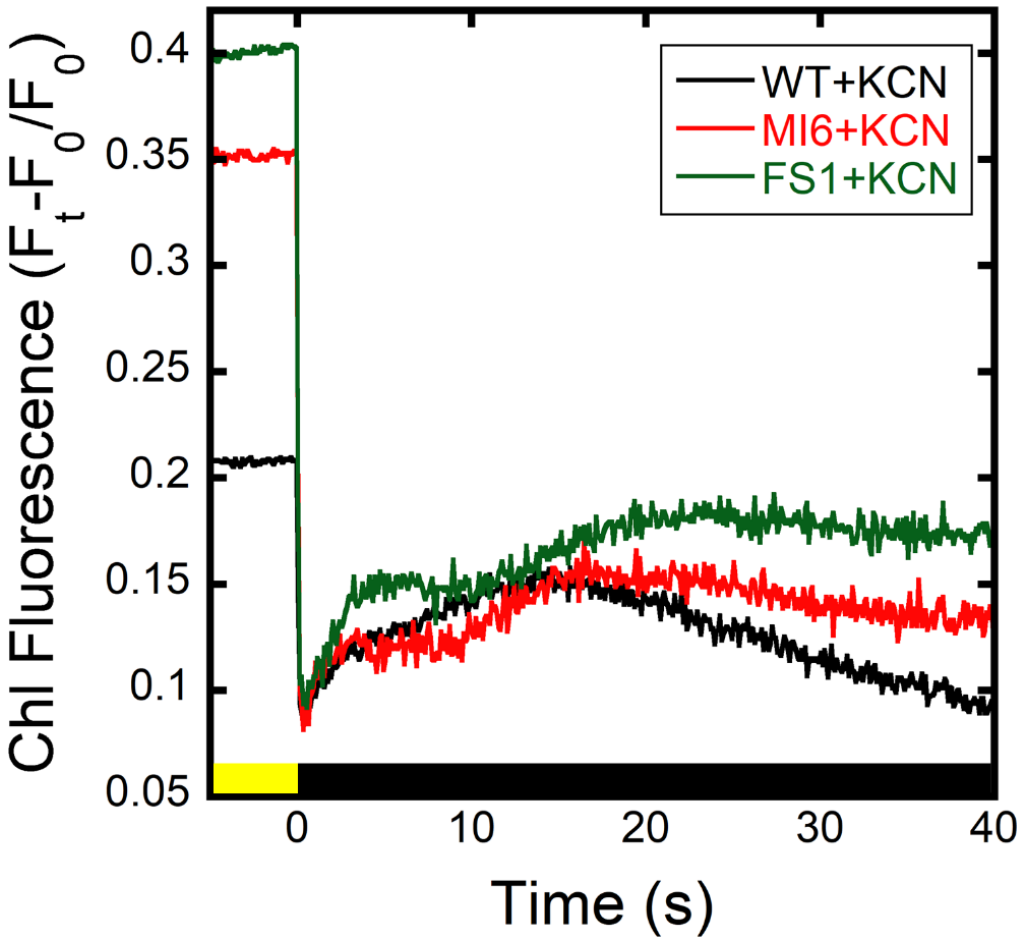

Figure 10. Post-illumination chlorophyll fluorescence rise is especially enhanced in FS1 after KCN addition. Chlorophyll fluorescence in the DUAL PAM-100 of WT (black), MI6 (red), and FS1 (green) cells in TCK buffer with 200µM KCN upon termination of 5 min illumination with 53 µmol m^{-2} s^{-1}.

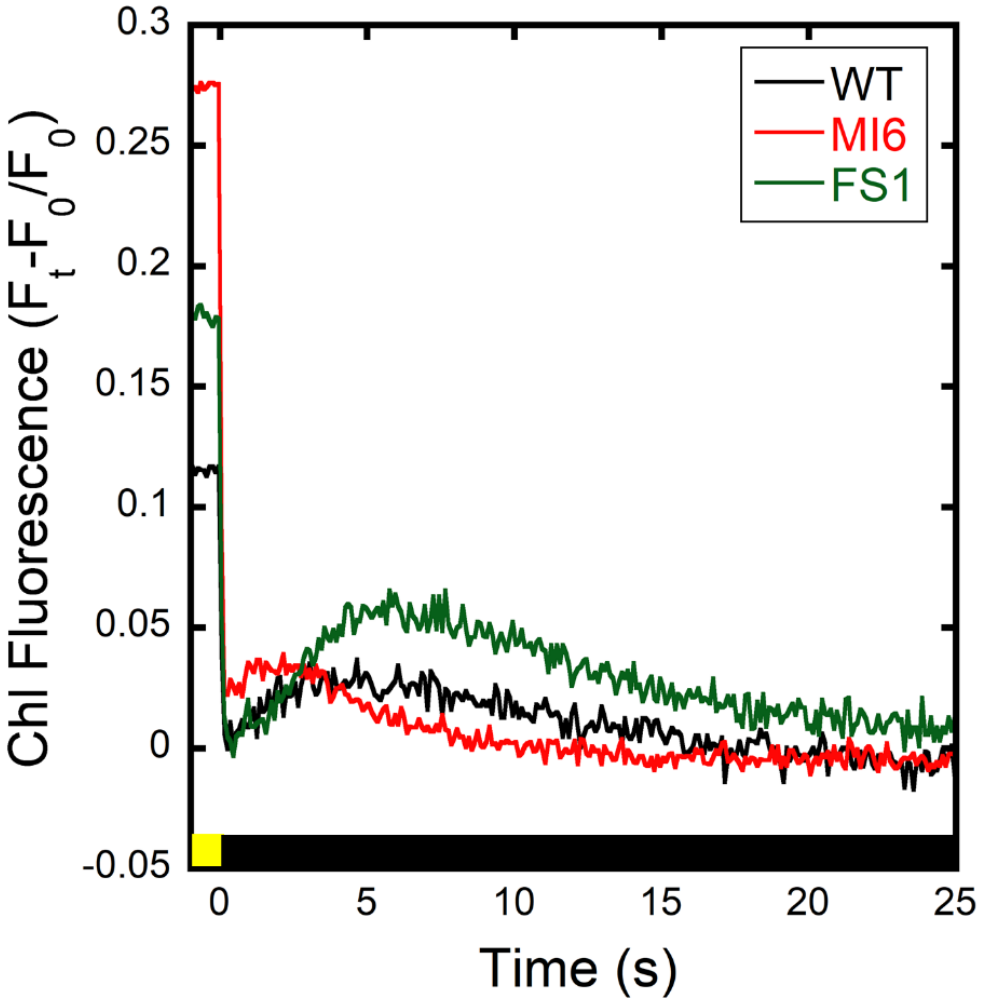

Figure 11. Post-illumination chlorophyll fluorescence rise enhanced in FS1 without inhibitors. Chlorophyll fluorescence in the DUAL PAM-100 of dark-adapted WT (black), MI6 (red), and FS1 (green) cells in TCK buffer after illumination with 53 µmol m^{-2} s^{-1} for 15 sec.

5.3.2 FNRs participates strongly in NADPH oxidation during illumination

NADPH fluorescence was measured concomitantly with chlorophyll fluorescence in the DualPAM-100 to observe the redox state of the soluble reductant pool during illumination (Holland *et al.* 2015). The MT flashes produce an artifact that was excluded in the graphics to emphasize the kinetics of fluorescence over time. As seen in **Fig. 12A**, the WT exhibits characteristics typical of NADPH fluorescence during 5 minutes illumination (Holland *et al.* 2015). Increase in fluorescence indicates reduction of $NADP^+$ and decrease in fluorescence is

indicative of NADPH oxidation. After the rapid reduction of the pool upon illumination, a smaller oxidation phase, likely due to the activation of FNR (Elanskaya *et al.* 2021), was seen before a large transient reduction associated with the production of NADPH and representative of the State-2 to State-1 transition, where light excitation energy is directed to PSII preferentially over PSI (Mullineaux *et al.* 1990, Ranjbar Choubeh *et al.* 2018, Bhatti *et al.* 2020). This was followed by a subsequent oxidation of NADPH associated with the activation of the CBB cycle and fixation of carbon after ~30sec of illumination (Holland *et al.* 2015). After illumination ceases, there was a rise in fluorescence that starts ~10 sec after the beginning of the dark period and continuing for ~10-20 sec associated with the oxidation of sugars (Holland *et al.* 2015). The delay before the rise correlates with the oxidation of trioses seen in the post-illumination rise of Chl fluorescence in KCN treated cells (**Fig. 10**), indicating that the delay in the rise was associated with Fd reduction before NADPH production by catabolism begins. The MI6 mutant has similar characteristics as the WT during and post-illumination, however the overall NADPH pool not as strongly reduced in the light, and its post-illumination rise was slightly smaller in magnitude (**Fig. 12C**). The FS1 mutant on the other hand had distinct characteristics in its NADPH redox state over the course of illumination (**Fig. 12E**). It had an initial reduction followed by a strong oxidation of NADPH to a steady state that was deeply oxidized compared to the WT or MI6, and even dropped below the baseline of fluorescence pre-illumination (**Fig. 12E**). The transient reduction peak was shifted to ~15 sec earlier than it was in the WT or MI6, potentially indicating changes in the regulation of the redox pools. After illumination, a large and dramatic rise was seen in FS1 to approximately the level of the initial NADPH reduction peak in a biphasic manner, first occurring quickly and then rising slowly to a point before minor oxidation was observed in the dark. This occurred on approximately the same timescale as the WT or MI6. Upon the addition of KCN, the WT has almost entirely reduced its NADPH pool in the dark, as upon illumination there was little increase in fluorescence (**Fig. 12B**). There was a transient oxidation, and then NADPH fluorescence rises slowly and reaches a steady state for the rest of illumination.

Given that the PQ pool was almost entirely reduced over the course of illumination (**Fig. 9B**), it might be that NADPH was as reduced as it can be as well, representing an acceptor side limitation for the photosynthetic electron transport chain. The MI6 has similar characteristics of NADPH fluorescence as before treatment with KCN, however the initial rise in fluorescence upon illumination was diminished (**Fig. 12D**), but not as much as in the wild type. A decrease in fluorescence was seen after the transient peak, possibly indicating dissipation of reductant by CO_2 fixation. Post-illumination it has a similarly sloped but greater rise than the WT has, and the pool continues to get reduced over time. FS1 interestingly, after its transient peak, has a strong oxidation of the NADPH pool, though not quite as quickly as without KCN, followed by a slow and steady rise in fluorescence, which seems to continue at a similar rate after the oxidation and subsequent reduction of NADPH after termination of illumination (**Fig. 12F**). This is consistent with enhanced CEF. Reductant is gradually being dissipated over the course of continuous illumination with dissipation attributed to COX and flavodiiron proteins in the absence of KCN and to flavodiiron proteins in its presence. The rise post-illumination was much smaller in magnitude than without KCN treatment, which is attributed to the already highly reduced level in the presence of KCN. Thus, in both cases, the post illumination reduction of NADPH is vigorous after the transient oxidation period after illumination and then approaches what appear to be a similar maximal level (**Fig. 12E,F**).

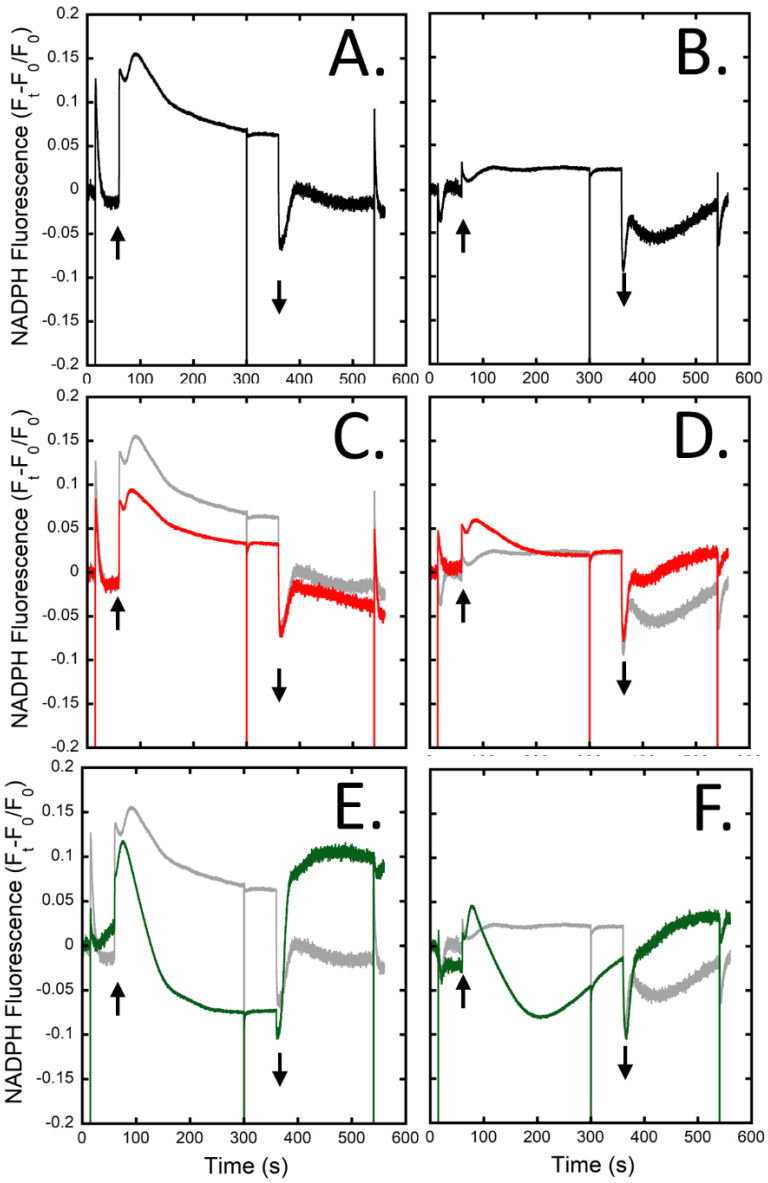

Figure 12. NADPH fluorescence kinetics distinct in strains lacking an FNR isoform. Panel A: NADPH fluorescence in the DUAL PAM-100 of dark-adapted WT cells in TCK buffer upon illumination for 5 min with 53 µmol m^{-2} s^{-1} and multiple turnover flashes before, during and after illumination (cropped here for emphasis). Arrows indicate actinic light on (up) or off (down). **Panel B:** NADPH fluorescence of the WT after treatment with KCN. The trace of the WT with and without KCN is repeated in panels C-F in grey for illustrative purposes. **Panel C**: NADPH fluorescence of the MI6 strain. **Panel D:** NADPH fluorescence of MI6 after treatment with KCN.

Panel E: NADPH fluorescence of the FS1 strain. **Panel F:** NADPH fluorescence of FS1 after treatment with KCN.

5.3.3 The presence of FNR_S enhances NDH-1 powered proton pumping

To investigate the ability of these strains to power CEF-driven proton pumping and assess the possibility that Fd is indeed being reduced by the strong NADPH oxidation seen in FS1 to power CEF, proton pumping upon actinic illumination was measured by acridine orange (AO) fluorescence quenching. This assay was performed essentially as described previously (Chapter IV), however the buffer used included 25mM KCl (TCK buffer) rather than 25mM NaCl (TCN). Switching the buffer dramatically reduced the rates of AO quenching (**Fig. 13**). The fast rate of quenching in the TCN buffer was further shown to be Na^+ gradient-dependent as the addition of the Na^+ ionophore, monensin (50µM), dissipating Na^+ gradients, reduced the rates to approximately those seen in TCK buffer. As discussed below, subtler changes in AO fluorescence quenching may be observed in TCK buffer, and it enhances the relative proportion of CEF-driven PMF formation. Because NDH-1 complexes have been shown to be the primary contributors to CEF-driven proton pumping in the dark-light transition in cells treated with DCMU (Chapter IV), and their primary reductant source is reduced Fd (Zhang *et al.* 2020), the action of FNR_S as an NADPH oxidizer should be most clearly seen when PSII is inhibited. The background inhibitors KCN, valinomycin, and DCCD were utilized as described previously to allow for measurement of near-maximal rates of proton pumping (Chapter IV). In dark adapted cells, the WT and FS1 have similar rates of PMF formation when treated with the background inhibitors or even with DCMU (**Fig. 14A,B, Table 3**). On the other hand, the ability of MI6 to establish PMF upon illumination was greatly diminished both with and without DCMU (**Fig. 14C, Table 3**), with very little CEF-driven proton pumping in the DCMU-treated samples. Overall, the ability for either CEF or LEF to drive ΔpH formation in MI6 was greatly diminished compared to that of the WT or FS1.

Repeated illumination of a sample in these conditions increased rates (not shown). To observe the effect of pre-illumination on photosynthetic electron flow driven proton pumping, cells were pre-illuminated for 2 minutes at 600 μmol m^{-2} s^{-1}, stirred in darkness for 4 minutes, then measured for the typical 15 sec illuminations. As seen in **Fig. 15** and **Table 3**, pre-illumination of the cells resulted in generally increased rates of proton pumping compared to dark-adapted cells (**Fig. 14**) in all conditions in all strains tested. The WT increased ~33% both with and without DCMU, indicating that the same process affects this rate increase. The MI6 increased dramatically in rates, essentially matching those of the WT (**Fig 15C, Table 3**). Rates of FS1 proton pumping also increased dramatically, with proton pumping rate outpacing the WT and MI6 both with and without DCMU (**Fig. 15C, Table 3**). In the WT, the proportion of CEF to LEF was not enhanced by pre-illumination, with a rate in the presence of DCMU ~50% that of the rate without DCMU regardless of pre-treatment. Results from MI6 show that pre-illumination more dramatically affects the CEF-dependent proton pumping rate, which increased nearly six-fold compared to the about two-fold increase of the rate when PSII is active (**Table 3**). FS1 also exhibits a dramatic increase in both LEF and, especially, CEF-dependent proton pumping approximately doubling and tripling, respectively, in comparison to the corresponding rates in dark-adapted samples (**Fig. 15B, Table 3**). Moreover, these rates are each considerably greater than the corresponding rates in the WT, underlining the large contribution of the FNR_S isoform to proton pumping.

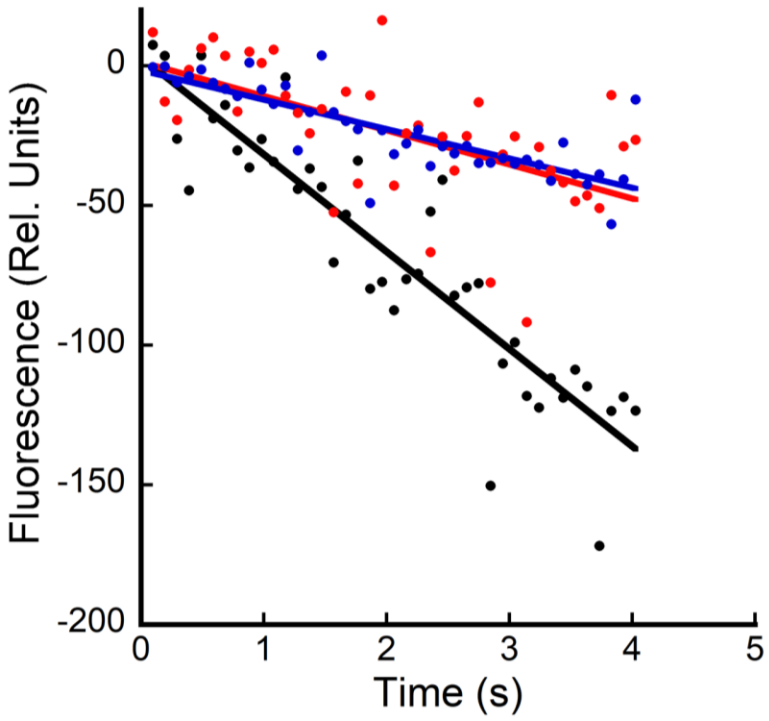

Figure 13. Acridine orange fluorescence quenching of WT cells treated with monensin in TCN buffer decreases rate to that seen in TCK buffer. Acridine orange fluorescence of dark-adapted WT cells in the JTS-100 in response to the presence of monensin in TCN buffer. Cells were dark adapted with acridine orange (5µM) for 20 min in either TCN buffer (black, red) or TCK buffer (blue). For samples in TCN buffer, a sample was prepared with KCl (150mM) plus Val (10µM), DCCD (500µM), and KCN (200µM) and stirred in the dark for 5 min (black trace) or with the addition of 50µM monensin (red). A sample in TCK buffer with the addition of Val (10µM), DCCD (500µM), and KCN (200µM) was otherwise treated the same as the black trace (blue trace).

Table 3. Relative rates of acidification in dark and light adapted states. The rate of acidification, j_{H^+}, upon illumination in WT, FS1, and MI6 in the presence of the background inhibitors with either no additional inhibitors, with DCMU, or DCMU and CCCP added. Values are averages of three technical replicates per condition. Data is presented with the standard deviation. Data normalized to [Chl]/OD_{750} of the WT to account for differences in the Chl content

per cell in the different strains. Rates are divided into either dark-adapted conditions (top) or light-adapted conditions (bottom).

	Inhibitors added	Wild-type	FS1	MI6
Dark-adapted	Val+DCCD+KCN	11.78 ± 0.74 s^{-1}	9.57 ± 0.63 s^{-1}	5.85 ± 2.28 s^{-1}
	Val+DCCD+KCN+DCMU	6.15 ± 1.17 s^{-1}	5.44 ± 1.17 s^{-1}	1.64 ± 0.81 s^{-1}
	Val+DCCD+KCN+DCMU+CCCP	0.31 ± 1.19 s^{-1}	0.0056 ± 0.38 s^{-1}	-0.56 ± 0.28 s^{-1}
Light-adapted	Val+DCCD+KCN	15.25 ± 1.20 s^{-1}	22.88 ± 5.94 s^{-1}	13.82 ± 0.95 s^{-1}
	Val+DCCD+KCN+DCMU	8.43 ± 0.76 s^{-1}	17.24 ± 5.11 s^{-1}	9.18 ± 5.30 s^{-1}
	Val+DCCD+KCN+DCMU+CCCP	-0.43 ± 0.15 s^{-1}	0.18 ± 0.38 s^{-1}	-0.74 ± 1.34 s^{-1}

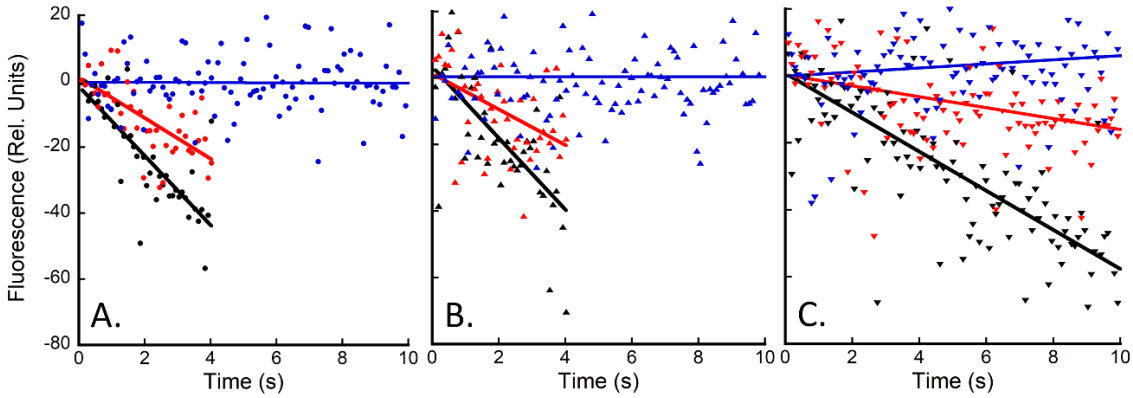

Figure 14. Rates of acidification, j_H^+, upon illumination of dark-adapted WT, FS1, and MI6. Acridine orange fluorescence of dark-adapted cells in the JTS-100. Cells were dark adapted with acridine orange (5µM) for 20 min in TCK buffer. Sample was prepared with Val (10µM), DCCD (500µM), and KCN (200µM) and stirred in the dark for 5 min as the background inhibitors. Actinic illumination (630 nm, 600 µE) was applied for 15 seconds for measurement. These plots are typical of 3 technical replicates. WT (A), FS1 (B), and MI6 (C) after treatment with the background inhibitors (black symbols), 10µM DCMU (red symbols), or DCMU and 250µM CCCP (blue

symbols). Data was normalized to the [Chl]/OD of the WT to account for differences in [Chl] per cell.

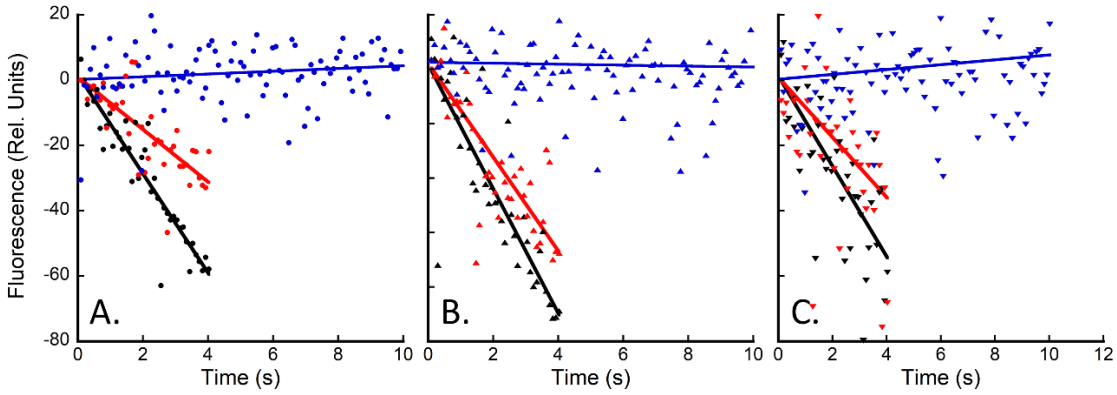

Figure 15. Rates of acidification, j_H^+, upon illumination of light-adapted WT, FS1, and MI6. Acridine orange fluorescence of dark-adapted cells in the JTS-100. Cells were dark adapted with acridine orange (5µM) for 20 min in TCK buffer. Sample was prepared with Val (10µM), DCCD (500µM), and KCN (200µM) and stirred in the dark for 5 min as the background inhibitors. After the addition of inhibitors, cells were pre-illuminated with 600 µmol m^{-2} s^{-1} actinic light for 2 min, and cells afforded 4 min in the dark before measurement with 15 sec of illumination at the same light intensity. These plots are typical of 3 technical replicates. WT (**A**), FS1 (**B**), and MI6 (**C**) after treatment with the background inhibitors (black symbols), 10µM DCMU (red symbols), or DCMU and 250µM CCCP (blue symbols). Data was normalized to the [Chl]/OD of the WT to account for differences in [Chl] per cell.

5.4 Discussion

The roles of FNR isoforms in electron transport pathways

The FNR isoforms in cyanobacteria, despite having small differences in their kinetics *in vitro* (Korn *et al.* 2009), have very different roles in the regulation of the redox state of the NADPH/Fd pools. FS1 has a higher $NADP^+$/NADPH ratio and does not exhibit a changed PSII/PSI ratio (Korn *et al.* 2009), indicating that the FNR_S isoform is involved in the reduction of Fd over the reduction of NADPH when it is the primary isoform. This was not the case in the

WT, which, under normal growth conditions, has a much larger proportion of FNR_L (Thomas *et al.* 2006), the isoform possessed by the MI6 mutant. Detectable amounts of the FNR_S isoform are present only during nutrient or light stress conditions (Thomas *et al.* 2006). When the WT was exposed to conditions of high light or low CO_2, conditions that enhance CEF (Deng *et al.* 2003), the FNR_S isoform constitutes approximately half the total amount of FNR in species that can express both isoforms (Thomas *et al.* 2006).

Consistent with earlier work (Korn 2010), it was shown that cyclic electron flow is enhanced in FS1, containing only FNR_S (**Fig. 1E, 10, 11**). This was determined by observing the post-illumination rise of chlorophyll fluorescence which has two main components: a fast rise associated with CEF and NDH-1, and a slower rise associated with carbohydrate oxidation (Holland *et al.* 2015). In FS1, a 5 min illumination produces a higher level of reduction in the PQ pool over the course of illumination to a more reduced steady-state, rather than oxidation to a steady-state like in the WT (**Fig. 9E**). This is indicative of enhanced flow of electrons into the PQ pool over the course of illumination. Upon cessation of illumination, there was a strong rise in FS1, but not in the WT or MI6 (**Fig. 9A, C, E**), indicative of increased electron flow to the PQ pool in the dark. When treated with KCN, the PQ pool generally reduces over the course of illumination, to a point near $F_{m'}$ in the WT, slightly in MI6, and slowly and steadily in FS1 (**Fig. 9B, D, F**). After illumination, each of the strains exhibits a strong post-illumination rise at similar rates, however FS1 had the largest rise of the three strains (**Fig. 10, 11**). To observe the rise without inhibition of COX, a shorter illumination that avoids the activation of the competing CBB cycle, and thus consumption of Fd_{red} and NADPH, was performed on dark adapted cells, and again FS1 was shown to have the largest rise in terms of magnitude, yet rises at approximately the same rate as the WT (**Fig. 11**, black and green). The MI6 strain had a small shoulder that declined well before FS1 or the WT started to oxidize PQ pool oxidation (**Fig. 11**, red). These results support the hypothesis established previously that FNR_S contributes more

strongly to cyclic electron flow than does FNR_L (Thomas *et al.* 2006, Korn *et al.* 2009, Korn 2010). Because the post-illumination rise is associated with NDH-1 activity (Battchikova *et al.* 2011, Holland *et al.* 2015, Artier *et al.* 2018, Zhang *et al.* 2020), and because NDH-1 complexes depend on Fd_{red} to power their proton pumping activity (Zhang *et al.* 2020), the oxidation state of the NADPH pool during illumination was investigated side-by-side with chlorophyll fluorescence.

The WT and MI6 had similar kinetics of NADPH fluorescence in the absence of KCN, with the WT having overall higher fluorescence during illumination, indicating a slightly more reduced NADPH pool during illumination (**Fig. 12A, C**). Their post-illumination rise, associated with carbohydrate oxidation, was similar in both, being slightly larger in the WT. The FS1 mutant, on the other hand, had strikingly unique kinetics. It had a sharp rise in fluorescence after illumination, shifted ~15 sec earlier than the peaks seen in WT and MI6 (**Fig. 12E**). This might be FNR_S operating as an NADPH reductase early in illumination due to a large influx of photosynthetically reduced Fd. Because the CBB cycle is regulated by the redox state of the NADPH pool, activating upon high levels of reduction (Tamoi *et al.* 2005), this could explain the shifting of the oxidation of the NADPH pool by CBB activity to an earlier point in FS1 (**Fig. 12E**). There was steady oxidation of NADPH after this initial peak that was sharper in its fluorescence decline than in the WT or MI6. This is likely due to CBB cycle activity drawing down NADPH, the activity of flavodiiron proteins and COX, as well as Fd reduction by FNR_S. This oxidation state of the NADPH pool then reaches a steady state where it was consumed as fast as it was produced with a higher $NADP^+$/NADPH ratio than the WT or MI6 in the same conditions, matching earlier data (Korn *et al.* 2009, Korn 2010). Post-illumination, FS1 was also interesting in these conditions, with a large post-illumination rise (**Fig. 12E**). It is unlikely that this peak can only be due to increased sugar oxidation activity, and that FNR_S was also acting to dissipate the reduced Fd now that it was no longer being photosynthetically produced at that

point. Upon treatment with KCN, the WT pool was almost entirely reduced in the dark, with little increase in fluorescence seen when illuminated (**Fig. 12B**). This was maintained throughout illumination and was followed by a small post-illumination rise. The MI6 has similar kinetics as it had before treatment with KCN, however fluorescence does not increase as much upon illumination (**Fig. 12D**). It reaches a steady state after the slow oxidation of NADPH by the CBB cycle, and post-illumination experiences a large increase in fluorescence. The FS1 had its fast reduction of NADPH followed by a rapid oxidation, though this was not as rapid as without KCN (**Fig. 12F**). After ~2.5 min, a trough was seen in fluorescence and it slowly and steadily rises for the rest of illumination. Due to the lack of COX as an electron sink in these conditions, it is possible that the slower oxidation followed by steady reduction of NADPH could be due to a strong reduction of both NADPH and Fd pools, which would result in a slower exchange of electrons between the two as they become further reduced. The slow rise could then be the FNR_S operating to reduce NADPH in conditions where Fd is overreduced, though still being consumed to balance reductant.

The roles of FNR isoforms in the establishment of proton motive force

The establishment of proton motive force in cyanobacteria is dependent upon photosynthetic electron transport upon illumination. When PSII is inhibited, the major driver of proton pumping by CEF-driven electron transport is NDH-1 (Chapter IV). Because NDH-1 is dependent upon Fd_{red} to supply electrons (Zhang *et al.* 2020), the ability to establish the proton gradient in the absence of PSII activity is indicative of the Fd reduction state. When dark-adapted, the WT has its fastest rate when PSII is active, with the addition of DCMU decreasing the rate by ~50% (**Fig. 14A, Table 3**). FS1 was similar in rates to the WT in these conditions (**Fig. 14B, Table 3**), while the rates in MI6 were severely reduced (**Fig. 14C, Table 3**), achieving only ~50% the rate of the WT when PSII is active. When PSII is inhibited, its rate is only 28% the rate of MI6 without DCMU, indicating a severe inhibition of CEF in these conditions for MI6, likely due to a lack of Fd_{red} for consumption. These data indicate that FNR_S is an important component

in the shifting from dark to light conditions, providing reductant for CEF and contributing to the formation of PMF, even when PSII is active.

Because repeated illumination of the same sample was seen to cause increases in the rate of AO quenching, a pre-illumination of 600 µmol m^{-2} s^{-1} over a period of 2 min was applied to the cells, followed by darkness for 4min and then measurement of the typical 15 sec illuminations at 600 µmol m^{-2} s^{-1}. This caused rate increases in all the strains measured. The rates in the WT increased by ~33% with and without DCMU, indicating the same process is responsible for this increase (**Fig. 15A, Table 3**). The MI6 mutant had dramatic increases in rate, nearly matching the WT after pre-illumination (**Fig. 15C, Table 3**). The FS1 mutant, however had the most dramatic increase in rate, more than doubling without DCMU, and tripling with DCMU (**Fig. 15B, Table 3**). When treated with DCMU, FS1 was able to achieve ~70% the rate without DCMU, a dramatic increase from the dark-adapted state. These data indicate that the pre-illumination period in the presence of the background inhibitors results in the accumulation of reductant which may then be consumed to generate PMF. Because the FS1 strain, containing only FNR_S, has such a dramatically increased rate compared to its counterparts, the FNR_a isoform must be providing Fd_{red} for consumption, as it also possesses a heavily oxidized NADPH pool. Because the pre-illumination also increased the rate in MI6, did so to near WT levels, and is the primary FNR isoform present in cells in normal growth conditions, it is clear that this subunit is able to provide Fd_{red} for CEF and is the likely isoform doing so in the WT, but only after a period of illumination to adapt to the new redox conditions. This indicates that these isoforms have different functions in maintaining the redox state of the NADP(H)/Fd pools.

Hypothesized roles of FNR isoforms in vivo

The presence of alternately regulated FNR isoforms in cyanobacteria capable of heterotrophy suggests that they have different roles in their maintenance of the NADPH/Fd redox state. Because the NADPH pool is oxidized over the course of illumination in a mutant

expressing only FNR_S (**Fig. 12E**), it has enhanced CEF (**Fig. 10, 11**), and it allows for enhanced CEF-driven proton pumping both with and without adaptation to light (**Fig. 14, 15, Table 3**). This suggests that FNR_S is primarily involved in NADPH oxidation/Fd reduction, as Fd_{red} is the source of reductant for NDH-1 complexes, the primary driver of proton pumping in the dark-light transition (Chapter IV). This also suggests that FNR_S is useful in the transition from dark to light, allowing faster adaptation to the light and establishing PMF more quickly to utilize the energy produced. When FNR_L is the only isoform present, the establishment of PMF is slowed until fully adapted to illumination where it approaches WT rates of AO quenching. The data then suggest that FNR_S is useful for allowing for fast adaptation to illumination and likely provides reductant for proton pumping through carbohydrate oxidation in the dark, and FNR_L is useful for long-term adaptation to illumination and may be used to reduce Fd for CEF given time in the light. The roles suggested here also raise a question of whether cyanobacteria that possess both FNR_L and FNR_S have a more robust response to fluctuating light conditions than do species that only possess FNR_L.

5.5 Conclusions

The FNR isoforms present in cyanobacteria capable of heterotrophy present an interesting and poorly understood system for regulating the redox state of the NADPH/Fd pools. The soluble FNR_S is utilized *in vivo* most generally as an NADPH oxidase in the light, allowing for rapid adaptation to the dark-light transition and produce a proton gradient quickly. This may allow these bacteria to more rapidly acclimate to altered conditions of photosynthetic electron flow. Alternatively, the FNR_L isoform attached to the PBS is mostly involved in the reduction of $NADP^+$ and may be utilized to reduce Fd when enough reductant as NADPH is available, allowing powering of NDH-1 and CEF proton pumping. The genetic redundancy of these isoforms suggests that there is a functional reason these isoforms are kept in some cyanobacteria,

and perhaps it allows these cyanobacteria capable of heterotrophy to more readily adapt to changes in the environment that affect the internal redox pools.

CHAPTER VI

CONCLUSION

6.1 Conclusions

The focus of this dissertation is on investigating the kinetics and contributions to the coupling mechanism between photosynthetic electron transport and the establishment of the proton motive force across the thylakoid membrane, which is used to drive the synthesis of ATP. To accomplish this, I was able to develop techniques to monitor the formation of the PMF by tracking the ΔpH component under conditions that shift the balance of the two interchangeable energetic components of the pmf, the electrical ($\Delta\psi$) and the proton concentration (ΔpH), towards ΔpH and utilize a fluorescent dye, acridine orange (AO) as a spectroscopic probe of changes in ΔpH. Moreover, I was able to combine this observational tool with more well-established spectroscopic probes of photosynthetic electron transport including chlorophyll fluorescence and NADPH fluorescence. These tools were then applied to the analysis of specific mutants of electron transport proteins that were known or hypothesized to be involved in the important, yet poorly understood process of cyclic electron flow (CEF). As noted, CEF is important in plants, algae, and cyanobacteria in tuning the output ratio of reducing and phosphorylating power, depending on changing cellular demands for NADPH and ATP. In Chapter IV, I presented evidence for CEF-driven proton pumping through cyanobacterial NDH-1 complexes and showed that they are major contributors to the formation of ΔpH in the dark-light transition. This data showed that the primary contributor to ΔpH formation is the water oxidation

activity of PSII, being the only source of light-induced ΔpH formation in the mutant M55, lacking functional NDH-1 complexes. The NDH-1 complexes were then shown to be the primary sources of proton pumping in the dark-light transition when PSII was inhibited, able to compensate for the loss of PSII by achieving ~40% of the uninhibited rate in the WT, highlighting the importance of NDH-1 complexes in the recycling of electrons via CEF. The role of the NDH-$1_{1/2}$ complexes was also highlighted as being the NDH-1 complexes mostly responsible for electron flow driven proton pumping as the inactivation of NDH-$1_{1/2}$ complexes by deletion of the *ndhF1* gene did not fully eliminate CEF-driven proton pumping, but did inhibit it severely.

To further investigate the mechanisms that allow CEF to power proton pumping by NDH-1 complexes, the roles of the FNR isoforms in *Synechocystis* sp. PCC 6803 were investigated in Chapter V with respect to the redox states of the PQ and NADPH pools as well as proton pumping activity. Two mutants were utilized, each lacking either the PBS-associatedFNR_L or the soluble FNR_S. The data in this chapter illustrated that these two isoforms have different functional roles despite being produced from the same gene at different translation start sites (Thomas *et al.* 2006). The FNR_S isoform functions primarily as an NADPH oxidase and provides Fd to enhance CEF via NDH-1. The FNR_L isoform, on the other hand, operates primarily as an $NADP^+$ reductase, though will operate as an NADPH oxidase after sustained (10's of seconds) exposure to actinic illumination. We also showed that proton pumping activity in the absence of PSII was dramatically enhanced by the presence of FNR_S, further implicating it in supplying reductant for CEF. The expression of the FNR_S isoform has been previously shown to increase in conditions of heterotrophy or stress such as high light exposure, conditions which increase CEF demands. The hypothesis was developed that FNR_S is utilized to power heterotrophic metabolism to aid in the transition and acclimation to fluctuations in light. The FNR_L isoform on the other hand is effective on a longer scale of illumination, being the primary photoautotrophic isoform and acting

primarily as an $NADP^+$ reductase until enough reductant is produced to push the reaction in the opposite direction. The results described in this study brings insights into the coupling and energetics of CEF to the driving of NDH-1 proton pumping, as well as shedding light on the system that mediates the supply of electrons to NDH-1 and other components of photosynthetic electron flow.

6.2 Future directions

This work opens a door for further work to be done on understanding the establishment of proton motive force in cyanobacteria. The techniques developed here may be utilized to understand the mechanisms of the cyanobacterial NDH-1 complexes, and particularly that of the complexes that hydrate CO_2 for later fixation, the NDH-$1_{3/4}$ complexes. These complexes have only recently had their structures determined, and there are surprising components in the active sites of the carbonic anhydrase-like subunits. Proton pumping assays, in combination with fluorescence and CO_2 uptake assays, could yield invaluable information on the mechanisms behind these complexes, potentially providing the groundwork for biomimetic CO_2 scrubbing technologies.

The roles of the FNR isoforms in the balancing of electron carriers is a subject that has been little explored but may yield some interesting insights about the fundamentals of photosynthetic electron flow as well as the evolution of photosynthesis. It remains unclear why some cyanobacteria have retained the isoform and others have not. Heterotrophy is a common thread for many of the species that possess both isoforms, however it is not only in those capable of heterotrophy. The utilization of the FNR_S isoform in stressful conditions such as fluctuating light, low carbon, or high light may indicate that strains possessing this isoform may outperform strains that lack it in terms of adapting to the stressors.

Toward the end of my thesis work, I was able to observe that excluding Na^+ from the cellular environment strongly influences the apparent rate at which proton pumping across the

thylakoids. Based upon the observation that the Na^+ ionophore monesin produces the same effect in Na^+-containing buffer, it is clear that a ΔNa^+ across either the cytoplasmic or thylakoid membrane is required to produce maximal rates of proton pumping across the thylakoids. Moreover, the in the absence of repeated illuminations when the Na^+ gradient is present, but the formation of the ΔpH gradient remains unaffected by pre-illumination when there is a Na^+ gradient suggesting that whatever physiological paremeter is being affected by the absence of a ΔNa^+ can be mitigated, but not overcome by some product of photosynthetic activity. Since a ΔNa^+ is know to be critical for cytoplasmic pH homeostasis in cyanobacteria (Ritchie 1998), perhaps monitoring cytoplasmic pH would be worthwhile. Overall, physiological basis for these intriguing phenomenon remains unknown and thus bears further investigation.

REFERENCES

Alberts, B., A. Johnson, J. Lewis, D. Morgan, M. Raff, K. Roberts and P. Walter (2017). Molecular Biology of the Cell, W.W. Norton.

Aleem, M. I. H. (1966). "Generation of reducing power in chemosynthesis. II. Energy linked reduction of pyridine nucleotides in the chemoautotroph, *Nitrosomonas europaea*." *Biochem Biophys Acta* **113**(2): 216-224.

Allen, J. F. (2002). "Photosynthesis of ATP - elecrons, proton pumps, rotors, and poise." *Cell* **110**: 273-276.

Allen, M. M. (1968). "Simple conditions for growth of unicellular blue-green algae on plates." *J Phycol* **4**: 1-4.

Arnon, D. I., F. R. Whatley and M. B. Allen (1954). "Photosynthesis by isolated chloroplasts. II. Photosynthetic phosphorylation, the converstion of light into phosphate bond energy." *J. Am. Chem. Soc* **43**(24): 6324-6329.

Artier, J., S. C. Holland, N. Miller, M. Zhang and R. L. Burnap (2018). "Synthetic DNA system for structure function studies of the high affinity CO_2 uptake (CupA) protein complex in cyanobacteria." *BBA - Bioenergetics* **1859**(10): 1108-1118.

Baird, T. T., A. Waheed, T. Okuyama, W. S. Sly and C. A. Fierke (1997). "Catalysis and inhibition of human carbonic anhydrase IV." *Biochemistry* **36**: 2669-2678.

Baradaran, R., J. M. Berrisford, G. S. Minhas and L. A. Sazanov (2013). "Crystal structure of the entire respiratory complex I." *Nature* **494**: 443-448.

Barber, J. and M. D. Archer (2001). "P680, the primary electron donor of photosystem II." *J Photochem Photobiol A* **142**: 97-106.

Battchikova, N., M. Eisenhut and E. M. Aro (2011). "Cyanobacterial NDH-1 complexes: novel insights and remaining puzzles." *Biochim Biophys Acta* **1807**(8): 935-944.

Battchikova, N., L. Wei, L. Du, L. Bersanini, E. M. Aro and W. Ma (2011). "Identification of novel Ssl0352 protein (NdhS), essential for efficient operation of cyclic electron transport around photosystem I, in NADPH:plastoquinone oxidoreductase (NDH-1) complexes of Synechocystis sp. PCC 6803." *J Biol Chem* **286**(42): 36992-37001.

Belkin, S., R. J. Mehlhorn and L. Packer (1987). "Proton gradients in intact cyanobacteria." *Plant Physiol* **84**: 25-30.

Bernat, G., J. Appel, T. Ogawa and M. Rogner (2011). "Distinct roles of multiple NDH-1 complexes in the cyanobacterial electron transport network as revealed by kinetic analysis of P700+ reduction in various Ndh-deficient mutants of Synechocystis sp. strain PCC6803." *J Bacteriol* **193**(1): 292-295.

Berrisford, J. M. and L. A. Sazanov (2009). "Structural basis for the mechanism of respiratory complex I." *J Biol Chem* **284**(43): 29773-29783.

Bhatti, A. F., R. R. Choubeh, D. Kirilovsky, E. Wientjes and H. van Amerongen (2020). "State transitions in cyanobacteria studied with picosecond fluorescence at room temperature." *Biochim Biophys Acta Bioenerg* **1861**(10): 148255.

Boone, C. D., M. Pinard, R. McKenna and D. Silverman (2014). Catalytic mechanism of alpha-class carbonic anhydrases: CO_2 hydration and proton transfer. Carbonic anhydrase: mechanism, regulation, links to disease, and industrial applications. S. C. Frost and R. McKenna. Springer Dordrecht Heidelberg New York London, Springer Science+Business Media Dordrecht.

Brandt, U. (2011). "A two-state stabilization-change mechanism for proton-pumping complex I." *Biochim Biophys Acta* **1807**(10): 1364-1369.

Campbell, D., V. Hurry, A. K. Clarke, P. Gustafsson and G. Öquist (1998). "Chlorophyll fluorescence analysis of cyanobacterial photosynthesis and acclimation." *Microbiol Mol Biol Rev* **62**(3): 667-683.

Chadwick, G. L., J. Hemp, W. W. Fischer and V. J. Orphan (2018). "Convergent evolution of unusual complex I homologs with increased proton pumping capacity: energetic and ecological implications." *ISME J* **12**(11): 2668-2680.

Checchetto, V., A. Segalla, G. Allorent, N. La Rocca, L. Leanza, G. M. Giacometti, N. Uozumi, G. Finazzi, E. Bergantino and I. Szabo (2012). "Thylakoid potassium channel is required for efficient photosynthesis in cyanobacteria." *Proc Natl Acad Sci U S A* **109**(27): 11043-11048.

Checchetto, V., E. Teardo, L. Carraretto, E. Formentin, E. Bergantino, G. M. Giacometti and I. Szabo (2013). "Regulation of photosynthesis by ion channels in cyanobacteria and higher plants." *Biophys Chem* **182**: 51-57.

Cooley, J. W. and W. F. Vermaas (2001). "Succinate dehydrogenase and other respiratory pathways in thylakoid membranes of Synechocystis sp. strain PCC 6803: capacity comparisons and physiological function." *J Bacteriol* **183**(14): 4251-4258.

Cooley, R. B., D. J. Arp and P. A. Karplus (2010). "Evolutionary origin of a secondary structure: pi-helices as cryptic but widespread insertional variations of alpha-helices that enhance protein functionality." *J Mol Biol* **404**(2): 232-246.

Debus, R. J., K. A. Campbell, W. Gregor, Z. L. Li, R. L. Burnap and R. D. Britt (2001). "Does Histidine 332 of the D1 polypeptide ligate the Manganese cluster in photosystem II? An electron spin echo envelope modulation study." *Biochemistry* **40**(12): 3690-3699.

Deng, Y., J. Ye and H. Mi (2003). "Effects of low CO_2 on NAD(P)H dehydrogenase, a mediator of cyclic electron transport around Photosystem I in the cyanobacterium *Synechocystis* PCC6803." *Plant Cell Physiol* **44**(5): 534-540.

Di Luca, A., A. P. Gamiz-Hernandez and V. R. I. Kaila (2017). "Symmetry-related proton transfer pathways in respiratory complex I." *PNAS* **114**(31): E6314-E6321.

Dismukes, G. C., R. Brimblecombe, G. A. N. Felton, R. S. Pryadun, J. E. Sheats, L. Spicca and G. F. Swiegers (2009). "Development of bioinspired Mn_4O_4-cubane water oxidation catalysts: lessons from photosynthesis." *Acc. Chem. Res.* **42**(12): 1935-1943.

Eaton-Rye, J. J. (2011). "Construction of gene interruptions and gene deletions in the cyanobacterium Synechocystis sp. strain PCC 6803." *Methods Mol Biol* **684**: 295-312.

Efremov, R. G. and L. Sazanov (2012). Structure of Complex I. A Structural Perspective on Respiratory Complex I. L. Sazanov, Springer Netherlands**:** 3-21.

Efremov, R. G. and L. A. Sazanov (2011). "Structure of the membrane domain of respiratory complex I." *Nature* **476**(7361): 414-420.

Elanskaya, I. V., A. A. Bulychev, E. P. Lukashev and E. M. Muronets (2021). "Deficiency in flavodiiron protein Flv3 promotes cyclic electron flow and state transition under high light in the cyanobacterium Synechocystis sp. PCC 6803." *Biochimica et Biophysica Acta (BBA) - Bioenergetics* **1862**(1): 148318.

Falkner, G., F. Horner, K. Werdan and H. W. Heldt (1976). "pH Changes in the Cytoplasm of the Blue-Green Alga Anacystis nidulans Caused by Light-dependent Proton Flux into the Thylakoid Space." *Plant Physiology* **58**(6): 717.

Falkner, G., F. Horner, K. Werdan and H. W. Heldt (1976). "pH changes in the cytoplasm of the blue-green alga *Anacystis nidulans* caused by light-dependent proton flux into the thylakoid space." *Plant Physiol* **58**: 717-718.

Fato, R., E. Estornell, S. D. Bernardo, F. Pallotti, G. P. Castelli and G. Lenaz (1996). "Steady-state kinetics of the reduction of coenzyme Q analogs by complex I (NADH:ubiquinone oxidoreductase) in bovine heart mitochondria and submitochondrial particles." *Biochemistry* **35**: 2705-2716.

Fedor, J. G., A. J. Y. Jones, A. Di Luca, V. R. I. Kaila and J. Hirst (2017). "Correlating kinetic and structural data on ubiquinone binding and reduction by respiratory complex I." *Proc Natl Acad Sci U S A* **114**(48): 12737-12742.

Fischer, W. W., J. Hemp and J. E. Johnson (2016). "Evolution of Oxygenic Photosynthesis." *Annual Review of Earth and Planetary Sciences* **44**(1): 647-683.

Fisher, N., T. M. Bricker and D. M. Kramer (2019). "Regulation of photosynthetic cyclic electron flow pathways by adenylate status in higher plant chloroplasts." *Biochim Biophys Acta Bioenerg* **1860**(11): 148081.

Folea, I. M., P. Zhang, M. M. Nowaczyk, T. Ogawa, E. M. Aro and E. J. Boekema (2008). "Single particle analysis of thylakoid proteins from Thermosynechococcus elongatus and Synechocystis 6803: localization of the CupA subunit of NDH-1." *FEBS Lett* **582**(2): 249-254.

Fujita, Y., A. Murakami, K. Ohki and N. Hagiwara (1988). "Regulation of Photosystem Composition in Cyanobacterial Photosynthetic System: Evidence Indicating that Photosystem I Formation is Controlled in Response to the Electron Transport State." *Plant and Cell Physiology* **29**(4): 557-564.

Galkin, A., S. Drose and U. Brandt (2006). "The proton pumping stoichiometry of purified mitochondrial complex I reconstituted into proteoliposomes." *Biochim Biophys Acta* **1757**(12): 1575-1581.

Galkin, A. S., V. G. Grivennikova and A. D. Vinogradov (1999). "$H^+/2e^-$ stoichiometry in NADH-quinone reductase reactions catalyzed by bovine heart submitochondrial particles." *FEBS Lett* **451**: 157-161.

Gao, F., J. Zhao, L. Chen, N. Battchikova, Z. Ran, E. M. Aro, T. Ogawa and W. Ma (2016). "The NDH-1L-PSI Supercomplex Is Important for Efficient Cyclic Electron Transport in Cyanobacteria." *Plant Physiol* **172**(3): 1451-1464.

Gao, F., J. Zhao, X. Wang, S. Qin, L. Wei and W. Ma (2016). "NdhV Is a Subunit of NADPH Dehydrogenase Essential for Cyclic Electron Transport in Synechocystis sp. Strain PCC 6803." *Plant Physiol* **170**(2): 752-760.

Gibson, D. G., L. Young, R. Y. Chuang, J. C. Venter, C. A. Hutchison, 3rd and H. O. Smith (2009). "Enzymatic assembly of DNA molecules up to several hundred kilobases." *Nat Methods* **6**(5): 343-345.

Haapanen, O. and V. Sharma (2018). "A modeling and simulation perspective on the mechanism and function of respiratory complex I." *Biochim Biophys Acta Bioenerg* **1859**(7): 510-523.

He, Z., F. Zheng, Y. Wu, Q. Li, J. Lv, P. Fu and H. Mi (2015). "NDH-1L interacts with ferredoxin via the subunit NdhS in Thermosynechococcus elongatus." *Photosynth Res* **126**(2-3): 341-349.

Herranen, M., N. Battchikova, P. Zhang, A. Graf, S. Sirpio, V. Paakkarinen and E. M. Aro (2004). "Towards functional proteomics of membrane protein complexes in Synechocystis sp. PCC 6803." *Plant Physiol* **134**(1): 470-481.

Hirst, J. (2013). "Mitochondrial complex I." *Annu Rev Biochem* **82**: 551-575.

Holland, S. C., J. Artier, N. T. Miller, M. Cano, J. Yu, M. L. Ghirardi and R. L. Burnap (2016). "Impacts of genetically engineered alterations in carbon sink pathways on photosynthetic performance." *Algal Research* **20**: 87-99.

Holland, S. C., A. D. Kappell and R. L. Burnap (2015). "Redox changes accompanying inorganic carbon limitation in Synechocystis sp. PCC 6803." *Biochim Biophys Acta* **1847**(3): 355-363.

Jensen, P. E., R. Bassi, E. J. Boekema, J. P. Dekker, S. Jansson, D. Leister, C. Robinson and H. V. Scheller (2007). "Structure, function and regulation of plant photosystem I." *Biochim Biophys Acta* **1767**(5): 335-352.

Jones, A. J., J. N. Blaza, F. Varghese and J. Hirst (2017). "Respiratory Complex I in Bos taurus and Paracoccus denitrificans Pumps Four Protons across the Membrane for Every NADH Oxidized." *J Biol Chem* **292**(12): 4987-4995.

Kana, R., E. Kotabova, O. Komarek, B. Sediva, G. C. Papageorgiou, Govindjee and O. Prasil (2012). "The slow S to M fluorescence rise in cyanobacteria is due to a state 2 to state 1 transition." *Biochim Biophys Acta* **1817**(8): 1237-1247.

Kaneko, T., S. Sato, H. Kotani, A. Tanaka, E. Asamizu, Y. Nakamura, N. Miyajima, M. Hirosawa, M. Sugiura, S. Sasamoto, T. Kimura, T. Hosouchi, A. Matsuno, A. Muraki, N. Nakazaki, K. Naruo, S. Okumura, S. Shimpo, C. Takeuchi, T. Wada, A. Watanabe, M. Yamada, M. Yasuda and S. Tabata (1996). "Sequence analysis of the genome of the unicellular cyanobacterium *Synechocystis* sp. strain PCC6803. II. Sequence determination of the entire genome and assignment of potential protein-coding regions." *DNA Res* **3**: 109-136.

Konneke, M., D. M. Schubert, P. C. Brown, M. Hugler, S. Standfest, T. Schwander, L. Schada von Borzyskowski, T. J. Erb, D. A. Stahl and I. A. Berg (2014). "Ammonia-oxidizing archaea use the most energy-efficient aerobic pathway for CO2 fixation." *Proc Natl Acad Sci U S A* **111**(22): 8239-8244.

Korn, A. (2010). Respective roles of the ferredoxin :NADP-oxidoreductase isoforms in the cyanobacterium Synechocystis sp. PCC 6803, Université Paris Sud - Paris XI.

Korn, A., G. Ajlani, B. Lagoutte, A. Gall and P. Setif (2009). "Ferredoxin:NADP+ oxidoreductase association with phycocyanin modulates its properties." *J Biol Chem* **284**(46): 31789-31797.

Kotlyar, A. B. and A. D. Vinogradov (1990). "Slow active/inactive transition of the mitochondrial NADH-ubiquinone reductase." *Biochem Biophys Acta* **1019**(2): 151-158.

Kramer, D. M. and J. R. Evans (2011). "The importance of energy balance in improving photosynthetic productivity." *Plant Physiol* **155**(1): 70-78.

Kramer, D. M., C. A. Sacksteder and J. A. Cruz (1999). "How acidic is the lumen?" *Photosynth Res* **60**: 151-163.

Kramer, D. M., C. A. Sacksteder and J. A. Cruz (1999). "How acidic is the lumen?" *Photosynthesis Research* **60**(2): 151-163.

Laughlin, T. G., A. N. Bayne, J. F. Trempe, D. F. Savage and K. M. Davies (2019). "Structure of the complex I-like molecule NDH of oxygenic photosynthesis." *Nature* **566**(7744): 411-414.

Liu, H., D. A. Weisz, M. M. Zhang, M. Cheng, B. Zhang, H. Zhang, G. S. Gerstenecker, H. B. Pakrasi, M. L. Gross and R. E. Blankenship (2019). "Phycobilisomes harbor FNR(L) in cyanobacteria." *mBio* **10**(2).

Lucker, S., M. Wagner, F. Maixner, E. Pelletier, H. Koch, B. Vacherie, T. Rattei, J. S. Damste, E. Spieck, D. Le Paslier and H. Daims (2010). "A Nitrospira metagenome illuminates the physiology and evolution of globally important nitrite-oxidizing bacteria." *Proc Natl Acad Sci U S A* **107**(30): 13479-13484.

Luz, B. and E. Barkan (2011). "Proper estimation of marine gross O2production with17O/16O and18O/16O ratios of dissolved O2." *Geophysical Research Letters* **38**(19): n/a-n/a.

Lyons, T. W., C. T. Reinhard and N. J. Planavsky (2014). "The rise of oxygen in Earth's early ocean and atmosphere." *Nature* **506**(7488): 307-315.

Ma, W. and H. Mi (2005). "Expression and activity of type 1 NAD(P)H dehydrogenase at different growth phases of the cyanobacterium, Synechocystis PCC 6803." *Physiologia Plantarum* **125**(1): 135-140.

Maeda, S., Badger, M.R., Price G.D. (2002). "Novel gene products associated with NdhD3/D4-containing NDH-1 complexes are involved in photosynthetic CO_2 hydration in the cyanobacterium *Synechococcus* sp. PCC7942." *Mol Microbiol* **43**(2): 425-435.

Martin, W., T. Rujan, E. Richly, A. Hansen, S. Cornelsen, T. Lins, D. Leister, B. Stoebe, M. Hasegawa and D. Penny (2002). "Evolutionary analysis of Arabidopsis, cyanobacterial, and chloroplast genomes reveals plastid phylogeny and thousands of cyanobacterial genes in the nucleus." *Proc Natl Acad Sci U S A* **99**(19): 12246-12251.

Martin, W. F., D. A. Bryant and J. T. Beatty (2017). "A physiological perspective on the origin and evolution of photosynthesis." *FEMS microbiology reviews* **42**(2): 205-231.

Matsushita, K., T. Ohnishi and H. R. Kaback (1987). "NADH-ubiquinone oxidoreductase of the *Escherichia coli* aerobic respiratory chain." *Biochemistry* **26**(24): 7732-7737.

Mi, H., T. Endo, T. Ogawa and K. Asada (1995). "Thylakoid Membrane-Bound, NADPH-Specific Pyridine Nucleotide Dehydrogenase Complex Mediates Cyclic Electron Transport in the Cyanobacterium Synechocystis sp. PCC 6803." *Plant and Cell Physiology* **36**(4): 661-668.

Mi, H., T. Endo, U. Schreiber, T. Ogawa and K. Asada (1992). "Electron donation from cyclic and respiratory flows to the photosynthetic intersystem chain is mediated by pyridine nucleotide dehydrogenase in the cyanobacterium *Synechocystis* PCC 6803." *Plant Cell Physiol* **33**(8): 1233-1237.

Mi, H., C. Klughammer and U. Schreiber (2000). "Light-induced dynamic changes of NADPH fluorescence in *Synechocystis* PCC 6803 and its *ndhB*-defective mutant M55." *Plant Cell Physiol* **41**(10): 1129-1135.

Mitchell, P. C. (1961). "Coupling of phosphorylation to electron and Hydrogen transfer by a chemi-osmotic type of mechanism." *Nature* **191**: 144-148.

Moal, G. and B. Lagoutte (2012). "Photo-induced electron transfer from photosystem I to NADP(+): characterization and tentative simulation of the in vivo environment." *Biochim Biophys Acta* **1817**(9): 1635-1645.

Morales, A., X. Yin, J. Harbinson, S. M. Driever, J. Molenaar, D. M. Kramer and P. C. Struik (2018). "In Silico Analysis of the Regulation of the Photosynthetic Electron Transport Chain in C3 Plants." *Plant Physiology* **176**(2): 1247.

Mullineaux, C. W. (2014). "Co-existence of photosynthetic and respiratory activities in cyanobacterial thylakoid membranes." *Biochim Biophys Acta* **1837**(4): 503-511.

Mullineaux, C. W. (2014). "Electron transport and light-harvesting switches in cyanobacteria." *Front Plant Sci* **5**: 7.

Mullineaux, C. W. and J. F. Allen (1990). "State 1-State 2 transitions in the cyanobacterium *Synechococcus* 6301 are controlled by the redox state of electron carriers between photosystems I and II." *Photosynth Res* **23**: 297-311.

Nagarajan, A. and H. B. Pakrasi (2016). Membrane-bound protein complexes for photosynthesis and respiration in cyanobacteria. Encyclopedia of Life Sciences.

Nakamaru-Ogiso, E., M. C. Kao, H. Chen, S. C. Sinha, T. Yagi and T. Ohnishi (2010). "The membrane subunit NuoL(ND5) is involved in the indirect proton pumping mechanism of Escherichia coli complex I." *J Biol Chem* **285**(50): 39070-39078.

Nakasugi, K., C. J. Svenson and B. A. Neilan (2006). "The competence gene, comF, from Synechocystis sp. strain PCC 6803 is involved in natural transformation, phototactic motility and piliation." *Microbiology* **152**(Pt 12): 3623-3631.

Nikkanen, L., A. Santana Sanchez, M. Ermakova, M. Rogner, L. Cournac and Y. Allahverdiyeva (2020). "Functional redundancy between flavodiiron proteins and NDH-1 in Synechocystis sp. PCC 6803." *Plant J* **103**(4): 1460-1476.

Ogawa, T., T. Harada, H. Ozaki and K. Sonoike (2013). "Disruption of the ndhF1 gene affects Chl fluorescence through state transition in the Cyanobacterium Synechocystis sp. PCC

6803, resulting in apparent high efficiency of photosynthesis." *Plant Cell Physiol* **54**(7): 1164-1171.

Ogawa, T. and K. Sonoike (2015). "Dissection of respiration and photosynthesis in the cyanobacterium Synechocystis sp. PCC6803 by the analysis of chlorophyll fluorescence." *J Photochem Photobiol B* **144**: 61-67.

Ohkawa, H., H. B. Pakrasi and T. Ogawa (2000). "Two types of functionally distinct NAD(P)H dehydrogenases in Synechocystis sp. strain PCC6803." *J Biol Chem* **275**(41): 31630-31634.

Ohnishi, T. (1998). "Iron-sulfur clusters/semiquinones in complex I." *Biochem Biophys Acta* **1364**: 186-206.

Palmgren, M. G. (1991). "Acridine orange as a probe for measuring pH gradients across membranes: Mechanism and limitations." *Analytical Biochemistry* **192**(2): 316-321.

Papageorgiou, G. C. and Govindjee (2011). "Photosystem II fluorescence: slow changes--scaling from the past." *J Photochem Photobiol B* **104**(1-2): 258-270.

Papageorgiou, G. C., M. Tsimilli-Michael and K. Stamatakis (2007). "The fast and slow kinetics of chlorophyll a fluorescence induction in plants, algae and cyanobacteria: a viewpoint." *Photosynth Res* **94**(2-3): 275-290.

Peschek, G. A., T. Czerny, G. Schmetterer and W. H. Nitschmann (1985). "Transmembrane Proton Electrochemical Gradients in Dark Aerobic and Anaerobic Cells of the Cyanobacterium (Blue-Green Alga) <em>Anacystis nidulans</em&gt." *Plant Physiology* **79**(1): 278.

Peschek, G. A., T. Czerny, G. Schmetterer and W. H. Nitschmann (1985). "Transmembrane proton electrochemical gradients in dark aerobic and anaerobic cells of the cyanobacterium (blue-green alga) *Anacystis nidulans*." *Plant Physiol* **79**: 278-284.

Pogoryelov, D., C. Reichen, A. L. Klyszejko, R. Brunisholz, D. J. Muller, P. Dimroth and T. Meier (2007). "The oligomeric state of c rings from cyanobacterial F-ATP synthases varies from 13 to 15." *J Bacteriol* **189**(16): 5895-5902.

Price, G. D., S. Maeda, T. Omata and M. R. Badger (2002). "Modes of active inorganic CO_2 uptake in the cyanobacterium, *Synechococcus* sp. PCC7942." *Funct. Plant Biol.* **29**: 131-149.

Ranjbar Choubeh, R., E. Wientjes, P. C. Struik, D. Kirilovsky and H. van Amerongen (2018). "State transitions in the cyanobacterium Synechococcus elongatus 7942 involve reversible quenching of the photosystem II core." *Biochim Biophys Acta Bioenerg* **1859**(10): 1059-1066.

Renger, G., U. Schreiber, J. Amesz and D. Fork (1986). Practical applications of fluorometric methods to algae and higher plant research. Light emission by plants and bacteria. Govindjee. Orlando, USA, Academic Press**:** 589-616.

Ritchie, R. J. (1998). "Bioenergetics of membrane transport in *Synechococcus* R-2 (*Anacystis nitulans*, *S. leopoliensis*) PCC7942." *Can. J. Bot.* **76**: 1127-1145.

Ritchie, R. J. (2006). "Consistent sets of spectrophotometric chlorophyll equations for acetone, methanol and ethanol solvents." *Photosynth Res* **89**(1): 27-41.

Ryu, J. Y., K. H. Suh, Y. H. Chung, Y. M. Park, W. S. Chow and Y. I. Park (2003). "NADPH dehydrogenase-mediated respiratory electron transport in thylakoid membranes of the cyanobacterium *Synechocystis* sp. PCC 6803 is inactive in the light." *Mol. Cells* **15**(2): 240-244.

Sacksteder, C. A., A. Kanazawa, M. E. Jacoby and D. M. Kramer (2000). "The proton to electron stoichiometry of steady-state photosynthesis in living plants: a proton-puming Q cycle is continuously engaged." *PNAS* **97**(26): 14283-14288.

Sanchez-Baracaldo, P. and T. Cardona (2020). "On the origin of oxygenic photosynthesis and Cyanobacteria." *New Phytol* **225**(4): 1440-1446.

Sato, M., J. Torres-Bacete, P. K. Sinha, A. Matsuno-Yagi and T. Yagi (2014). "Essential regions in the membrane domain of bacterial complex I (NDH-1): the machinery for proton translocation." *J Bioenerg Biomembr* **46**(4): 279-287.

Sazanov, L. (2007). "Respiratory complex I: mechanistic and structural insights provided by the crystal structure of the hydrophilic domain." *Biochemistry* **46**(9): 2275-2288.

Sazanov, L. A. (2015). "A giant molecular proton pump: structure and mechanism of respiratory complex I." *Nat Rev Mol Cell Biol* **16**(6): 375-388.

Schluchter, W. M. and D. A. Bryant (1992). "Molecular characterization of ferredoxin NADP+ oxidoreductase in cyanobacteria: cloning and sequence of the petH gene of Synechococcus sp. PCC 7002 and studies on the gene product [published erratum appears in Biochemistry 1992 Jun 30;31(25):5952]." *Biochemistry* **31**: 3092 3102.

Schreiber, U., T. Endo, H. Mi and K. Asada (1995). "Quenching Analysis of Chlorophyll Fluorescence by the Saturation Pulse Method: Particular Aspects Relating to the Study of Eukaryotic Algae and Cyanobacteria." *Plant and Cell Physiology* **36**(5): 873-882.

Schreiber, U. and C. Klughammer (2009). "New NADPH/9-AA module for the DUAL-PAM-100: Description, operation and examples of application." *PAM application notes* **2**: 1-13.

Schuller, J. M., J. A. Birrell, H. Tanaka, T. Konuma, H. Wulfhorst, N. Cox, S. K. Schuller, J. Thiemann, W. Lubitz, P. Setif, T. Ikegami, B. D. Engel, G. Kurisu and M. M. Nowaczyk (2019). "Structural adaptations of photosynthetic compolex I enable ferredoxin-dependent electron transfer." *Science* **363**(6424): 257-260.

Schuller, J. M., P. Saura, J. Thiemann, S. K. Schuller, A. P. Gamiz-Hernandez, G. Kurisu, M. M. Nowaczyk and V. R. I. Kaila (2020). "Redox-coupled proton pumping drives carbon concentration in the photosynthetic complex I." *Nat Commun* **11**(1): 494.

Screpanti, E. and C. Hunte (2007). "Discontinuous membrane helices in transport proteins and their correlation with function." *J Struct Biol* **159**(2): 261-267.

Sharma, V., G. Belevich, A. P. Gamiz-Hernandez, T. Rog, I. Vattulainen, M. L. Verkhovskaya, M. Wikstrom, G. Hummer and V. R. Kaila (2015). "Redox-induced activation of the proton pump in the respiratory complex I." *Proc Natl Acad Sci U S A* **112**(37): 11571-11576.

Shibata, M., H. Ohkawa, T. Kaneko, H. Fukuzawa, S. Tabata, A. Kaplan and T. Ogawa (2001). "Distinct constitutive and low-CO2-induced CO2 uptake systems in cyanobacteria: genes involved and their phylogenetic relationship with homologous genes in other organisms." *Proc Natl Acad Sci U S A* **98**(20): 11789-11794.

Shikanai, T. and H. Yamamoto (2017). "Contribution of Cyclic and Pseudo-cyclic Electron Transport to the Formation of Proton Motive Force in Chloroplasts." *Mol Plant* **10**(1): 20-29.

Simon, J. and M. G. Klotz (2013). "Diversity and evolution of bioenergetic systems involved in microbial nitrogen compound transformations." *Biochim Biophys Acta* **1827**(2): 114-135.

Stanier, R. Y. and G. Cohen-Bazire (1977). "Phototrophic prokaryotes: the Cyanobacteria." *Annu Rev Microbiol* **31**: 255-274.

Strand, D. D., N. Fisher, G. A. Davis and D. M. Kramer (2016). "Redox regulation of the antimycin A sensitive pathway of cyclic electron flow around photosystem I in higher plant thylakoids." *Biochim Biophys Acta* **1857**(1): 1-6.

Strand, D. D., N. Fisher and D. M. Kramer (2017). "The higher plant plastid NAD(P)H dehydrogenase-like complex (NDH) is a high efficiency proton pump that increases ATP production by cyclic electron flow." *Journal of Biological Chemistry* **292**(28): 11850-11860.

Strand, D. D., N. Fisher and D. M. Kramer (2017). "The higher plant plastid NAD(P)H dehydrogenase-like complex (NDH) is a high efficiency proton pump that increases ATP production by cyclic electron flow." *J Biol Chem* **292**(28): 11850-11860.

Tamoi, M., T. Miyazaki, T. Fukamizo and S. Shigeoka (2005). "The Calvin cycle in cyanobacteria is regulated by CP12 via the NAD(H)/NADP(H) ratio under light/dark conditions." *Plant J* **42**(4): 504-513.

Teuber, M., M. Roegner and S. Berry (2001). "Fluorescent probes for non-invasive bioenergetic studies of whole cyanobacterial cells." *BBA* **1506**: 31-46.

Thomas, J. C., B. Ughy, B. Lagoutte and G. Ajlani (2006). "A second isoform of the ferredoxin:NADP oxidoreductase generated by an in-frame initiation of translation." *PNAS* **103**(48): 18368-18373.

Tikhonov, A. N. (2013). "pH-dependent regulation of electron transport and ATP synthesis in chloroplasts." *Photosynth Res* **116**(2-3): 511-534.

van Thor, J. J., O. W. M. Gruters, H. C. Matthijs and K. J. Hellingwerf (1999). "Localization and function of ferredoxin:$NADP^+$ reductase bound to the phycobilisomes of *Synechocystis*." *The EMBO Journal* **18**(15): 4128-4136.

van Thor, J. J., R. Jeanjean, M. Havaux, K. A. Sjollema, F. Joset, K. J. Hellingwerf and H. C. Matthijs (2000). "Salt shock-inducible photosystem I cyclic electron transfer in *Synechocystis* PCC6803 relies on binding of ferredoxin:$NADP^+$ reductase to the thylakoid membranes via its CpcD phycobilisome-linker homologous N-terminal domain." *BBA* **1457**: 129-144.

Verkhovskaya, M. L., N. Belevich, L. Euro and M. Wikstrom (2008). "Real-time electron transfer in respiratory complex I." *PNAS* **105**(10): 3763-3767.

Vermaas, W. F. J. (2001). Photosynthesis and Respiration in Cyanobacteria. Encyclopedia of Life Sciences.

Vinogradov, A. D. (1998). "Catalytic properties of the mitochondrial NADH-ubiquinone oxidoreductase (complex I) and the pseudo-reversible active/inactive enzyme transition." *Biochem Biophys Acta* **1364**: 169-185.

Wang, D. and G. A. Voth (2009). "Proton transport pathway in the ClC Cl-/H+ antiporter." *Biophys J* **97**(1): 121-131.

Wang, H. L., B. L. Postier and R. L. Burnap (2002). "Polymerase chain reaction-based mutageneses identify key transporters belonging to multigene families involved in Na+ and pH homeostasis of Synechocystis sp. PCC 6803." *Molecular microbiology* **44**(6): 1493-1506.

Wang, H. L., B. L. Postier and R. L. Burnap (2004). "Alterations in global patterns of gene expression in Synechocystis sp. PCC 6803 in response to inorganic carbon limitation and the inactivation of ndhR, a LysR family regulator." *J Biol Chem* **279**(7): 5739-5751.

Wickstrand, C., P. Nogly, E. Nango, S. Iwata, J. Standfuss and R. Neutze (2019). "Bacteriorhodopsin: Structural Insights Revealed Using X-Ray Lasers and Synchrotron Radiation." *Annu Rev Biochem.*

Wikstrom, M. and G. Hummer (2012). "Stoichiometry of proton translocation by respiratory complex I and its mechanistic implications." *Proc Natl Acad Sci U S A* **109**(12): 4431-4436.

Wikstrom, M., V. Sharma, V. R. Kaila, J. P. Hosler and G. Hummer (2015). "New perspectives on proton pumping in cellular respiration." *Chem Rev* **115**(5): 2196-2221.

Williams, J. G. K. (1988). "Construction of Specific Mutations in Photosystem II Photosynthetic Reaction Center by Genetic Engineering Methods in *Synechocystis* 6803." *Methods Enzymol* **167**: 766-778.

Wirth, C., U. Brandt, C. Hunte and V. Zickermann (2016). "Structure and function of mitochondrial complex I." *Biochim Biophys Acta* **1857**(7): 902-914.

Yoshihara, S., X. Geng, S. Okamoto, K. Yura, T. Murata, M. Go, M. Ohmori and M. Ikeuchi (2001). "Mutational analysis of genes involved in pilus structure, motility, and transformation competency in the unicellular motile cyanobacterium *Synechocystis* sp. PCC6803." *Plant Cell Physiol.* **42**(1): 63-73.

Zhang, C., J. Shuai, Z. Ran, J. Zhao, Z. Wu, R. Liao, J. Wu, W. Ma and M. Lei (2020). "Structural insights into NDH-1 mediated cyclic electron transfer." *Nat Commun* **11**(1): 888.

Zhang, P., N. Battchikova, T. Jansen, J. Appel, T. Ogawa and E. M. Aro (2004). "Expression and functional roles of the two distinct NDH-1 complexes and the carbon acquisition complex

NdhD3/NdhF3/CupA/Sll1735 in Synechocystis sp PCC 6803." *Plant Cell* **16**(12): 3326-3340.

Zhao, J., F. Gao, D. Y. Fan, W. S. Chow and W. Ma (2017). "NDH-1 Is Important for Photosystem I Function of Synechocystis sp. Strain PCC 6803 under Environmental Stress Conditions." *Front Plant Sci* **8**: 2183.

Zubay, G. (1996). Orgins of life on earth and in the cosmos, Academic Press.

FIGURE APPENDIX

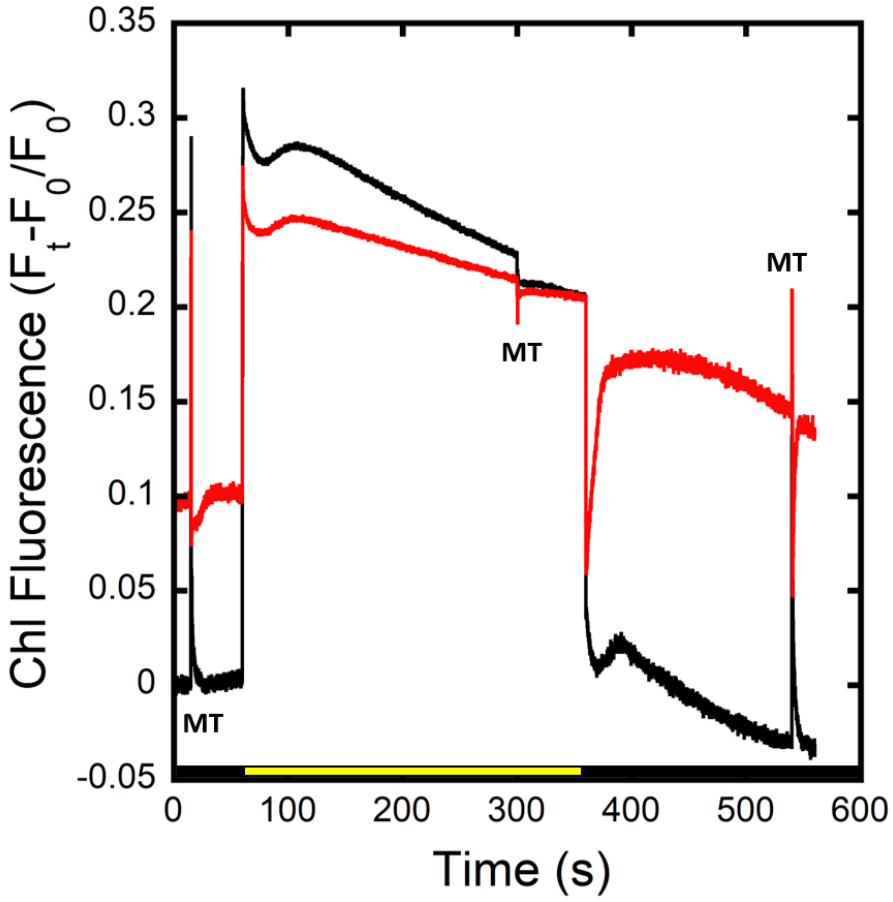

Figure S1. Effect of KCN on chlorophyll fluorescence in near saturating actinic light in the wild type. Chlorophyll fluorescence of dark-adapted cells in TCN buffer with 150mM KCl without (black) and with (red) the addition of KCN to cells in the presence of 330μE actinic light. Multiple turnover flashes (MT) were provided where indicated. Data are normalized to F_0 of the

trace with no KCN.

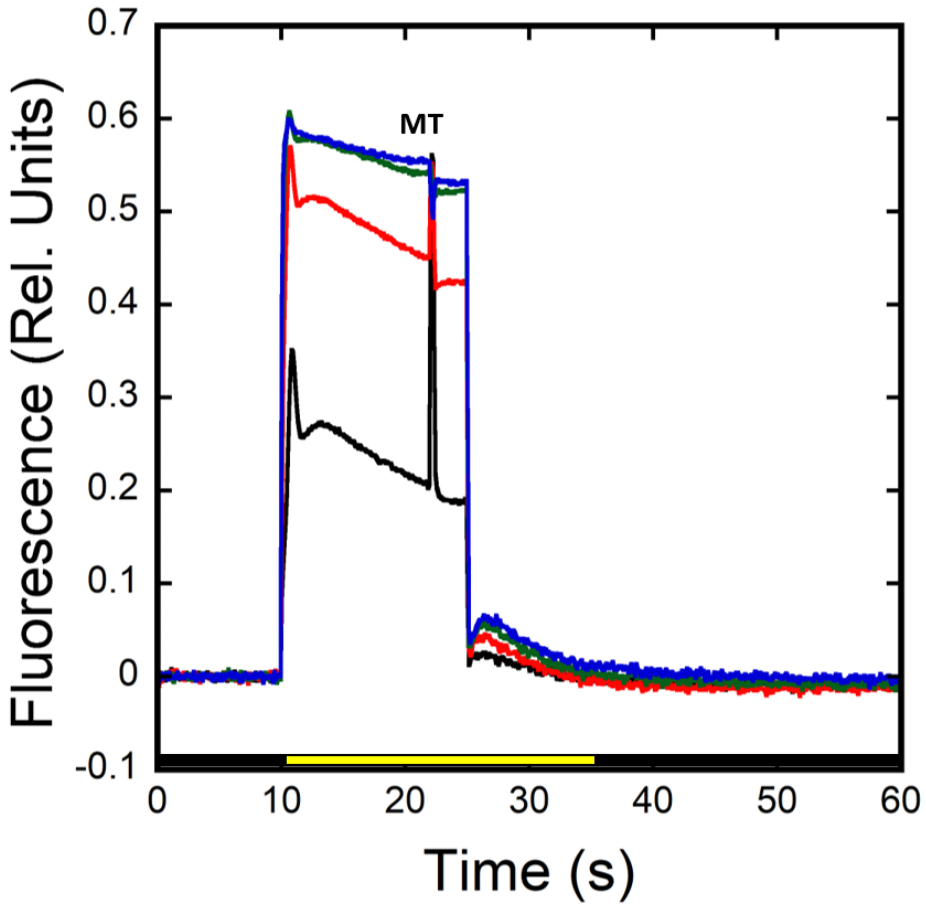

Figure S2. Light intensity dependence of chlorophyll fluorescence. Chlorophyll fluorescence traces were measured in dark adapted wild type cells in TCN buffer with 70uE (black), 166uE (red), 339uE (green), 660uE (blue) actinic light with a multiple turnover flash after 22 seconds of illumination. Traces normalized to F_m and values used to calculate q_p in **Fig. 7B**.

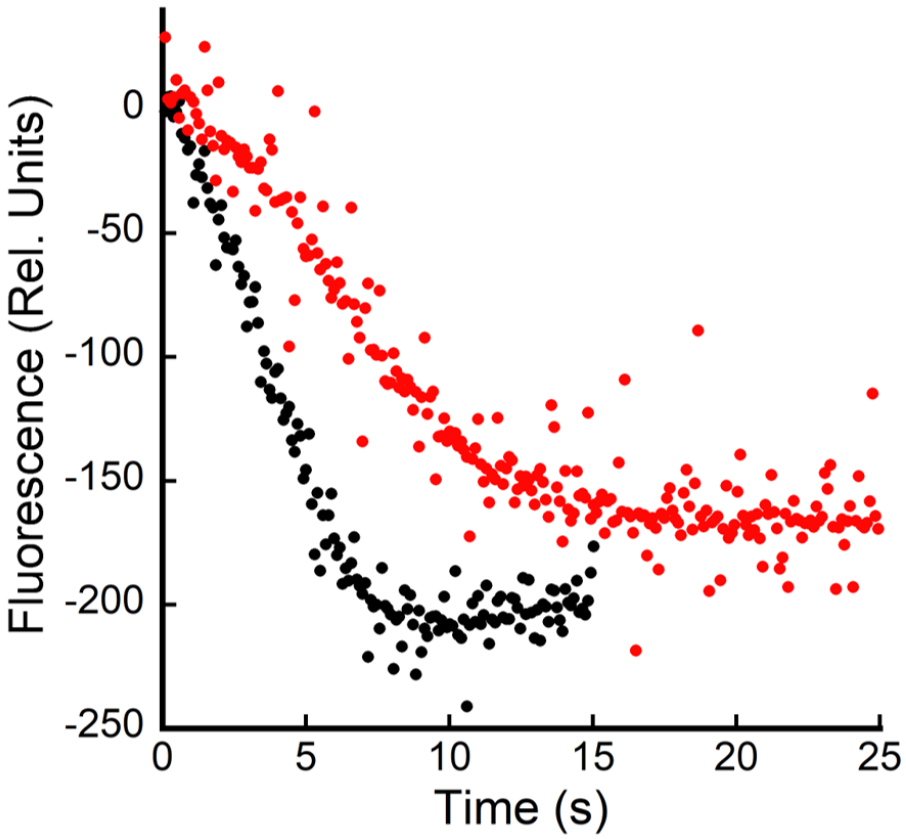

Figure S3. Quenching of AO fluorescence in the presence of DCMU with a longer illumination time. Acridine orange fluorescence of dark-adapted WT cells in TCN buffer with acridine orange (5µM), KCl (150mM) plus Val (10µM), DCCD (500µM), and KCN (200µM) (black) or with the addition of DCMU (red). Actinic illumination of 600 µmol m^{-2} $sec^{-1}$was applied at time zero.

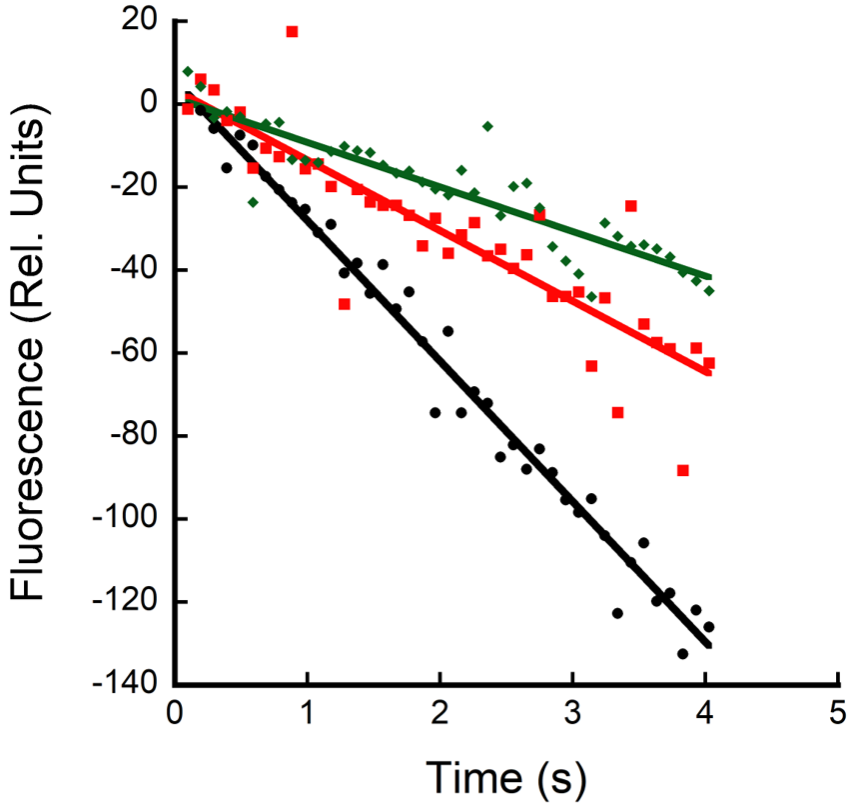

Figure S4. Effect of the addition of glucose on AO quenching rate in cells treated with DCMU. WT cells treated with background inhibitors were measured with no other additions (black circles), in the presence of DCMU (red squares), or in the presence of DCMU and glucose (green diamonds). Traces representative of three technical replicates.

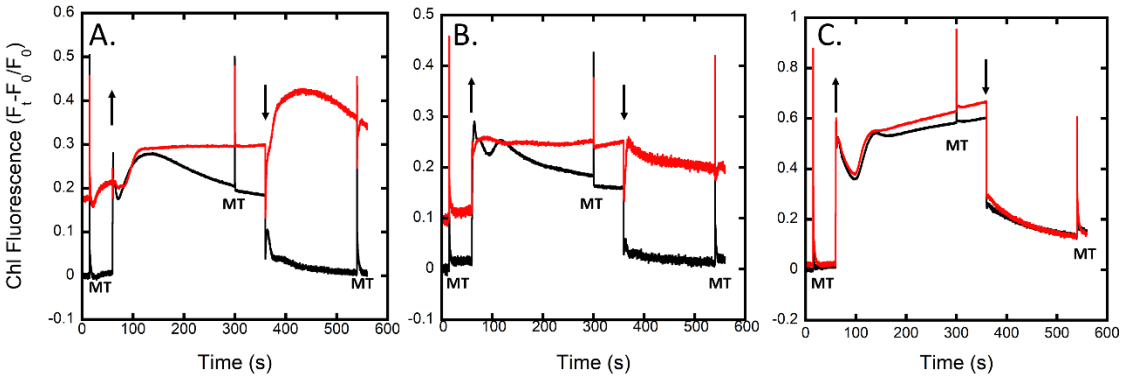

Figure S5. Effect of the addition of KCN on chlorophyll fluorescence in the strains measured. Cells of the WT (**A**), Δ*ndhF1* (**B**), and M55 (**C**) were dark adapted in TCN buffer +

150mM KCl and chlorophyll fluorescence measured with 53μE actinic illumination. Cells were either left untreated (black) or treated with 200μM KCN (red). Multiple turnover flashes (MT) were provided where indicated. Data normalized to F_0 with no KCN. Arrows indicate actinic illumination beginning (up) or ceasing (down).

Table S1. Primers used to generate Δ*ndhF1* by Gibson assembly.

Primer name	Sequence	Target
ndhF1_US_F	AGCAGATTGTACTGAGAGTGCACCAGCTCACAGGACAAAGCATAATC	Upstream of *ndhF1*
ndhF1_US_R	AGGTTTCGGTCTCGTTCATTGTTGCACGGAG	Upstream of *ndhF1*
ndhF1_DS_F	CAAGCCGAGATCGGCTAAGCTTTCCAGCCAAAC	Downstream of *ndhF1*
ndhF1_DS_R	CCCGGGGATCCTCTAGAGTCGACCTGCACGCCTTGTTCGGTAGCAAC	Downstream of *ndhF1*
Gm_F	TGCAACAATGAACGAGACCGAAACCTTGCGC	GmR cassette of HT-3
Gm_R	TGGAAAGCTtAGCCGATCTCGGCtTGAACGAATTG	GmR cassette of HT-3

VITA

Neil Thomas Miller

Candidate for the Degree of

Doctor of Philosophy

Dissertation: CYANOBACTERIAL CYCLIC ELECTRON FLOW DRIVES PROTON PUMPING THROUGH NDH-1 COMPLEXES

Major Field: Microbiology and Molecular Genetics

Biographical:

Education:

Completed the requirements for the Doctor of Philosophy in Microbiology and Molecular Genetics at Oklahoma State University, Stillwater, Oklahoma in December, 2020.

Completed the requirements for the Bachelor of Science in Biology at John Brown University, Siloam Springs, AR, USA in 2013.